THÈSE

En vue de l'obtention du

DOCTORAT DE L'UNIVERSITÉ DE TOULOUSE

Délivré par :
Institut National Polytechnique de Toulouse (INP Toulouse)

Discipline ou spécialité :

Génie des Procédés et de l'Environnement

Présentée et soutenue par :
G. HERNANDEZ-RODRIGUEZ

le : lundi 19 septembre 2011

Titre :

Optimisation multiobjectif de réseaux de transport de gaz naturel

Multiobjective optimization of natural gas transportation networks

---

Ecole doctorale :
Mécanique, Energétique, Génie civil et Procédés (MEGeP)

Unité de recherche :
Laboratoire de Génie Chimique-UMR 5503

Directeur(s) de Thèse :
C. AZZARO-PANTEL (INP-Toulouse, France)

Rapporteurs :
A. ESPUNA (UPC-Barcelone, Espagne)
P. SIARRY (UPEC-Créteil, France)

Autre(s) membre(s) du jury

L. PIBOULEAU (INP-Toulouse, France)
A. A. AGUILAR-LASSERRE (ITO-Veracruz, Mexique)
P. BAUDET (ProSim SA-Labège, France)

Abstract

⋆ TITLE: *Multiobjective optimization of natural gas transportation networks*
The optimization of a natural gas transportation network *(NGTN)* is typically a multiobjective optimization problem, involving for instance energy consumption minimization at the compressor stations and gas delivery maximization. However, very few works concerning multiobjective optimization of gas pipelines networks are reported in the literature. Thereby, this work aims at providing a general framework of formulation and resolution of multiobjective optimization problems related to *NGTN*.
In the first part of the study, the *NGTN* model is described. Then, various multiobjective optimization techniques belonging to two main classes, scalarization and evolutionary, commonly used for engineering purposes, are presented. From a comparative study performed on two mathematical examples and on five process engineering problems (including a *NGTN*), a variant of the multiobjective genetic algorithm *NSGA-II* outmatches the classical scalararization methods, Weighted-sum and ε-Constraint. So *NSGA-II* has been selected for performing the triobjective optimization of a *NGTN*. First, the monobjective problem related to the minimization of the fuel consumption in the compression stations is solved. Then a biojective problem, where the fuel consumption has to be minimized, and the gas mass flow delivery at end-points of the network maximized, is presented. The non dominated solutions are displayed in the form of a Pareto front. Finally, the study of the impact of hydrogen injection in the *NGTN* is carried out by introducing a third criterion, i.e., the percentage of injected hydrogen to be maximized. In the two multiobjective cases, generic Multiple Choice Decision Making tools are implemented to identify the best solution among the ones displayed of the Pareto fronts.
⋆ KEYWORDS: *Multiobjective optimization, Natural gas transportation network, Weighted-Sum, ε-Constraint, Genetic algorithm, Hydrogen*

Résumé

⋆ TITRE : *Optimisation multiobjectif de réseaux de transport de gaz naturel*
L'optimisation de l'exploitation d'un réseau de transport de gaz naturel *(RTGN)* est typiquement un problème d'optimisation multiobjectif, faisant intervenir notamment la minimisation de la consommation énergétique dans les stations de compression, la maximisation du rendement, etc. Cependant, très peu de travaux concernant l'optimisation multiobjectif des réseaux de gazoducs sont présentés dans la littérature. Ainsi, ce travail vise à fournir un cadre général de formulation et de résolution de problèmes d'optimisation multiobjectif liés aux *RTGN*.
Dans la première partie de l'étude, le modèle du *RTGN* est présenté. Ensuite, diverses techniques d'optimisation multiobjectif appartenant aux deux grandes classes de méthodes par scalarisation, d'une part, et de procédures évolutionnaires, d'autre part, communément utilisées dans de nombreux domaines de l'ingénierie, sont détaillées. Sur la base d'une étude comparative menée sur deux exemples mathématiques et cinq problèmes de génie des procédés (incluant en particulier un *RTGN*), un algorithme génétique basé sur une variante de *NSGA-II*, qui surpasse les méthodes de scalarisation, de somme pondérée et d'ε-Contrainte, a été retenu pour résoudre un problème d'optimisation tricritère d'un *RTGN*. Tout d'abord un problème monocritère relatif à la minimisation de la consommation de fuel dans les stations de compression est résolu. Ensuite un problème bicritère, où la consommation de fuel doit être minimisée et la livraison de gaz aux points terminaux du réseau maximisée, est présenté ; l'ensemble des solutions non dominées est répresenté sur un front de Pareto. Enfin l'impact d'injection d'hydrogène dans le *RTGN* est analysé en introduisant un troisième critère : le pourcentage d'hydrogène injecté dans le réseau que l'on doit maximiser. Dans les deux cas multiobjectifs, des méthodes génériques d'aide à la décision multicritère sont mises en œuvre pour déterminer les meilleures solutions parmi toutes celles déployées sur les fronts de Pareto.
⋆ MOTS-CLÉS : *Optimisation multiobjectif, Réseau de transport de gaz naturel, Somme pondérée, ε-Contrainte, Algorithme génétique, Hydrogène*

Acknowledgments

Creating a thesis such as this one requires the help of many people. Firstly, I would like to thank Catherine AZZARO-PANTEL and Luc PIBOULEAU, my supervisors, for encouraging me to finish this work.

I express my sincere appreciation to Serge DOMENECH, Ludovic MONTRASTUC, Alberto AGUILAR and André DAVIN for providing their knowledge and deep understanding of the pipeline networks optimization.

I also want to thank to CONACyT (the Mexican council of science and technology) for encouraging and supporting for over three years by providing the resources including my research scholarships.

During all my years working at the Laboratoire de Génie Chimique, I met a lot of people with who I spent grateful moments, particularly Nicolas, Jean Sebastien, Moises, Ali, Weifeng, Antony, Attia, Juliette and many others. Also, it has been a pleasure working with my working team: Adrien, Adama, Dan, Mary, Marianne and Marie.

I am thankful to the Mexican community. I appreciate all the time spent with Jorge, José Luis, Manuel, Raúl, Sofía, Lalo, Denisse, Fernando, Lizbeth, Marco, Víctor and Antonio.

Last but not least, I owe a debt of gratitude to my family: María Antonia (mother), María Inés (grandmother), Ulises (brother), Marta and Mercedes for encouraged me in this excellent experience. Without their help, my work would had never been finished.

I also express my gratitude to BERTANI-HERNANDEZ family for their valuable help in all my endeavors throughout my adult life.

I am indebted to my future wife Monica for her loving support, encouragement and understanding not only in preparing this thesis but in everything I pursue.

Contents

Introduction and general formulation

1

Contents

1 Introduction

Natural gas *(NG)* systems are becoming more and more complex as the use of this energy source increases. Many investigators have studied the problem of compressible fluid flow through pipelines and compressors. Although much effort has been and continues to be spent on unsteady mathematical models, many design and operating problems can and will be solved by steady-state modelling. Mathematical modelling is one of the most important tools used to aid in design and operation studies. In this chapter, some guidelines are presented concerning the typical features of the *NG* pipeline networks and of their main components. Then, a review of the modelling background dedicated to pipeline transmission systems is presented. The principles of the optimization procedures that can be used to tackle the problem are recalled, with a special focus on their applications. Later, the principle of extension for Natural gas-Hydrogen *(NG-H_2)* mixtures is presented. Finally, a general outline of this work is proposed and introduces the structure of the following chapters.

2 Fossil energy sources: natural gas

Fossil fuel is the most important source of energy for the humanity. There are three major fuels: coal, oil and natural gas. Coal is used primarily to produce electricity. It therefore provides us with light, motive power from electric motors, and our many electronic devices. Oil gives us our mobility, our cars, planes, trains, trucks and boats. *NG* is used primarily to produce heat, for our buildings, hot water, and industrial processes. It is one of the principal sources of energy for many of our day-to-day needs and activities (Figure 1.1). There is an abundance of *NG* but it is a non-renewable resource, the formation of which takes thousands and possibly millions of years. Therefore, understanding the availability of our supply of *NG* is important as we increase our use of this fossil fuel.

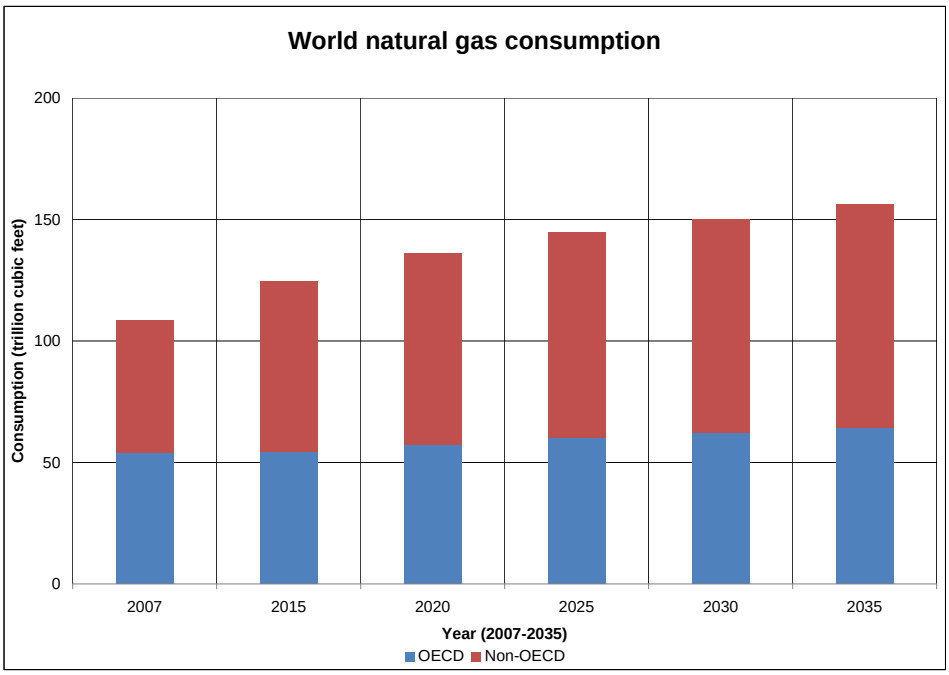

Figure 1.1: World natural gas consumption, 2007-2035 (*EIA*, 2010).

Unlike other fossil fuels, *NG* is clean burning and emits lower levels of potentially harmful byproducts into the air. We require energy constantly, to heat our homes, cook our food, and generate our electricity. It is this need for energy that has elevated *NG* to such a level of importance in our society, and in our lives (Figure 1.2).

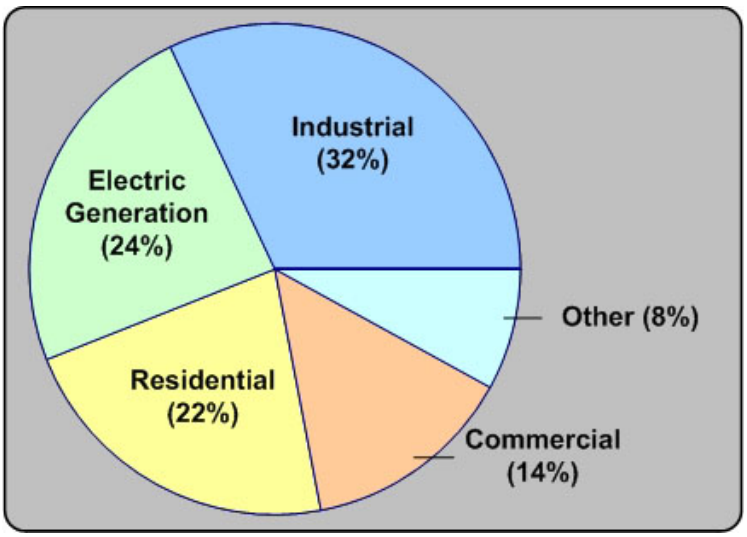

Figure 1.2: Natural gas use by sector in 2010 (*EIA*, 2010).

Gas name	Symbol	Value
Methane	CH_4	70-90%
Ethane	C_2H_6	0-20%
Propane	C_3H_8	
Butane	C_4H_{10}	
Carbon dioxide	CO_2	0-8%
Oxygen	O_2	0-0.2%
Nitrogen	N_2	0-5%
Hydrogen sulphide	H_2S	0-5%
Rare gases	A, He, Ne, Xe	Trace

Table 1.1: Typical composition of natural gas.

The process of extracting *NG* out of the ground, and transport it to its final destination, is a complicated one. There is a great deal of behind-the-scenes activity that goes into delivering *NG* to your homes, even though it takes only the flick of a switch to turn it on (Figure 1.3). There are six major technical processes that allow the *NG* industry to get its product out of the ground, and transform it into the *NG* that is used in your homes and in industry.

1. The Exploration section outlines how *NG* is found, and how companies decide where to drill wells for it.
2. The Extraction section focuses on the drilling process, and how *NG* is brought from its underground reservoirs to the surface.
3. The Production section discusses what happens once the well is drilled, including the processing of *NG* once it is brought out from underground.
4. The Transport section outlines how the *NG* is transported from the well-head and processing plant, using the extensive network of pipelines.
5. The Storage section describes the storage of *NG*, how it is accomplished, and why it is necessary.
6. The Distribution section focuses on the delivery of *NG* from the major pipelines to the end users, whoever they may be.
7. The Marketing section discusses the role that *NG* marketers play in getting the gas from the wellhead to the end-user.

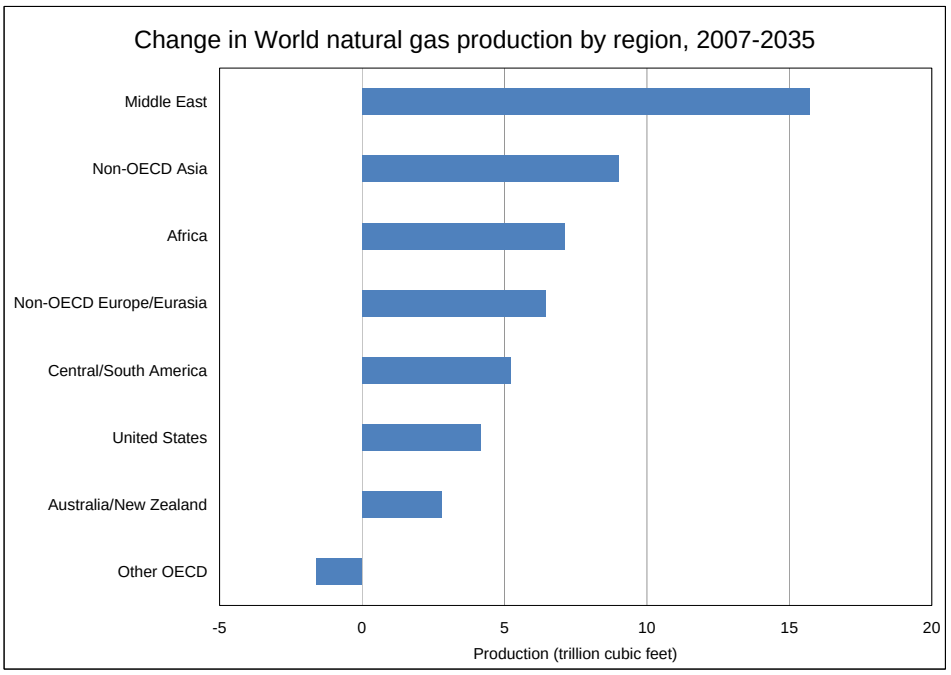

Figure 1.3: World natural gas production by region, 2007-2035 (*EIA*, 2009).

The efficient and effective movement of *NG* from producing regions to consumption regions requires an extensive and elaborate transportation system. In many instances, *NG* produced from a particular well will have to travel a great distance to reach its point of use. The transportation system for *NG* consists of a complex network of pipelines, designed to quickly and efficiently transport *NG* from its origin, to areas of high *NG* demand.

There are three major types of pipelines along the transportation route: the gathering system, the interstate pipeline system, and the distribution system. The gathering system consists of low pressure, small diameter pipelines that transport raw *NG* from the wellhead to the processing plant. Pipelines can be characterized as interstate or intrastate. Interstate pipelines are similar to an interstate highway system: they carry *NG* across state boundaries, in some cases clear across the country. Intrastate pipelines, on the other hand, transport *NG* within a particular state. This work will cover only the fundamentals of interstate *NG* pipelines.

Finally, the preservation of our environment is a very important and pressing topic, particularly when dealing with energy issues. *NG* is an extremely important source of energy for reducing pollution and maintaining a clean and

healthy environment (Table 1.2). In addition to being a domestically abundant and secure source of energy, the use of *NG* also offers a number of environmental benefits over other sources of energy, particularly other fossil fuels.

NG, as the cleanest of the fossil fuels, can be used in many ways to help reduce the emissions of pollutants into the atmosphere. Burning *NG* in the place of other fossil fuels emits fewer harmful pollutants, and an increased reliance on *NG* can potentially reduce the emission of many of these most harmful pollutants.

Pollutant	**Natural gas**	**Oil**	**Coal**
Carbon Dioxide	117,000	164,000	208,000
Carbon Monoxide	40	33	208
Nitrogen Oxides	92	448	457
Sulfur Dioxide	1	1,122	2,591
Particulates	7	84	2,744
Mercury	0.000	0.007	0.016

**Pounds per Billon Btu of Energy input*

Table 1.2: Fossil fuel emission levels (*EIA*, Natural gas issues and trends 1998).

3 The natural gas transportation system

The *NG* transmission pipeline infrastructure in Europe represents one of the largest and most complex mechanical systems in the world. The European natural gas system is very well developed and consists, inter alia, of 1.4 million kilometers pipelines of which 145,000 kilometers concern high pressure transmission pipelines. In addition, 93 storage facilities with a total working volume of 60,000 million cubic meters are in operation.

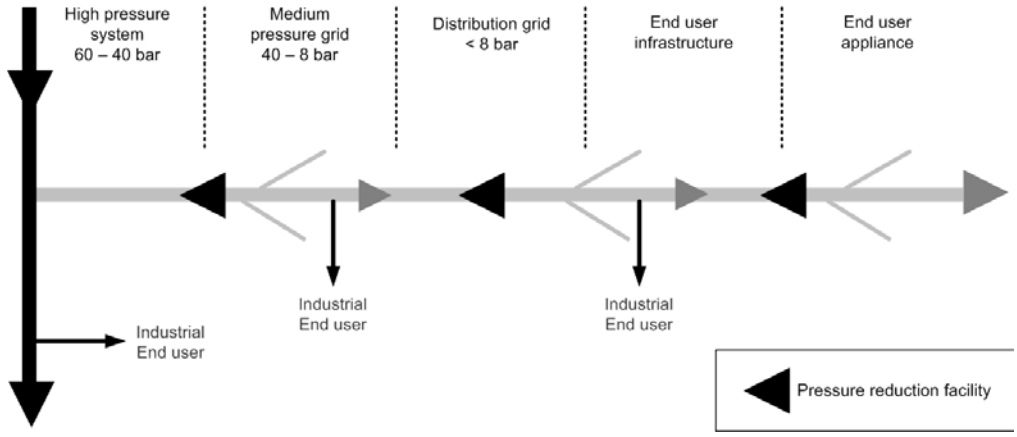

Figure 1.4: Schematic view of the different parts of a natural gas delivery system.

The *NG* chain is generally constituted by various components as represented in Figures 1.4 & 1.5. The pressure regimes are just indicative and may differ from country to country. The transport lying system between the *NG* deposits and the consumers is quite complex. After the gas has been extracted, so-called trunk lines are connected with pipeline compressor stations. The *NG* is then pumped into long distance pipelines called transmission lines and sent to the take-off stations for the consumers. Later, the gas is further transported to the control station of the regional distribution system. It then finally goes to industrial customers and households. A schematic view of a pipeline section is displayed in Figure 1.6 with six compression stations, delivery and supply points.

Part of the NG system	Operating pressures (bar)	Active components (besides valves and pressure regulators)	Material of pipelines	Connected end users
Natural gas production and theatment facilities	> 65	Various	Steel	-
High pressure transmission system	< 70 and > 40	Compressors, LNG-facilities, underground storages, gas bleding stations	Steel	Power plants, iron mills, large chemical plants using natural gas as feedstock, etc
Medium pressure transmission system	< 40 and > 8	-	Steel	Chemical plants, ceramic, industry, District heat&power plants (WKK-facilities), etc
Distribution grid	< 8	-	Steel, cast iron, PE, PVC	Offices, domestic end users, greenhouse, etc
End user infrastructure	< 8	-	Copper, PE	-

Figure 1.5: Technical features of the different parts of a natural gas delivery system [Tabkhi, 2007].

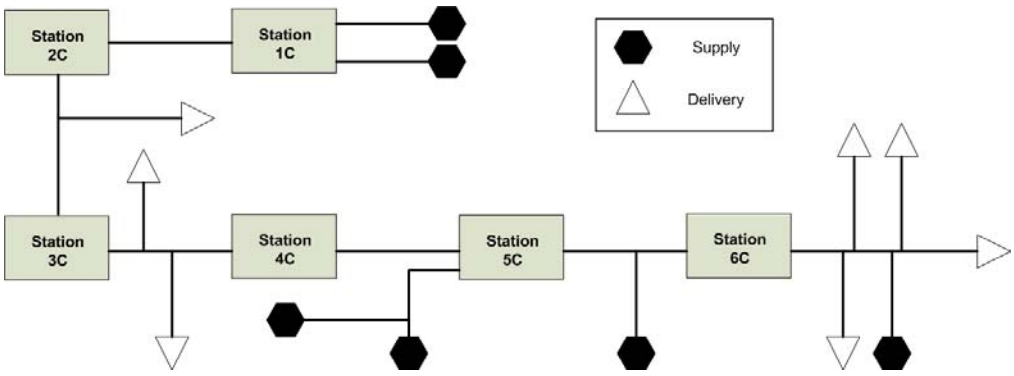

Figure 1.6: Schema showing a selected pipeline section with six compression stations.

Pipeline pressures, diameters and materials used at the different stages of transport vary considerably from country to country, with minor differences also within national systems, depending on the supplier. Figure 1.7 shows some typical ranges of pressures, diameters and materials involved in the different stages of transport. According to the International Energy Agency *(IEA)*, several hundreds of thousands of both large-size transportation and mid/small-size distribution lines have been constructed over the last 30 years all over the world, to match with the increase in *NG* consumption.

Transport stage	Pressure (bar)	Diameter (cm)	Material
To head station	70-100	40-150	LA, HSS
Long distance	60-90	50-130	LA, HSS
Local/Regional	8-40	7.5-30	LA, LCS
Customer	0.050-0.100	2.5-5	LCS, PVC, PE

LA: low alloy, **HSS:** high strength steels, **LCS:** low-carbon steel, **PVC:** poly-vinyl-chloride, **PE:** polyethylene

Figure 1.7: Stages of pipeline transport [Castello et al., 2005].

The didactic example that will be treated in this work will fall into transmission network domain although the approach may be extended easily to the treatment of other distribution systems. Compressor stations in a pipeline system can be sub-divided in two classes: the originating stations, which are positioned at the inlet to the pipeline and are usually the most complex ones, and the booster stations, which are located along the pipeline to compensate for the pressure decrease due to friction and elevation losses. In principle, the longer the pipeline and the elevation of the terrain increased, the more compressor horsepower is required to achieve the required delivery pressure at destination. However, under a fixed route and flow capacity, the number and size of booster stations can vary depending on circumstances and design.

Although systems with fewer stations can be easier to operate, they have the disadvantage of introducing a need for high inlet pressures. Actual transmission systems represent a compromise between very few powerful originating stations and a large number of small booster points. The essential components of a compressor station are the following:

1. The gas compressors and their drivers (gas turbines, electric motors, steam turbines, internal combustion engines).
2. Measuring equipment and metering systems.
3. Inlet separators or gas scrubbers, to remove liquid and solid impurities from the gas and protect the compressors.
4. Heat exchangers and inter-stage coolers, to remove the heat of compression between subsequent compressor stages.
5. Piping manifolds, valves and controllers to direct and regulate the gas flow, valves for vent and relief.

Compressors used for gas transmission in pipelines can be divided in two categories:

1. Positive displacement, or intermittent flow compressors. They can be further sub-divided in reciprocating and rotary compressors. In the first type, the gas is compressed within a cylinder by a moving piston; in the other case the gas is displaced from inlet to outlet by the vanes or lobes of a turning rotor.

2. Dynamic, or continuous flow compressors. They increase the pressure of the gas by increasing its velocity and converting the energy into pressure by slowing the gas flow up in a diffuser. These machines can be further sub-divided in the centrifugal and axial types, which accelerate the gas molecules respectively by subjecting them to centrifugal forces or by transferring them the energy of a spinning rotor: *turbo-compressors* [Gorla and Khan, 2003].

In the present work, centrifugal compressors are used for gas transmission in pipelines. They are assumed to be driven by turbines whose supply energy is provided from a line of the gas derived from the pipeline passed through the station in order to be compressed. The compressors within the compressor station are modelled using centrifugal compressor map-based polynomial equations. These equations are used to define the pipeline conditions across the compressor: flow, discharge pressure, suction pressure and suction temperature. Then, if the operating point is on the *compressor-map*, the fuel consumption of the driver (gas turbine engined) is determined. The use of the so-called *performance-map* will be explained in Chapter 2.

Finally, the volume of gas that a centrifugal compressor can handle depends on the size and speed of the impeller and on the discharge pressure. For a given compressor, performance curves can be drawn that define, for a given value of the impeller rotational speed, the relationship between the inlet flow and the compression work (or compressor's head), which in turn increases with the ratio between the suction and discharge pressures.

4 Transmission pipeline representation: modelling, simulation and optimization

As the gas industry has grown, gas pipeline networks have evolved over decades into very large and complex systems. A typical network today might consist of thousands of pipes, dozens of stations, and many other devices, such as valves and regulators. Inside each station, there can be several groups of compressor units of various vintages that were installed as the capacity of the system expanded. Designing gas pipe distribution networks involves numerous variables, which include pipe diameter, pressure, temperature, line length, space between pumping or compressor stations, required inlet and delivery pressures and quantities. Each of these parameters influences the overall construction and operating cost in some degree and the selection of one or more items will determine the economics of the construction and operation of the system. Indeed, the only real difference between the design and operation of gas pipeline networks is: the extent to which some of the variables are already fixed. Because of the high number of variables involved, the task of establishing the optimum can be quite difficult and in order to ensure a robust solution, many options may have to be investigated.

In more detail, many investigators have studied the problem of compressible fluid flow through pipelines and compressors. Some of these efforts are reported in what follows: *Steady-state solutions and compressor stations*. Stoner [1969, 1972] presented a new method for obtaining a steady-state solution of an integrated gas system model made up of pipelines, compressors, control valves and storage fields. Berard and Eliason [1978] developed a computer program that simulated steady-state gas transmission networks using the Newton-Raphson method for solving nonlinear equations. Hoeven [1992] described some mathematical aspects of gas network simulation using a linearization technique. Rhoads [1983]; Ouyang and Aziz [1996]; Schroeder [2001] give a new description of the equations which govern the flow of compressible fluids through pipes. Tian and Adewumi [1994] used a one-dimensional compressible fluid flow equation without neglecting the kinetic energy term to determine the flow of natural gas through a pipeline system. Costa et al. [1998] provided a steady-state gas pipeline simulation. Here, compressors are

modelled by simply employing a functional relationship between the pressure increase and the mass flow rate of gas through the compressor.

Since 30 years, there has been a successive great deal on the optimization approach of gas pipe networks. Foremost, Turner and Simonson [1984, 1985] developed a computer program for a compressor station that is added to *SIROGAS*, which is a program for solving pipeline networks for steady-state and transient mode.

Botros [1989]; Botros et al. [1991] and Botros [1994] presented a dynamic simulation for a compressor station that consists of nonlinear partial differential equations describing the pipe flow together with nonlinear algebraic equations describing the quasi-steady flow through various valves, constrictions, and compressors.

Botros [1990] presented a numerical study of gas recycling during surge control, and furnished a basic understanding of the thermodynamic point of view and showed the variation of gas pressure, temperature and flow.

Odom and Langenbacher [1990] reviewed the theory of centrifugal compressor performance, and also presented a set of polynomial equations for the centrifugal compressor map. By using different values for the coefficients in these equations, it is possible to model different types of compressors.

Letniowski [1993] presented an overview of the design process for a compressor station model that is part of a network model.

Greyvenstein and Laurie [1994] used the well-known *SIMPLE* algorithm of the Patankar method [Patankar, 1980], which is well known in Computational Fluid Dynamics to deal with pipe network problems.

Jenicek and Kralik [1995] developed optimized control of a generalized compressor station. The work described an algorithm for optimizing the operation of the compressor station with fixed configuration.

Carter [1996] presented a hybrid mixed-integer-nonlinear programming method, which is capable of efficiently computing exact solutions to a restricted class of compressor models and attempted to place station optimization in the context with regard to simulation.

Bryant [1997] modelled compressor station control, which had some advantages such as the ability to set individual unit swing priority, the ability to try and meet multiple set-points, and the ability to automatically come on-line and off-line.

Doonan et al. [1998] used $Simulink^{TM}$ to simulate a pipeline system.

Cameron [1999] presented the package *TFlow* using an *Excel-based* model for steady-state and transient simulation. All information needed to model a pipeline system is contained in an *Excel* workbook, which also displays the simulation result.

Metcalf [2000] presented the effect of compressor valves to improve reciprocating compressor performance, compressor efficiency and horsepower consumption, by choosing the best types of valves.

Fauer [2002] suggested a general equation model and contributed each variable to make accurate predictions.

The state-of-the-art shows that there is growing interest on the subject for dealing on the existing technologies that are used to model the performance and operation of the various components that collectively make up the natural gas pipeline system. Furthermore, from an industrial point of view, the problem of minimizing fuel cost is of great importance, since the reduction of the energy used in pipeline operations will have a significant economical and environmental impact. Thus, efficient operation of compressor stations is of major importance for enhancing the performance of the pipeline network. It is estimated that the global optimization of operations can save considerably the fuel consumed by the stations. Moreover, for a *NG* delivery company, the demand may vary according to climatic conditions or industrial requirements. So, another problem which arises is to determine, for a given supply at the network entrance nodes, the minimal and maximal network capacities in terms of *NG* mass flow delivery and fuel consumption in compressor stations. This problem can be formulated as a biobjective optimization problem. A new industrial perspective consists to take into account the amount of hydrogen that can be added to the pipeline network traditionally devoted to the transportation of natural gas, without any modification in the system. The transition towards the situation in which H_2 will become an important energy carrier, will need decades but worldwide great efforts are made nowadays in the field of H_2 production, delivery, storage and utilization. In this view, an analysis of the potential of using the actual *NG* pipeline systems for the delivery of H_2 is a valid argument. So, defining the conditions under which hydrogen can be added to natural gas constitutes a key point of this investigation as well as how much hydrogen can be injected into the existing pipeline network while minimizing fuel consumption

and maximizing the pipeline throughput. Meeting together all these multiple-criteria aspects, let us introduce to the multiobjective optimization area.

Actually, the two main approaches that are classically encountered in gas networks representation are numerical simulation and optimization. The main purpose of simulation is to determine the actual behaviour of a gas network under given conditions. Simulation basically answers the question: *what happens if we run our grid with given control variables and known boundary flows?* Typical questions like finding a control regime which achieves several target values, usually require a series of simulation runs by expert users who are familiar with the network. Two disadvantages of numerical simulation will be noted. First, finding an adequate regime may even take a large number of runs, and second, it cannot ensure that the solution achieved is optimal.

This explains mainly why the searching process must be substituted with more sophisticated algorithms. Yet, optimization generally works with simplified models, but it yields optimum results where limits or certain target values will be achieved automatically if they are defined as optimization problem constraints. If the effort has been focused on steady-state flow conditions, researchers have identified the need for transient flow simulations for long. Nevertheless, it has been proven that they require a sophistication level that may be difficult to take into account as far as optimization of large systems is concerned.

Hence, as abovementioned, the optimization of a *NG* transportation network is typically a multiobjective optimization problem, where the practitioner has to cope simultaneously with throughput maximization and fuel consumption minimization. Insofar as the objective of this work is the multiobjective optimization of gas transmission networks, only steady-state behaviour of the gas flow is considered. The problem is to implement, for a given mathematical model of a pipeline network, a numerical method that meets the multi-criteria aspect which embeds both solution quality and reasonable resolution time.

5 Multiobjective optimization procedures

A great diversity of optimization methods were implemented to meet the industrial stakes and provide competitive results. But if they prove to be well fitted to

the particular case they consider, the numerical performances cannot be constant whatever the treated problem is. Actually, the efficiency of a given method for a particular example is hardly predictable, and the only certainty we have is expressed by the *No Free Lunch Theory* [Wolpert and Macready, 1997]: there is no method that outdoes all the other ones for any considered problem. In the 19^{th} century, Francis Y. Edgeworth and Vilfredo Pareto introduced the concept of non-inferiority in the field of economics, giving birth to multiobjective optimization. Since then, multiobjective optimization has permitted all engineering areas and has developed at a rapidly increasing speed, particularly during the last decade for chemical engineering and process design.

According to De Weck [2004] there is general consensus that multiobjective optimization methods can be broadly decomposed into two categories: first scalarization approaches, second genetic and evolutionary methods. From a popular classification, scalarization methods apply in well mathematically defined problems with explicit formulations of objectives and constraints, while genetic and evolutionary methods based on evolutionary strategies mainly apply in black-box problems, where objectives and/or constraints are returned by a computer code for each value of optimization variables. Besides the black-box problems, the possibility to mutate out of a local optimum and the ability to compute the entire Pareto front in one run, make also this type of methods attractive.

In the first group of methods the multiobjective problem is solved by translating it back to a single (or a series of) objective, scalar problem. Miettinen [1999] gives an interesting review of various techniques and Engau and Wiecek [2007] present seven types of scalarization methods, but the two most popular ones are the Weighted-sum *(WS)* and the ε-constraint *(ε-C)* procedures. *WS* methods are based on the formation of an overarching objective function containing contributions from each sub-objective. The formulation of the aggregate objective function requires that the preferences or weights between objectives are assigned a priori, i.e. before the results of the optimization process are known. The second important sub-group is constituted by ε-*C* methods; it is also based on a scalarization, where one of the objective functions is minimized while all the other objective functions are upper bounded in the form of additional constraints. In the second group (genetic and evolutionary methods), the elements of the objective vector are kept separate throughout the optimization

process; these approaches typically use the concept of dominance to distinguish between dominated and non-dominated solutions.

Both classes of methods have their own inconveniences: scalarization methods need to know the Nadir values which are the worst values of objective functions over the efficient solutions, that may be very difficult. Furthermore, for problems involving crisp equality constraints (like balance equations for example), an external solver has to be used for each point generated by a genetic and evolutionary method.

Since, the consideration of multiobjective problems is concerned in this study, the stochastic way is adopted in what follows. This approach presents some advantages related to the treatment of the underlying combinatorial aspect linked to industrial problems and to its easy extension to the treatment of multiobjective problems. Nevertheless, since the number of equality constraints associated with the problem formulation may be important, the deterministic approach is also presented in this study [Rodriguez et al., 2010]. The choice between deterministic and evolutionary approaches is carried out on the basis of classical chemical engineering problems.

6 Towards a hydrogen economy

In a world where energy demand is growing at unprecedented rates, pipelines will continue to play an important role in safely and efficiently transporting oil and gas from often remote areas to their markets. Hydrogen is foreseen as an important and reliable energy carrier in the future sustainable energy society. This energy vector, which can be produced from different primary sources among which the renewable energies, is exploitable in different stationary or portable applications. Hydrogen deployment scenarios can be based on one of two different fundamental assumptions concerning the level of decentralization in production. Regardless of the primary energy sources and technologies used, hydrogen can be produced by large scale facilities and then distributed to individual customers over a range of few tens to some hundreds kilometers (centralized production), or it can be produced in the immediate proximity of dispensing facilities or end-use appliances (on-site generation). Consequently, this yields principally to two separate families of production and distribution

pathways made of neighboring stages allowing the adoption of different technologies.

Gaseous hydrogen can be transported using several modes like pipeline, railroad, tanker truck, and tanker ship. The chosen method depends on the distance of transportation, the production method, the use, etc. Regarding transportation of hydrogen with conventional means, the solution via pipelines has been employed to make hydrogen available to a specific range of mass consuming users.

The current aggregated length of pipelines for hydrogen transport that are known to be either in service, or under planning, reaches almost 2500 km comprising a total of some 1500 km in Europe as a whole, and at least 700 km in North America. The oldest hydrogen pipeline is a 220 km started in 1938 in the German Ruhr Valley [Whaley and Long, 2001]. The longest hydrogen pipeline in Europe runs more than 400 km between France and Belgium [Kruse et al., 2002]. The most extensive hydrogen pipeline network in the U.S.A. is about 720 km long and runs almost continuously along the Gulf Coast from Corpus Christi, Texas to New Orleans, Louisiana [Mintz et al., 2002]. Other shorter hydrogen pipelines include a 80 km pipeline in South Africa and two short pipelines in Texas that supply hydrogen to industrial users. *NASA* has piped hydrogen through short pipelines at their space centers for several years [Whaley and Long, 2001].

Of course, the idea of adding hydrogen to gas via pipelines to satisfy the increased demand for energy will require changes in the natural gas pipeline infrastructure to enhance the reliability of the existing systems.

According to the analysis of the dedicated literature concerning hydrogen, it is foreseeable that the hydrogen economy will have to rely on a combination of different delivery options and the share of application of each option will change and evolve with time. This study only considers Natural gas-Hydrogen mixture transmission via pipeline networks. Thorough technical and economic studies on the whole energy chain including production, storage, transport, distribution and utilization are the basic steps to provide new industrial perspectives.

7 Conclusions and general outline

In this introducing chapter, a review of the typical problems of *NG* transmission pipelines and different methodologies to deal with this problem have been presented. Some guidelines can be mentioned concerning the main goal of this study, being the multiobjective optimization of gas transmission networks.

First, the idea is to implement, for a given mathematical model of a pipeline network [Tabkhi et al., 2009], a numerical method that meets the multi-criteria aspect which embeds both solution quality and resolution time. For this purpose, steady-state behaviour of the gas is considered and will be assumed in the momentum and mass balances, that will be presented in details in the Chapter 2.

Second, although various optimization techniques can be used, the choice of a stochastic one is performed, since it is generally recognized that this kind of methods is particularly well-fitted to take into account the multi-criteria aspect despite the important number of constraints that are likely to be involved in the problem formulation. Adequate solvers within the MATLAB toolbox were used *(fmincon, fsolve)* since this optimization tool is often considered as a standard for the solution of *Process Systems Engineering problems*.

Third, the formulation is based on multiobjective optimization problems. Of course, the variables and objective function may differ according to the problem which is considered; however, the nature of variables is continuous (for instance, set points values of compression facilities).

Fourth, concerning to the pipeline optimization, it must be pointed out that the goal of minimizing the energy consumption in compressor stations will have not only economic benefits but also a positive environmental impact, since pipelines emit CO_2 mainly due to energy used at compressor stations.

Fifth, it must be pointed out that the majority of the works presented are based on classical mathematical formulations for gas natural problems. Although the problem may be highly combinatorial for industrial sized problems, the literature review only mentions very few works devoted to stochastic algorithms (for instance, Simulated Annealing or Genetic Algorithms). This is probably due to the important number of constraints (inequalities and equalities) which condition the problem numerical solution. However very few works con-

cerning multiobjective optimization of *NG* transportation networks are reported in the literature.

In that context, this work illustrates their application in a series of case studies covering a range of significant chemical process engineering problems. The work presented here attempts to provide a general methodology in a manner useful to both the scientist/engineer engaged in process development or design, finding the most appropriate operating conditions. This manuscript is now logically presented as follows:

- **Chapter 1** starts with an introduction to gas pipelines, outlining their main technical features. This chapter also highlights the importance of modelling and optimization of such networks and presents the results of the literature review. Finally, the guidelines of the work are presented.
- **Chapter 2** details the modelling approach that serves as a methodology framework.
- **Chapter 3** is devoted to the multiobjective optimization. Typical methods that can be broadly decomposed into two categories: first scalarization approaches, second genetic and evolutionary methods are presented.
- **Chapter 4** studies the efficiency of classical methods in treating 2 mathematical problems and 4 multiobjective chemical engineering problems. On the basis of both problems types, the choice of the best procedure, namely the Genetic algorithm, will be performed in what follows.
- **Chapter 5** considers a Natural gas transmission network *(NGTN)*, involving the simultaneous consideration of fuel consumption minimization and gas mass flow delivery maximization. In a more prospective concern, *NGTN* is dedicated to the transport of a mixture of natural gas-hydrogen mixture in a transition period towards the so-called predicted *hydrogen economy*. Later, some generic tools like the *TOPSIS* and *FUCA* procedures are used for determining a *good* solution on the Pareto front or set of efficient solutions.
- **Chapter 6** gives the conclusions and perspectives for future works.

Review on modelling and optimization of natural gas pipeline networks

2

Contents

1 Introduction

The transportation of large quantities of Natural gas *(NG)* is carried out by pipeline network systems across long distances. As the gas flows through the network, pressure (and energy) is lost due to both friction between the gas and the pipe inner wall, and heat transfer between the gas and its environment. Typically, compressor stations are located at regular intervals along the pipeline to boost the pressure lost through the friction of the *NG* moving through the steel pipe. They consume a significant part of the transported gas (3% to 5%, Suming et al. [2000]), thus resulting in an important fuel consumption cost on the one hand, and in a significant contribution to CO_2 emissions, on the other hand. Nowadays, more than 50% of the total human-caused Greenhouse gas *(GHG)* emissions result from the production and use of energy. About 70% of *GHG* emissions from *NG* occur when it is burned to produce heat or energy. Pipelines emit CO_2 mainly due to energy used at compression stations. Therefore, pipeline companies reduce *GHG* emissions mainly by improving the use of energy by acquiring more efficient equipment and by adopting better operating practices [Mora and Ulieru, 2005].

Thus, efficient operation of compressor stations is of major importance for enhancing the performance of the pipeline network. This chapter first presents a gas transportation model taking into account the elements of the network under steady-state conditions. Then, different approaches for optimizing the performance of natural gas networks are discussed in the last section.

2 Natural gas pipeline modelling

Due to operating problems, a gas transmission line is not usually designed to handle two-phase flows. Exceptions lie for example in oil/gas wells, gathering systems and separation units. The formulation presented here is only valid for single phase gas flow.

The pressure drop in a gas pipeline, i.e., the essential parameter to determine the required compression power for the transmission, is derived from the differential momentum balance. Friction between fluid boundary layer and interior surface of the tube induces energy losses and, consequently, reduces the gas pressure.

The material balance and the equations of momentum conservation on the basic elements of the network as well as the other governing equations constitute the modelling core. The necessary equations in the system of the gas transmission network in order to determine the dynamic conditions, such as pressure and flow rate, are developed. First of all, the momentum balance for a single pipeline is given.

2.1 One dimensional compressible gas flow

The application of one-dimensional flow model to gas pipeline pressure drop calculation, in which the fluid conditions vary only along the pipe, is a good approximation which is usually adopted in the dedicated literature [Osiadacz, 1987]. A reason for using it, is that the cross section area is assumed constant and the curvature of the pipe centre-line is very large compared with the cross-sectional dimensions.

In general, basic equations describing the flow of gas in pipes are derived from a momentum balance that is named also equation of motion, equation of continuity, energy balance and equation of state. In practice, the form of the mathematical models varies with the assumptions made corresponding to the conditions of the operation. Simplified models are based on neglecting some terms in the basic model.

Parameter	**Value magnitude**	**Unit**
Gas molecular weight	18-25	g/mol
Gas critical pressure	45-50	bar
Gas critical temperature	200-250	K
Gas heat capacity at constant pressure	35-45	$J/mol.K$
Gas isentropic exponent	1.2-1.4	-
Specified minimum yield strength	2000-5000	bar
Design factor	0.4-0.7	-
Seam join factor	0.6-1	-
Temperature deration factor	0.85-1	-
Pipeline internal roughness	50-100	μm
Network temperature	260-315	K
Compressor mechanical efficiency	80-98	%
Compressor driver efficiency	25-45	%

Table 2.1: Some parameters and their order of magnitude.

Nomenclature

Symbol	Meaning
A	Cross section area of the pipe (m^2)
Cp	Heat capacity at constant pressure $(J/kmol.K)$
D	Diameter (m)
f	Darcy friction factor
h	Compressor isentropic head (kJ/kg)
HHV	High heating value (J/kg)
L	Length (m)
LHV	Low heating value (J/kg)
$\dot{m}$	Mass flow rate (kg/s)
M	Molecular mass (kg/mol)
$MAOP$	Maximum allowable operating pressure (bar)
P	Pressure (bar)
$\bar{P}$	Average pressure (bar)
Q	Volumetric flow rate (m^3/s)
R	Universal gas constant $(J/mol.K)$
Rg	Roughness of the interior surface of pipes (m)
$SMYS$	Specified minimum yield strength (bar)
Re	Reynolds number
t	Time (s)
T	Temperature (K)
W	Power (MW)
x	Pipe centerline direction (m)
y	Mole fraction $(Decimal)$
Z	Compressibility factor
Greek letters	
β	Thickness (m)
η	Efficiency
κ	Average isentropic exponent
ν	Velocity (m/s)
ρ	Gas density (kg/m^3)
φ	Factor
$\bar{\omega}$	Rotational speed (rps)
Subscripts	
c	Critical
$comp$	Compressor
d	Discharge
dr	Driver $(Decimal)$
e	Erosional
E	Seam joint
F	Design
i	Supply
IS	Adiabatic or Isentropic (%)
j	Delivery
k	Natural gas component
m	Mechanical $(Decimal)$
s	Suction
t	Total $(Decimal)$
T	Temperature derating

Table 2.2: Nomenclature of the Natural gas transmission networks.

2.2 Conservation of mass: continuity equation

Generally, the one-dimensional conservation of mass is expressed in the form of following equation where ρ is the gas density, v is the gas velocity, x is the pipeline centerline direction and t is the time:

$$\frac{\partial(\rho v)}{\partial x} + \frac{\partial \rho}{\partial t} = 0 \tag{2.1}$$

The relation between mass flow rate, $\dot{m}$, also called pipe throughput, the density and the velocity of gas is expressed in Equation 2.2. Unlike a liquid pipeline, due to compressibility, the gas velocity depends upon the pressure and, hence, will vary along the pipeline even if the pipe diameter is constant.

$$\dot{m} = \frac{\pi}{4} D^2 \rho v \tag{2.2}$$

The cross section area of the pipe, A, remains constant over its entire length. D is the pipe internal diameter. Gas density and pressure are represented in the form of the following equation by introducing the compressibility factor, Z, in the model.

$$\rho = \frac{PM}{ZRT} \tag{2.3}$$

R is the universal gas constant and M is the molecular mass of the gas and depends on its composition. Molecular mass of the gas is calculated using a simple mixing rule expressed by the following equation in which y_k and M_k are the mole fractions and the molecular masses of species respectively.

$$M = \sum_{k=1}^{n} M_k y_k \tag{2.4}$$

The compressibility factor, Z, is used to alter the ideal gas equation to account for the real gas behaviour. Traditionally, the compressibility factor is calculated using an equation of state. Yet, for natural gas, it may be estimated from the empirical relationship proposed for simulation goals in the literature [Mohring et al., 2004]. For example, this factor can be expressed as a function of the critical properties of the gas mixture, average pressure of the pipe segment and

the temperature that have been considered as constant:

$$Z = 1 + \left(0.257 - 0.533\frac{T_c}{T}\right)\frac{\bar{P}_{ij}}{P_c} \tag{2.5}$$

$$T_c = \sum_{k=1}^{n} T_{ck} y_k \tag{2.6}$$

$$P_c = \sum_{k=1}^{n} P_{ck} y_k \tag{2.7}$$

The pseudo-critical temperature of natural gas, T_c, and its pseudo-critical pressure, P_c, can be calculated using an adequate mixing rule starting from the critical properties of the natural gas components. The critical point of a material is the point where the distinction between the liquid and vapour phases disappears. In this work, average pseudo-critical properties of the gas are determined from the given mole fractions of its components by Kay's rule which is a simple linear mixing rule shown in Equations 2.6 & 2.7. Average pressure, $\bar{P}_{ij}$, can be calculated from two end pressures [Mohring et al., 2004]:

$$\bar{P}_{ij} = \frac{2}{3}\left(P_i + P_j - \frac{P_i P_j}{P_i + P_j}\right) \tag{2.8}$$

Using Equation 2.3, the continuity equation can be rearranged in the basis of mass flow rate and pressure expressed as:

$$\frac{1}{A}\frac{\partial \dot{m}}{\partial x}\frac{M}{R}\frac{\partial}{\partial t}\left(\frac{P}{ZT}\right) = 0 \tag{2.9}$$

2.3 Equation of motion: momentum balance

The conservation law of momentum is applied to a cylindrical control volume in steady-state to derive the pattern of the pressure changes along a pipe and time. So the governing equation to calculate the pressure at each point of a pipe can be derived as follows:

$$\frac{\partial P}{\partial x} + \frac{f}{2D}\rho v^2 \pm g\rho \ sin\alpha \frac{\partial(\rho v^2)}{\partial x} + \frac{\partial(\rho v)}{\partial t} = 0 \tag{2.10}$$

In this equation, P is the pressure in (Pa), g is the acceleration of gravity in (m/s^2) and α is the acute angle between the horizon and the pipe centerline direction, x. The sign of gravity term in the Equation 2.10 is positive if the gas flows upward and is negative when the gas flows downward. The Darcy friction factor, f, is a dimensionless value that is a function of the Reynolds number, Re, and relative roughness of the pipeline, (Rg/D). Darcy friction factor is numerically equal to four times of the Fanning friction factor that is preferred by some engineers. The Reynolds number quantifies the ratio of inertial forces to viscous forces for given flow conditions and helps to identify different flow regimes, such as laminar or turbulent flows:

$$Re = \frac{\rho v D}{\mu} \tag{2.11}$$

Traditionally, to characterize roughness of pipelines the equivalent sand-grain roughness is used. The sand-grain roughness refers to the rough pipe experiments of Nikuradse and it is commonly used in practice; the hydraulic properties of a pipeline are compared to Nikuradse's work to arrive at an equivalent roughness [Sletfjerding and Gudmundsson, 2003]. In turbulent flow, the wall roughness is often a limiting factor as compared with the Reynolds number to find out the value of the friction factor. In offshore gas pipelines, for example, where Re has an order of magnitude of 13000, the wall roughness will strongly influence the pipeline pressure drop. In such pipelines, it is a common practice to apply coating on pipe walls to reduce wall roughness and pressure drop [Sletfjerding and Gudmundsson, 2003]. Another example concerns the flow around merchant ships where the viscous drag dominates the resistance, and the wall roughness has a significant influence on drag [Grigson, 1992]. Since the flow is considered fully developed here, which is the case concerning gas pipelines, the friction factor is estimated through the equation deduced by Prandtl-von Karman [Romeo et al., 2002] in which the friction factor depends only on the relative roughness:

$$f = \left(-2\ log\frac{Rg/D}{3.71}\right)^{-2} \tag{2.12}$$

The momentum balance in terms of pressure and throughput can be written with the following equation:

$$\frac{\partial P}{\partial x}+\frac{f}{2D}\frac{ZRT}{PMA^2}\dot{m}^2 \pm g\frac{PM}{ZRT}sin\alpha+\frac{2\dot{m}R}{A^2M}\frac{ZT}{P}\frac{\partial \dot{m}}{\partial x}+\frac{\dot{m}^2R}{A^2M}\frac{\partial}{\partial x}\left(\frac{ZT}{P}\right)+\frac{1}{A}\frac{\partial \dot{m}}{\partial t}=0 \tag{2.13}$$

The derivation of this equation is presented in Tabkhi [2007]. In the case of the steady-state, the flow properties do not change with time at each point of the pipe. This clause can be presented mathematically as the Equations 2.14 & 2.15. Therefore, according Equation 2.9, the mass flow rate through the pipe remains constant across it:

$$\frac{\partial \dot{m}}{\partial t}=0 \tag{2.14}$$

$$\frac{\partial}{\partial t}\left(\frac{P}{ZT}\right)=0 \tag{2.15}$$

$$\frac{1}{A}\frac{\partial \dot{m}}{\partial x}=0 \rightarrow \dot{m}=constant \tag{2.16}$$

Consequently, Equation 2.13 which is a general equation can be written in steady-state operating as follows:

$$\frac{\partial P}{\partial x}+\frac{f}{2D}\frac{ZRT}{PMA^2}\dot{m}^2 \pm \frac{PM}{ZRT}sin\alpha+\frac{\dot{m}^2R}{A^2M}\frac{\partial}{\partial x}\left(\frac{ZT}{P}\right)=0 \tag{2.17}$$

In gas transmission lines, changes in elevation may seem to have a negligible contribution to the overall pressure drop, but it turns out that, particularly in high pressure lines this contribution could be appreciable. The associated equation for the pressure drop calculation in a pipe segment with the change in elevation is shown in Equation 2.19 [Tabkhi, 2007]. For a horizontal pipe, by assuming that the temperature and compressibility factor remain constant between the points 1 and 2 of the pipe, the steady-state pressure drop can be calculated using the following expression:

$$(P_2^2-P_1^2)-\frac{32\dot{m}^2ZRT}{\pi^2D^4M}ln\left(\frac{P_2}{P_1}\right)+\frac{16f}{\pi^2D^5}\frac{ZRT}{M}\dot{m}^2L=0 \tag{2.18}$$

In general, when considering compressible flow, as pressure changes along the line, so does the density. A rigorous calculation of pressure loss for long

pipelines involves dividing it into segments, performing the calculation for each segment (considering variable parameters) and integrating over the entire length. The relationship between pressure and flow exhibits a high degree of nonlinearity. So, the Equation 2.19 evaluates the pressure drop corresponding to a given flow magnitude and direction. This equation is used to estimate the pressure profile of pipelines and can incorporate the pressure head that occurs due to the location of the pipeline via the elevation changes as presented in Equation 2.19 [Tabkhi, 2007], as well as for the other cases. Introducing flow direction, pressure loss equation yields to the form below:

$$(P_1^2 - P_2^2) - \frac{32\dot{m}^2 ZRT}{\pi^2 D^4 M} ln\left(\frac{P_1}{P_2}\right) = \frac{16f}{\pi^2 D^5}\frac{ZRTL}{M}\dot{m}^2 sign(\dot{m}) \tag{2.19}$$

2.4 Maximum allowable operational pressure

The internal pressure in a pipe causes the pipe wall to be stressed, and if allowed to reach the yield strength of the pipe material, it could cause permanent deformation of the pipe and ultimate failure. In addition to the internal pressure due to gas flowing through the pipe, the pipe might also be subjected to external pressure which can result from the weight of the soil above the pipe in a buried pipeline and also by the probable loads transmitted from vehicular traffic. The pressure transmitted to the pipe due to vehicles above ground will diminish with the depth of the pipe below the ground surface. In most cases involving buried pipelines the effect of the internal pressure is more than that of external loads. Therefore, the necessary minimum wall thickness will be dictated by the internal pressure in a gas pipeline. The pressure at all points of the pipeline should be less than the maximum allowable operating pressure ($MAOP$) which is a design parameter in the pipeline engineering. This upper limit is calculated using Equation 2.21:

$$P < MAOP \tag{2.20}$$

$$MAOP = SMYS\frac{2\beta}{D-\beta}\varphi_F\varphi_E\varphi_T \tag{2.21}$$

$$\beta = 52 \times 10^{-3} D + 989 \times 10^{-5} \tag{2.22}$$

The derivation of this equation is given in Tabkhi [2007]. According to this equation, to withstand the internal pressure in a gas pipeline, the required minimum wall thickness depends upon the pipe diameter and pipe material (Equation 2.22). This equation is obtained using the scheduled dimensions provided by *ASME B36.19M* standard that concerns stainless steel pipes. In addition other factors such as population density of the region wherein the pipeline goes through are introduced [Shashi Menon, 2005]. The yield stress used in Equation 2.21 is called the specified minimum yield strength ($SMYS$) of pipe material. *SMYS* is a mechanical property of the construction material of the gas pipeline. The factor φ_F has been named the design factor. This factor is usually 0.72 for cross-country or offshore gas pipelines, but can be as low as 0.4, depending on class location and type of construction. The class locations, in turn, depends on the population density in the vicinity of the pipeline. The seam joint factor, φ_E, varies with the type of pipe material and joint type. Seam joint factors are between 1 and 0.6 for the most commonly used material types. The temperature derating factor, φ_T, is equal to 1 for the gas temperature below $120°C$ but it arrives to 0.867 at $230°C$. These three factors are explained in more details in Tabkhi [2007].

2.5 Critical velocity

The gas velocity is directly related to the flow rate. As flow rate increases due to the augmentation in pressure drop, so does the gas velocity. An important factor in the treatment of compressible fluid flow is the so-called critical flow. For a compressible flow, the increase in flow owing to the pressure drop increase is limited, to the velocity of sound in the fluid, i.e., the critical velocity. Sonic or critical velocity is the maximum velocity which a compressible fluid can reach in a pipe. For trouble-free operation, the velocities must be maintained under a half of sonic velocity. Sonic velocity in a gas, v_c, is calculated with a satisfactory approximation using Equation 2.24. Here κ is the average isentropic exponent of the gas. Cp is the heat capacity at constant pressure.

$$v < \frac{v_c}{2} \tag{2.23}$$

$$v_c = \sqrt{\frac{\kappa ZRT}{M}} \tag{2.24}$$

$$\kappa = \frac{\sum_{k=1}^{n}(Cp_k y_k)}{\sum_{k=1}^{n}(Cp_k y_k) - R} \tag{2.25}$$

2.6 Erosional velocity

Increasing gas velocity in a pipeline can have a particular effect on the vibration level and increase the noises too. Moreover, higher velocities in the course of a long period of time will cause the erosion of the inside surface of the tubes, elbows and other joints. The upper limit of the velocity range should be such that erosion-corrosion cavitations or impingement attack will be minimal. The upper limit of the gas velocity for the design purposes is usually computed empirically with the following equation [Shashi Menon, 2005]. In pipeline design domain, the erosional velocity, v_e, falls always underneath the speed of sound in the gas.

$$v < v_e \tag{2.26}$$

$$v_e = 122\sqrt{\frac{ZRT}{PM}} \tag{2.27}$$

Consideration should be given such that the flow velocity remains within a range where corrosion is minimized. The lower limit of the flow velocity range should be so that the impurities keep suspended in the pipeline, thereby minimizing accumulation of corrosion matter within the pipeline.

2.7 Compressor characteristics

As shown in Figure 2.1, a centrifugal gas compressor is characterized by means of its delivered flow rate and its pressure ratio, the ratio between suction side pressure and its discharge pressure. The compression process in a centrifugal compressor can be well formulated using isentropic process aiming for calculating horsepower for a compressor station. The pressure ratio of a centrifugal

compressor is usually linked with a specific term named: Head. It is carried over from pump design nomenclature and expressed in (kJ/kg) even for compressors. The compressor isentropic head, h, developed by the compressor is defined as the amount of energy supplied to the gas per unit mass of gas.

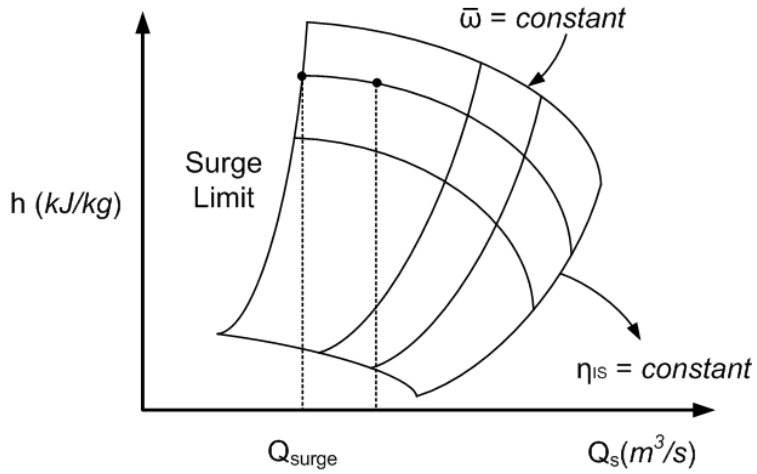

Figure 2.1: A typical centrifugal compressor map.

Therefore, by multiplying the mass flow rate of compressed gas, $\dot{m}_{comp}$ by the compressor isentropic head, h, the total energy supplied to the gas is calculated. Dividing this by compressor isentropic efficiency, η_{IS}, the required power, W, to compress the gas is obtained. Thus, the equation for power calculation can be expressed as follows:

$$W = \frac{\dot{m}_{comp}(h)}{\eta_{IS}} \tag{2.28}$$

This equation is obtained by considering compression adiabatic process that is a reasonable assumption because the heat transfer between gas and the outside is very low. For adiabatic compressor firstly the adiabatic efficiency is defined:

$$\eta_{IS} = \frac{W_{ideal}}{W} \tag{2.29}$$

As shown in the following equation, considering adiabatic compression, h is an index of the pressure ratio across the compressor. In this equation, P_d is the discharge pressure of the compressor and P_s is the suction pressure and κ is isentropic exponent and will be calculated using Equation 2.25. The compressibility factor and the temperature are considered here at suction side of

the compressor [Smith and Van Ness, 1998].

$$h = \frac{Z_s R T_s}{M} \frac{\kappa}{\kappa - 1} \left[\left(\frac{P_d}{P_s} \right)^{\frac{\kappa-1}{\kappa}} - 1 \right] \tag{2.30}$$

Centrifugal compressors devices are commonly moved by electric motors, steam turbine or internal combustion engines. Combustion turbines can also supply the required energy for compression process. Turbine compressors gain their energy by using up a small proportion of the natural gas that they compress. The turbine itself serves to operate a centrifugal compressor, which contains a type of fan that compresses and pumps the natural gas through the pipeline. Some compressor stations are operated by using an electric motor to turn the same type of centrifugal compressor. This type of compression does not require the use of any of the natural gas from the pipe; however it does require a reliable source of electricity nearby. Reciprocating natural gas engines are also used to power some compressor stations. These engines are similar to a very large truck engine, and they are powered by natural gas provided from the pipeline. The combustion of the gas powers pistons on the outside of the engine, which serves to compress the natural gas.

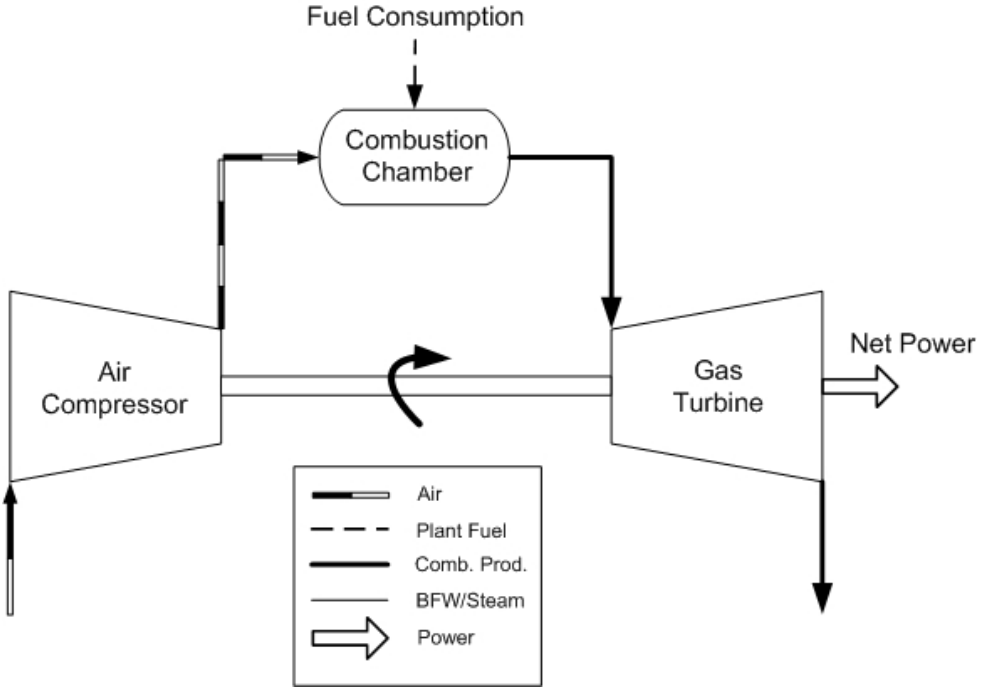

Figure 2.2: Representation of a compressor and its incorporated turbine.

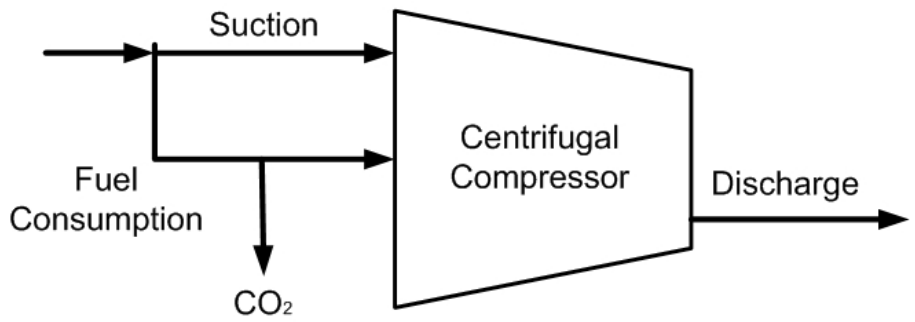

Figure 2.3: General schema of the fuel consumption in the centrifugal compressor.

In this work, centrifugal compressors in the stations are assumed to be driven by turbines whose supply energy is provided from a line of the gas derived from the pipeline passed through the station in order to be compressed as shown in Figures 2.2 & 2.3. The flow rate of the consumed gas as fuel for the compression process in each compressor is obtained by dividing the required power for compression (W) by the mechanical efficiency (η_m), driver efficiency (η_{dr}) and low heating value (LHV):

$$\dot{m}_f = \frac{10^6 \dot{m}_{comp}(h)}{\eta_{IS}\eta_m\eta_{dr}LHV} \tag{2.31}$$

Here LHV represents the quantity of energy released by mass unity of the gas during complete combustion. It is considered at $25°C$ and $1\ bar$ and it is calculated from the mass lower heating values, LHV_k of the molecules composing the gas:

$$LHV = \frac{\sum_{k=1}^{n} y_k M_i LHV_k}{\sum_{k=1}^{n} y_k M_k} \tag{2.32}$$

HHV is not introduced here as the released water after the combustion reactions. It is assumed to be in gaseous state. Feasible operating domain of a single compressor is constituted using the inequalities shown in Equations 2.35 & 2.36.

The compressors within the compressor stations are modelled using compressor map-based polynomial equations. Normalized head, $h_i/\bar{\omega}^2$ and normalized flow rate, $Q_s/\bar{\omega}$, are used to describe the performance map of the compressors

[Odom and Langenbacher, 1990]. Q_s is volumetric flow rate at suction side and $\bar{\omega}$ is rotational speed. The set of polynomial equations uses constant coefficients. If the compressor driver allows, the compressor speed can be varied to control the pressure ratio. Applying standard polynomial curve-fit procedures for each compressor, the normalized head can thus be obtained under the form of the following equation [Abbaspour et al., 2005].

$$\frac{h_i}{\bar{\omega}^2} = b_1 + b_2\frac{Q_s}{\bar{\omega}} + b_3\left(\frac{Q_s}{\bar{\omega}}\right)^2 \tag{2.33}$$

As well, contours of constant isentropic efficiency could be fitted in the polynomial form of second degree shown in Equation 2.34:

$$\eta_{IS} = b_4 + b_5\frac{Q_s}{\bar{\omega}} + b_6\left(\frac{Q_s}{\bar{\omega}}\right)^2 \tag{2.34}$$

The rotation speed of all compressors is comprised between lower and upper bounds as represented below.

$$\bar{\omega}_l \leq \bar{\omega} \leq \bar{\omega}_u \tag{2.35}$$

The lower limit on flow is marked by surge or pumping phenomenon that is an unsteady flow condition characterized by increased noise and flow reversal through the machine. To prevent from surge phenomenon, by considering surge margin, λ_{surge}, the following constraint is introduced [Odom and Langenbacher, 1990].

$$\lambda_{surge} \leq \frac{Q_s - Q_{surge}}{Q_s} \tag{2.36}$$

There is a surge flow rate, Q_{surge}, corresponding to each compressor rotational speed (Figure 2.1). The line joining the surge points at different speeds gives the surge line. The surge line will be sketched using the following equation [Pugnet, 1999]:

$$Q_{surge} = b_7\left[\left[\frac{Z_sRT_s}{MP_s^2}\frac{\kappa-1}{\kappa}h_{surge} + \left(\frac{Z_sRT_s}{P_sM}\right)^2\right]^{\frac{\kappa}{\kappa-1}} - \left(\frac{Z_sRT_s}{P_sM}\right)^2\right]^{\frac{1}{2}} \tag{2.37}$$

In this equation, h_{surge} is the surge head at specified compressor speed and can be calculated using following equation:

$$\frac{h_{surge}}{\bar{\omega}^2} = b_1 + b_2\frac{Q_{surge}}{\bar{\omega}} + b_3\left(\frac{Q_{surge}}{\bar{\omega}}\right)^2 \tag{2.38}$$

A fixed value for the surge pseudo efficiency is considered, it will be introduced like a parameter in the optimization procedure. The previous equation represents a nonlinear correlation between surge flow rate and rotational speed of the compressor. The right portions of the head-flow characteristics curves drop because of choking. Choking phenomenon which occurs at high flow rates also limits the compressor's operating range. At a given speed, the upper limit on flow is set by stall in the inlet, diffuser or impeller passages. To avoid chocking occurrence at inlet, the inequality shown in Equation 2.39 should be considered. In this inequality, A_s is the cross sectional area and v_c is the gas sonic velocity at the compressor inlet.

$$Q_s \leq A_s v_c \left[\frac{2}{\kappa+1}\right]^{\frac{\kappa+1}{2(\kappa+1)}} \tag{2.39}$$

3 Previous works on natural gas network optimization

3.1 Monobjective optimization

One of the first works on natural gas network optimization is the Ph.D. thesis of De Wolf [1992]. The objective to be minimized was the sum of investment and operating costs. Osiadacz [1987] has presented a dynamic optimization of high-pressure gas networks using hierarchical system theory. Mohitpour et al. [1996] have used a dynamic simulation approach for the design and optimization of pipeline transmission systems. Sung et al. [1998] have based their modelling approach on a hybrid network using minimum cost spanning tree. Sun et al. [2000] have used a software support system, called the *Gas Pipeline Operation Advisor* for minimizing the overall operating costs, subject to a set of constraints such as the horsepower requirement, availability of individual compressors, types of compressor and the cycling of each compressor. A reduction technique for natural gas transmission network optimization problems was implemented by Ríos-Mercado et al. [2002]. Nestor et al. [2002] have used the

software package *Gas Net*. A Mixed Integer Non Linear Programming *(MINLP)* model for the problem of minimizing the fuel consumption in a pipeline network was implemented by Cobos-Zaleta and Ríos-Mercado [2002]. Mora and Ulieru [2005] have determined the pipeline operation configurations requiring the minimum amount of energy (e.g. fuel, power) needed to operate the equipment at compressor stations for given transportation requirements. Chauvelier-Alario et al. [2006] have developed *CARPATHE*, a simulation package (GdF-Suez) for representing the behaviour of multi-pressure networks and including functionalities for both network design and network operation. Optimization methods for planning reinforcement on gas transportation networks and for minimizing the investment cost of an existing gas transmission network were used by André et al. [2006]; André [2010]. Recently, Tabkhi et al. [2009] have minimized the fuel consumption in the compressor stations by using the *GAMS* package; they carried out a post-optimal analysis based on Lagrange multipliers to identify the most sensitive problem constraints on the optimal solution.

3.2 Multiobjective optimization

In the natural gas network optimization problems, the references on multiobjective optimization are rarer than in the monobjective case. Surry et al. [1995] and Surry and Radcliffe [1997] have developed the *COMOGA* method for solving monobjective constrained optimization problem by means of a multiobjective genetic algorithm; the procedure is illustrated by a gas network pipe-sizing problem. However this application is only related to monobjective case. Babonneau et al. [2009] solved the biobjective optimization of investment and energy in a gas transmission network. As the problem was formulated in a convex form, convex solvers presented by Abbaspour et al. [2005] were used.

4 Conclusion

The modelling equations presented in Section 2 will be used in Chapter 5 for modelling a didactic network [Abbaspour et al., 2005]. These equations will be also used to take into account hydrogen injection into natural gas transmission network.

Nowadays, most of optimization studies in process engineering have to be performed within a multiobjective framework, where some objectives related to environmental impacts, security, etc., must be simultaneously optimized with classical economic or technical criteria. In natural gas network optimization problems a lack of published works on multiobjective optimization can be observed, and this thesis aims at filling this gap. So this topic will be the main purpose of the present study. In the following chapter, the most commonly used approaches in multiobjective optimization (scalarization and evolutionary procedures) are reviewed and three specific algorithms (Weighted-sum, ε-constraint and Genetic algorithm) are detailed. On the basis of two mathematical problems and four multiobjective chemical engineering problems, the choice of the best procedure, namely the Genetic algorithm, will be performed in Chapter 5. Then in the first part of Chapter 5, the didactic network is optimized according to two objectives: the fuel consumption in compression stations and the mass load of gas delivery. In the second part, this didactic network is considered again for hydrogen transportation, and three objectives are taken into account: the fuel consumption in compression stations, the mass load of gas delivery and the percentage of injected hydrogen into the network.

Multiobjective optimization methods

3

Contents

1 Introduction

As shown in Chapter 2, the natural gas network system can be formulated as a multiobjective optimization problem. In many other engineering fields, most of process optimization problems became multiobjective optimization ones. When dealing with process optimization, the current trend is to consider other objectives besides the traditional economic criterion, related to sustainability, environment and safety. So, this chapter deals with the most commonly used multiobjective methods in chemical engineering. Two mathematical examples are presented as comparison purposes. Then, from the basis of well-known chemical engineering problems, the choice of the multiobjective optimization algorithm is performed in Chapter 4.

Among the diversity of multiobjective optimization methods, two important classes have to be distinguished: first scalarization approaches, second genetic and evolutionary methods. Complete reviews are proposed in literature for both classes [Hao et al., 1999; Grossmann, 2002; Biegler and Grossmann, 2004]. A thorough analysis of both classes was previously studied by Ponsich [2005] with the support of batch plant design problems.

The first class, namely deterministic methods, assumes the verification of mathematical properties of the objective function and constraints, such as continuity, differentiability and convexity. In practice, these assumptions (particularly convexity) do not always hold, and the convergence towards a global optimum is no longer guaranteed. This working mode enables only to ensure to get a local optimum, what is a great advantage versus stochastic methods.

The second class, namely stochastic methods, is based on the evaluation of the objective function at different points of the search space. These points are chosen through a set of heuristics, combined with generations of random numbers. Thus, stochastic procedures cannot guarantee to obtain an optimum. However by allowing occasional objective function increases (for minimization problems) they may go out of local optimum gaps. Even if stochastic methods do not require any mathematical property for the objective function and constraints, they may be difficult to implement for problems involving a significant number of equality constraints.

Besides, the efficiency of a given method for a particular example is hardly predictable, and the only certainty we have is expressed by the *No Free Lunch*

(NFL) Theory [Wolpert and Macready, 1997]: there is no method that outdoes all the other ones for any considered problem. This feature generates a common lack of explanation concerning the use of a method for the solution of a particular example. Several works were carried out on the *NFL*: Droste et al. [2002] show that each heuristic which is able to optimize some functions efficiently follows some ideas about the structure of considered functions in black-box optimization; Griffiths and Orponen [2005] study the *NFL* in the framework of Boolean functions; Service [2010] generalizes the *NFL* theorem to non totally ordered objectives spaces. However, for any particular application, the resolution strategy has to be selected in one of the two classes of methods.

This chapter recalls three classical types of procedures used in multiobjective optimization. The choice of the most adequate method will be performed in the next chapter, where several chemical process optimization problems are studied. The present chapter is organized as follows. First, the general properties of a multiobjective problem are presented. Then, three classical solution procedures (Weighted-sum, ε-constraint and Evolutionary procedures) are recalled. More precisely, three algorithms (Adaptive Weighted-Sum, Augmented ε-Constraint and *NSGA-IIb*) are described. Finally, two mathematical problems are solved for performing a preliminary comparison of the three algorithms.

2 General properties of a multiobjective constrained optimization problem

2.1 A general definition of optimality for multiobjective problems

Like many real world examples, the problem under consideration involves several competing measures of performance, or objectives [Collette and Siarry, 2002].

General Abbreviations

Abbreviation	Meaning
AUGMECON	Augmented ε-Constraint
AWS	Adaptive Weighted-Sum
GA	Genetic Algorithm
GRG	Generalized Reduced Gradient
MGA	Multiobjective Genetic Algorithm
MINLP	Mixed Integer Non Linear Programming
MOGA	MultiObjective Genetic Algorithm
MOSA	MultiObjective Simulated Annealing
MOOP	MultiObjective Optimization Problem
NFL	No Free Lunch
NLP	Non Linear Programming
NPGA	Niched Pareto Genetic Algorithm
NSGA	Non dominated Sorting Genetic Algorithm
RHS	Right-Hand-Side
SQP	Successive Quadratic Programming
VBA	Visual Basic for Applications
WS	Weighted-Sum
ε-C	ε-Constraint

Table 3.1: Nomenclature of the multiobjective optimization.

A *MOOP* can be formulated as shown in Equation 3.1. Each $f_i(x)$ may be nonlinear, but also discontinuous with respect to some components of the general decision variable x in an *n-dimensional* universe X.

$$Min \;\; F(x) = \left[f_1(x), f_2(x), ..., f_p(x)\right]^T \tag{3.1}$$

$$x \in X \subset R^{n'} \times N^{n''} \tag{3.2}$$

$$n = n' + n'' \tag{3.3}$$

This formulation (Equations 3.1 to 3.3) holds for general mixed problems, involving continuous and integer variables (n is the total number of variables). When integer variables are boolean ones, the set N is restricted to $[0, 1]$.

The subspace X is defined by a set of equality-inequality constraints (linear or nonlinear) and bounds on variables:

$$\begin{aligned} X \;\; = \;\; & \{x \in R^{n'} \times N^{n''} / g_i(x) \leq 0,\; i = 1 \; to \; n_1;\; r_j(x) < 0,\; j = 1 \; to \; n_2; \\ & h_k(x) = 0,\; k = 1 \; to \; n_3;\; l_i \leq x_i \leq u_i\} \end{aligned} \tag{3.4}$$

In a *MOOP*, the concept of optimality is replaced with that of efficiency or Pareto optimality. The efficient (or Pareto optimal, non dominated, non-inferior) solutions are the solutions that cannot be improved in one objective function without deteriorating their performance in at least one of the rest. The mathematical definition of an efficient solution (x^*) is the following:

$$f_i(x) \leq f_i(x^*) \ \ \forall \ \ i \in \{1, ..., p\} \tag{3.5}$$

A feasible solution (x^*) of a *MOOP* is efficient (non dominated), if there is no other feasible solution (x) such as shown in Equation 3.5 with at least one strict inequality. If we replace the large inequality in Equation 3.5 by a strict inequality, we obtain the weakly efficient solutions. Weakly efficient solutions are not usually pursued in *MOOP* because they may be dominated by other efficient solutions. The set of non dominated solutions constitute the Pareto front. The Pareto front can be viewed as an equilibrium curve composed of *good* solutions for the *MOOP*, i.e., the set of problem solutions among which the decision maker has to perform his choice. Branke et al. [2004] and Taboada and Coit [2006] suggest picking the knees in the Pareto front, that is to say, solutions where a small improvement in one objective function would lead to a large deterioration in at least one other objective. Several other methods can be found in the literature; they are discussed in Chapter 5.

2.2 Constraint handling in evolutionary methods

Constrained multiobjective optimization is the most common kind of problem in engineering applications. When implementing scalarization methods, the problem related to constraints does not arise. The constraints are directly treated by the *MINLP* solver. In the case of continuous problems considered in this study (no integer or binary variables, $n'' = 0$) the solver is a *NLP*, generally based on a *SQP* or a *GRG* strategy. However for evolutionary procedures, each solution generated from an elementary move can be unfeasible with regard to a constraint set. In general, three types of constraints are considered (Equation 3.6):

simple inequality ($\leq$), strict inequality ($<$), and equality ($=$).

$$\left.\begin{array}{l} g(x) \leq c1 \\ r(x) < c2 \\ h(x) = c3 \end{array}\right\} \Leftrightarrow \left\{\begin{array}{l} constr1(x) = c1 - g(x) \geq 0 \\ constr2(x) = c2 - r(x) > 0 \\ constr3(x) = c3 - h(x) = 0 \end{array}\right. \tag{3.6}$$

Where (g, r, h) are real-valued functions of a decision variable $x = (x_1, \ldots, x_n)$ on the *n-dimension* decisional search space X, and (c_1, c_2, c_3) are constant values. In the more general case, these constraints are written as vectors of the type :

$$\begin{array}{lcl} \vec{constr1}(x) & = & ((c1 - g(x))_1, \cdots, (c1 - g(x))_{n1}) = (contr1(x)_1, \cdots, contr1(x)_{n1}) \geq 0 \\ \vec{constr2}(x) & = & ((c2 - r(x))_1, \cdots, (c2 - r(x))_{n2}) = (contr2(x)_1, \cdots, contr2(x)_{n2}) > 0 \\ \vec{constr3}(x) & = & ((-|c3 - h(x)|)_1, \cdots, (-|c3 - h(x)|)_{n3}) = (contr3(x)_1, \cdots, contr3(x)_{n3}) = 0 \end{array} \tag{3.7}$$

Where $n_1, n_2,$ *and* n_3 are respectively, the number or inequality, strict inequality and equality constraints. This constraint formulation implies that each constraint value will be negative if and only if this constraint is violated. The conversion of Equation 3.6, that is a classical representation of constraint sets, to Equation 3.7 constitutes the first step of an unified formulation of constrained-optimization problems. In practice, due to round-off error on real numbers, the equality constraint $\vec{constr3}$ was modified as shown in Equations 3.8 & 3.9.

$$\vec{constr3}(x) = (-|c3 - h(x)|_1 + \epsilon_1, \cdots, -|c3 - h(x)|_{n3} + \epsilon_{n3}) = \vec{contr3}(x) + \vec{\epsilon} \tag{3.8}$$

$$\vec{\epsilon} = (\epsilon_1, \cdots, \epsilon_{n3}), \forall i \in \{1, \cdots, n3\}, \epsilon_i \in R \tag{3.9}$$

$\vec{\epsilon}$ is called a precision vector of the equality vector, and takes low values (less than 10^{-6} for example). This approximation is not necessary when equality constraint involves only integer or binary variables. From Equation 3.9, the constraint satisfaction implies the maximization of violated constraints in vectors $\vec{constr1}$, $\vec{constr2}$, and $\vec{constr3}$. According to Fonseca and Fleming [1998], the satisfaction of a number of violated constraints is, from Equation 3.7, a multiobjective minimization problem. From a theoretical point of view, a constrained multiobjective optimization problem can be formulated as a two-step optimization problem. The first step implies the comparison of constraint satisfaction degrees between two solutions, using the Pareto's domination defined by Equation 3.5, but a more simple solution consists in comparing the

sum of values of violated constraints only, as in *NSGA-II* algorithm of Deb et al. [2002], which implies there are no priority rules between constraints. This step is performed first, before the second one which concerns the comparison of the objective function vectors.

3 General Multiobjective Optimization methods

3.1 Weighted-sum method *(WS)*

Historically, the first method for solving *MOOPs* is the *WS* method. The method transforms multiple objectives into an aggregated single objective function by multiplying each objective function by a weighting factor and summing up all weighted objective functions. So, the minimization problem is transformed as shown in Equations 3.10 to 3.12:

$$Min \;\; F_w = \omega_1 f_1 + \omega_2 f_2 + ... + \omega_p f_p \tag{3.10}$$

$$0 \leq \omega_i \leq 1 \tag{3.11}$$

$$\sum_{i=1}^{p} \omega_i = 1 \tag{3.12}$$

In Equation 3.10, ω_i is a weighting factor for the (i) objective function (f_i). Due to Equations 3.11 & 3.12, the *WS* is said to be convex. Each single objective optimization determines one particular optimal solution point on the Pareto front. The *WS* method then changes weights systematically, and each different single objective optimization determines a different optimal solution. The solutions obtained approximate the Pareto front.

Initial works on *WS* method can be found in Zadeh [1963]. Oski [1988] applied the *WS* method to structural optimization. Li and Guangwen [1990] used the method to solve a river water quality management problem. Jin et al. [2001] proposed a dynamic weighted aggregation for evolutionary multiobjective optimization. Kim and de Weck [2006] presented an Adaptive Weighted-Sum method *(AWS)* and Ding et al. [2006] described a normalization procedure for weighting factors.

3.2 ε-constraint method *(ε-C)*

In the *ε-C* method, one of the objective functions is minimized while all the other objective functions are upper bounded by introducing additional constraints. So the problem defined by Equations 3.1 to 3.3 is transformed into the following problem (f_k):

$$Min \;\; f_k(x) \tag{3.13}$$

$$x \in X \subset R^{n'} \times N^{n''} \tag{3.14}$$

$$f_i(x) \leq \varepsilon_i \;\; i = 1 \;\; to \;\; p, \;\; i \neq k \tag{3.15}$$

By parametric variation in the Right-Hand-Side *(RHS)* of the constrained objective functions (Equation 3.15), the efficient solutions of the problem can be obtained. The method was first presented by Chankong and Haimes [1983].

In practical applications, it may be very difficult to select the initial design values inside the feasible region. So in many works, the optimization is conducted successively; the previous optimization results are used as initial values for the current optimization. Hence, the solution time is increased linearly with the increased number of Pareto solutions. Kim et al. [1997] proposed to define initial values independently, and each Pareto solution can be found independently by using parallel processing. The initial vector (x_0) is defined as a convex combination of results of single optimization of each objective function of the problem. By changing the coefficients of the convex combination, various Pareto optimal solutions can be obtained.

In order to properly apply the *ε-C* method, the range of the *(p-1)* objective functions that are used as constraints must be known. The calculation of the range of the objective functions over the efficient set is not a trivial task [Isermann et al., 1988; Reeves and Reid, 1988]. While the best value is easily attainable as the optimum of the individual optimization, the worst value over the efficient set (Nadir value) is not. The most common approach is to calculate these ranges from the payoff table (the table with the results from the individual optimization of the p objective functions). From Figueira et al. [2005], the optimal solution of Equations 3.13 to 3.15 is guaranteed to be an efficient solution only if all the *(p-1)* objective function constraints are binding. To overcome this

difficulty, Mavrotas [2009] proposes the transformation of the objective function constraints to equalities by explicitly incorporating appropriate slack ($+S_i$) or surplus ($-S_i$) variables for minimization or maximization respectively. In the same time, the sum of these slack or surplus variables is used as a second term (with lower priority) in the objective function forcing the constraints on objective functions to be binding, so as to produce only efficient solutions. This proposed version of the ε-C method will be described in Section 4.2.1. A quite similar approach based on slack variables is presented in Ehrgott and Ruzika [2008].

3.3 Genetic and evolutionary methods

In this class of methods, the elements of the objective vector are kept separate throughout the optimization process; these approaches typically use the concept of dominance (Equation 3.5) to distinguish between dominated and non dominated solutions for passing from the current solution to the next one. An evolutionary procedure is a heuristic method for solving a large class of combinatorial problems by combining user-given black-box procedures whose derivatives are not available with heuristics, in order to obtain a good solution for the problem. Some heuristics maintain at any time a single current state, and replace that state by a new one (transition state or move). Heuristics often work on pool of states containing several candidate states. The new states (evolution) are generated by combination or crossover of two or more states of the pool. Since 1975, many evolutionary procedures have appeared. For example, one can cite genetic algorithms [Holland, 1975; Chafekar et al., 2005], simulated annealing [Kirkpatrick et al., 1983], artificial immune systems [Farmer et al., 1986], ant colonies [Dorigo, 1992], particle swarms [Kennedy and Eberhart, 1995], artificial bee colonies [Nakrani and Tovey, 2004] and artificial neural networks [Ang et al., 2007].

All these algorithms can be adapted to the multiobjective case, as it can be observed in the list of references proposed by Coello Coello [2009]. Recently, Coello and Becerra [2009] indicate the most representative evolutionary algorithms in the fields of materials science and engineering, and give some potential areas for future research in these domains. They distinguish three main classes of *MGA*: *MOGA* where the rank of an individual corresponds to the num-

ber of individuals in the current population by which it is dominated [Fonseca et al., 1993]; *NSGA* where several layers of classifications of the individuals are established on the basis of non domination [Srinivas and Deb, 1994]; *NPGA* where a binary tournament selection scheme based on Pareto domination is used [Horn et al., 1994]. The book of Deb [2001] presents several performance metrics for convergence, metrics for diversity, and metrics for both convergence and diversity. Obayashi et al. [1999] published the Proceedings of the 4^{th} International Conference on Evolutionary Multi Criterion Optimization held in Matsushima (Japan, March 2007) and gave a good review of the domain. Another recent evolution concerns the evolutionary neural networks that evolve their architecture through multiobjective genetic algorithms as a Pareto trade-off between the accuracy of training and the problem complexity [Pettersson et al., 2007, 2009].

The two most popular methods in the chemical engineering field are *MGA* [Konak et al., 2006], and *MOSA* [Shu et al., 2004; Smith et al., 2004; Bandyopadhyay et al., 2008]. None of these two methods is perfect and selecting one depends on the requirements of the particular situation considered. From the literature survey [Deb et al., 2002; Branke et al., 2004; Turinsky et al., 2005; Mansouri et al., 2007], it appears that *MGA* is generally preferred to *MOSA*. One of the most efficient genetic algorithm is *NSGA-II* [Deb et al., 2002], an upgrade of *NSGA* which estimates the density of solutions surrounding a particular solution. From Coello and Becerra [2009], its performance is so good, that it has gained a lot of popularity in the last few years.

4 Solution procedures

4.1 Adaptive Weighted-sum

4.1.1 A procedure for implementing the Weighted-sum method: *AWS* algorithm

In this section, a classical Weighted-sum *(WS)* procedure with a convex combination of objective functions is implemented. This procedure is an improvement of the one proposed by Kim and de Weck [2005]. The so-called, Adaptive Weighted-Sum *(AWS)* method, is briefly presented for a biobjective problem. For

convex Pareto fronts, the *AWS* procedure allows to obtain a front with a given density of multiobjective solutions. However, in the case of non-convexity, the secant line between the points P_1 and P_2 does not over-estimate the Pareto front (Figure 3.1(a)) and the method can fail. So, on a theoretical point of view, the *AWS* procedure is restricted to convex Pareto fronts. All basic steps of the procedure are recalled in what follows.

Nomenclature

Symbol	**Meaning**
C	Constant
J	Objective function
$\bar{J}$	Normalized objective function
l	Length
$\bar{l}$	Average length
n	Number of divisions or refinements
x	Solution vector
Greek letters	
δ	Offset distance
Δ	Uniform step size
ϵ	Prescribed distance
θ	Angle
λ	Weighting factor
Subscripts	
s	Segment
Superscripts	
$i*$	Optimal solution vector
N	Nadir point
U	Utopia point

Table 3.2: Nomenclature of the *AWS* method.

Step 1: Perform a multiobjective optimization using the classical *WS* approach with a small number of divisions. The uniform step size of the weighting factor is determined by the number of divisions:

$$\Delta\lambda = \frac{1}{n_{initial}} \tag{3.16}$$

By using a large step size on the weighting factor, a small number of solutions are obtained.

Step 2: Compute the lengths of the segments between all the neighboring solutions. Delete nearly overlapping solutions. Overlapping occurs often whereas several nearly identical solutions are obtained. The Euclidian distances between

these solutions are nearly zero, and among these, only one solution is needed to represent the Pareto front. In the computer implementation, if the distance among solutions is less than a prescribed distance (ε), then all solutions except one are deleted.

Step 3: Determine the number of further refinements (additional number of divisions) in each of the regions. The longer the segment is, the more it needs to be refined. The refinement is determined based on the relative length of the segment:

$$n_s = round\left(C\frac{l_s}{\bar{l}_s}\right) \tag{3.17}$$

In Equation 3.17, n_s is the number of further refinements for the segment, l_s is the length of the segment, $\bar{l}_s$ is the average length of all the segments, and C is a constant of the algorithm *(C=1)*. The function *(round)* rounds off to the nearest integer.

Step 4: If n_s is zero or one, no further refinement is carried out in the segment. For other segments whose number of further refinements is greater than one, go to the following step.

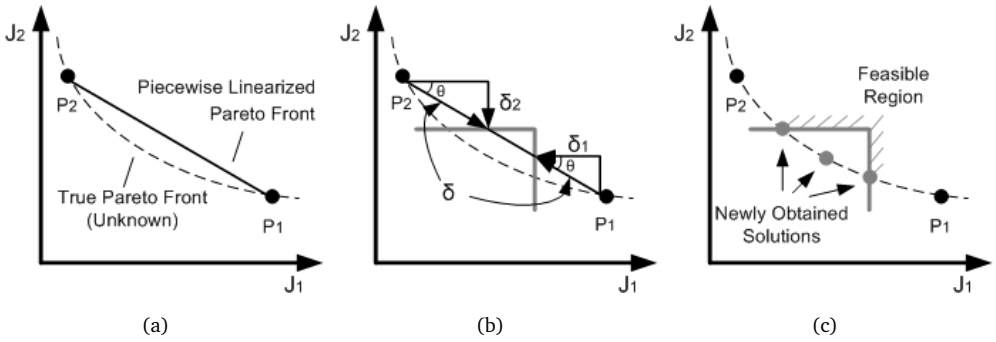

Figure 3.1: Determining the offset distances, δ_1 and δ_2, based on δ.

Step 5: Determine the offset distances from the two end points of each segment. First, a piecewise linearized secant line is built by connecting the end points, P_1 and P_2, as shown in Figure 3.1(a). Then, the user selects the offset distance (δ) along the piecewise linearized Pareto front. The offset distance, δ, determines the final density of the Pareto solution distribution, because it becomes the maximum segment length during the last phase of the algorithm. In order to find the offset distances parallel to the objective axes, the angle θ in

Figure 3.1(b) is computed as:

$$\theta = tan^{-1}\left(-\frac{P_1^y - P_2^y}{P_1^x - P_2^x}\right) \tag{3.18}$$

Where P_i^x and P_i^y are the x (J_1) and y (J_2) positions of the end points, P_1 and P_2, respectively. Then, δ_1 and δ_2 are determined with δ and θ as follows:

$$\delta_1 = \delta cos\theta \tag{3.19}$$

$$\delta_2 = \delta sin\theta \tag{3.20}$$

Step 6: Impose additional inequality constraints and then conduct sub-optimization with the *WS* method in each of the feasible regions. As shown in Figure 3.1(b), the feasible region is offset from P_1 and P_2 by the distance of δ_1 and δ_2 in the direction of J_1 and J_2. Performing sub-optimization in this region, the problem is stated as:

$$Min\left[\lambda J_1(x) + (1-\lambda)J_2(x)\right] \tag{3.21}$$

$$J_1(x) \leq P_1^x - \delta_1 \tag{3.22}$$

$$J_2(x) \leq P_2^y - \delta_2 \tag{3.23}$$

$$h(0) = 0, \quad g(x) \leq 0, \quad \lambda\epsilon[0,1] \tag{3.24}$$

Where δ_1 and δ_2 are the offset distances obtained in Step 5, P_i^x and P_i^y are the x and y position of the end points. The uniform step size of the weighting factor for each feasible region is determined by the number of refinements, n_s, obtained in Step 3:

$$\Delta\lambda_s = \frac{1}{n_s} \tag{3.25}$$

The segments in which no converged optimal solutions are obtained are removed from the segment set for further refinement, because in this case these regions are non-convex and do not contain Pareto optimal solutions.

Step 7: Compute the length of the segments between all the neighboring solutions. Delete nearly overlapping solutions. If all the segment lengths are less than a prescribed maximum length, δ, terminate the optimization procedure. If there are segments whose lengths are greater than the maximum length, go to Step 3 and iterate.

AWS ALGORITHM

As indicated above, the *AWS* procedure can fail on non-convex Pareto fronts. This new method can effectively solve multiobjective optimization problems whose Pareto front has: (i) convex regions with non-uniform curvature, (ii) non-convex regions of non-dominated solutions, and (iii) non-convex regions of dominated solutions. The so-called *AWS* algorithm is based on the work of Kim and de Weck [2005]. The issue of controlling values of various parameters of an algorithm is one of the most important and critical area of calculation: it has the potential of adjusting the algorithm to solve a particular problem. Note that the solver *fmincon* of MATLAB toolbox (version *R2008a*) was used in the method implementation.

4.1.2 Parameters of the algorithm

The current description and values of the algorithm tuning parameters are indicated in Tables 3.3 & 3.4. These values include the tuning parameters of all the chemical engineering problems performed in Chapters 4 & 5.

Tuning parameters description

Parameter	Description
nInitial	Initial number of solutions (solving by *WS* method)
loop	Sub-optimization number (solving by *AWS* method)
c1,2	Optimization criterion for the objectives. All functions must be *cmin* because of *fmincon* function always minimizes
exitflag1,2	Describe the exit condition *(exitflag)* of *fmincon*. It means the convergence status described in MATLAB
Refinement	Determine the algorithm ending by limiting the number of further refinements in each of the regions.
C	A constant value that determines the Refinements number in each region
ED	Delete nearly overlapping solutions according to this condition: *Euclidian Distance* $<$ *ED*
delta	Determine the final density of the Pareto solution (Figure 3.1(b))
tolerance	Nominal tolerance authorized in the algorithm

Table 3.3: Tuning parameters description of the *AWS* algorithm.

Parameter	Range of values
nInitial	10 - 20
loop	10 - 50
c1,2	*cmin*
exitflag1,2	1 and 2
Refinement	1
C	1
ED	10^{-10} - 10
delta	0.01 - 10^4
tolerance	10^{-10}

Table 3.4: Tuning parameters values of the *AWS* algorithm.

4.2 Augmented ε-constraint

4.2.1 A procedure for implementing the ε-constraint method: *AUGMECON* algorithm

In this section, a classical ε-constraint *(ε-C)* procedure is implemented. This classical procedure has been improved based on the work of Mavrotas [2006]. The so-called *AUGMECON* method is briefly presented for a biobjective problem. All basic steps of the procedure are recalled in what follows.

Nomenclature

Symbol	Meaning
f	Objective function
q	Equal intervals
r	Range of the objective function
$+S$	Slack variable
$-S$	Surplus variable
ε	Parametrical variation

Table 3.5: Nomenclature of the *AUGMECON* method.

The *AUGMECON* method uses slack or surplus variable ($\pm S_i$) as shown in [Mavrotas, 2006]. The classical formulation given by Equations 3.13 to 3.15 is replaced by:

$$Min \left[f_k(x) + \varepsilon_i \times \sum_{i=1}^{p(i\neq k)} \frac{S_i}{r_i} \right] \tag{3.26}$$

$$n = n' + n'' \tag{3.27}$$

$$g_i(x) = \ f_i(x) + S_i = \varepsilon_i \ \ where \ \ i = 1 \ \ to \ \ p, i \neq k \tag{3.28}$$

$$S_i \in R^+, \ \ r_i \in R \tag{3.29}$$

In order to avoid any scaling problems, it is recommended to replace the slack or surplus variable ($\pm S_i$) in the second term of the objective function by S_i/r_i, where r_i is the range of the *ith* objective function (calculated from the payoff table). By parametrical variation in the *RHS* of the constrained objective functions (ε_i), efficient solutions to the problem can be obtained.

Practically, this *AUGMECON* method is implemented as follows: from the payoff table [Mavrotas, 2006], the range of each one of the *(p-1)* objective functions that are going to be used as constraints can be determined. Then the range of the *ith* objective function is divided into q_i equal intervals using intermediate equidistant grid points. Thus we have $(q_i + 1)$ grid points that are used to vary parametrically the *RHS* (ε_i) of the *ith* objective function. If the first objective is chosen *(k=1)* as the objective function and the other f_i *(i=2 to p)* considered as constraints, the total number of runs becomes $(q_2+1) \times (q_3+1) \times \ldots \times (q_p+1)$. An interesting characteristic of this *AUGMECON* method is that the

density of the Pareto front can be tuned by properly assigning the values to the q_i. The higher the number of grid points the more dense is the representation of the efficient set, but the higher is the computational time. A trade-off between the density of the efficient set and the computation time is always advisable.

AUGMECON ALGORITHM

The *AUGMECON* procedure can solve multiobjective optimization problems that produces only efficient solutions (no weakly efficient solutions). The so-called *AUGMECON* algorithm is based on the Mavrotas [2006]. Similar to the *AWS* method, the issue of controlling values of various parameters of an algorithm is one of the most important and critical area of calculation. Note that, as in the previous case, the solver *fmincon* of MATLAB toolbox was used.

4.2.2 Parameters of the algorithm

The current description and values of the algorithm tuning parameters are indicated in Tables 3.6 & 3.7. These values include the tuning parameters of all the chemical engineering problems performed in Chapter 4 & 5.

Tuning parameters description

Parameter	Description
nSolution	Final number of solutions
NadirPoint	The worst value (Range 1) of f_i
UtopiaPoint	The best value (Range 2) of f_i
exitflag1,2	Describe the exit condition *(exitflag)* of *fmincon*. It means the convergence status described in MATLAB

Table 3.6: Tuning parameters description of the *AUGMECON* algorithm.

Parameter	Value
nSolution	100
NadirPoint	Depending on problem
UtopiaPoint	Depending on problem
exitflag1,2	1 and 2

Table 3.7: Tuning parameters values of the *AUGMECON* algorithm.

4.3 Evolutionary procedure: *NSGA-IIb*

4.3.1 A procedure for implementing the genetic algorithm: *NSGA-IIb*

Concerning evolutionary procedures reviewed at Section 3.3, Multiobjective Genetic Algorithms *(MGA)* are generally preferred in the chemical engineering community, so genetic algorithms *(GA)* have been retained in this work for solving the *MOOP*. These procedures belong to the genetic algorithm library *(MULTIGEN)* recently developed in Gomez et al. [2010]. The *MULTIGEN* tools, written in Visual Basic for Applications *(VBA)*, use *Excel* sheets as interface. The use of *VBA* was imposed by the industrial partner *(CEA: Commissariat à l'Energie Atomique, French agency of nuclear studies and applications)* when the *MULTIGEN* library was developed [Gomez et al., 2010]. The *MULTIGEN* library involves several algorithms, distinguishing them by their structure and by their type of variables (continuous, integer, binary); eight different algorithms are now available. The aim was to treat multiobjective constrained optimization problems involving mixed variables (boolean, integer, real), where some of these problems can be structural optimization ones [Gomez et al., 2010].

According to all the previous items mentioned in Section 3.3, *NSGA-II* [Deb et al., 2002] was chosen as a basis of development of the *MULTIGEN* library. The step-by-step procedure is illustrated in Figures 3.2 to 3.4 showing the use of dominance concepts in the procedure implementation. Its principles are now briefly summarized in what follows.

Initially, a random parent population P_0 of size N is created. The population is sorted based on the non domination principle. At each individual is assigned a fitness (or rank) equal to its non domination level (1 is the best level, 2 is the next-best level, and so on). Thus, maximization of fitness can be performed. At first, the usual binary tournament selection, recombination and mutation operators are used to create an offspring population Q_t of size N (Figure 3.2). Since elitism is introduced by comparing current population with the previously best found non dominated solutions, the procedure is different after the initial generation.

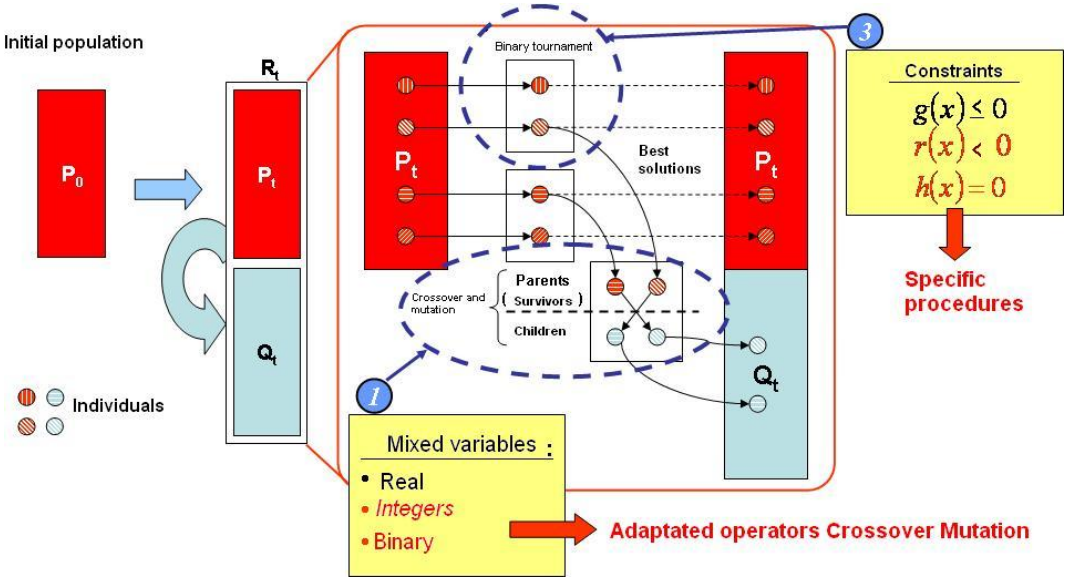

Figure 3.2: Operating principle of the *NSGA-II* (Part 1) [Gomez, 2008].

First, a combined population $R_t = P_t \ U \ Q_t$ is formed (Figure 3.3). The population R_t is of size $2N$. Then, the population is sorted according to non domination. If the size of F_1 (set of individuals of rank 1) is smaller then N, we definitely choose all members of the set F_1 for the new population P_{t+1}. The remaining members of the population P_{t+1} are chosen from subsequent non dominated fronts in the order of their ranking. Thus, solutions from the set F_2 are chosen next, followed by solutions from the set F_3, and so on. This procedure is continued until no more sets can be accommodated. Say that the set F_l is the last non dominated set beyond which no other set can be accommodated. In general, the number of solutions in all sets from F_1 to F_l is greater than the population size.

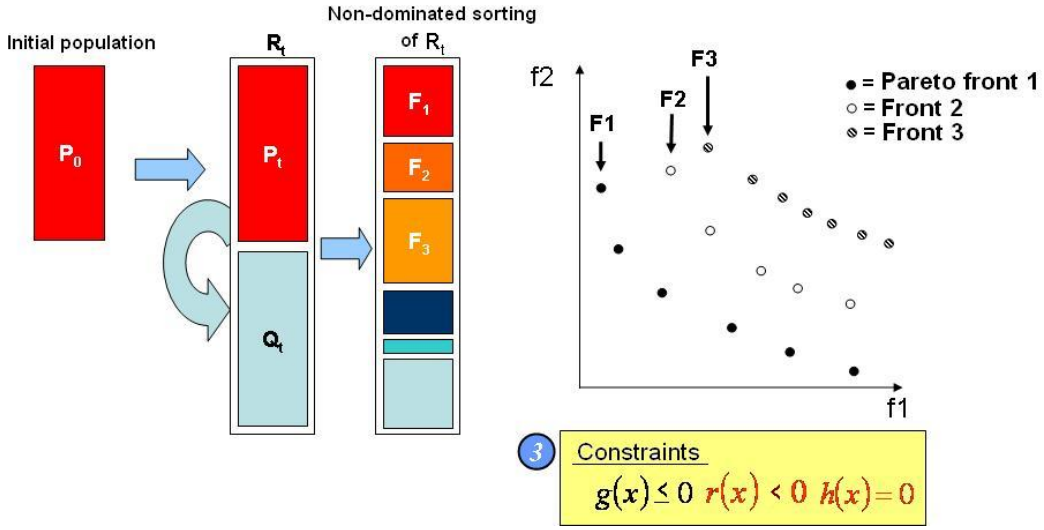

Figure 3.3: Operating principle of the *NSGA-II* (Part 2) [Gomez, 2008].

In order to choose exactly population members, we sort the solutions of the last front using the crowded-comparison operator in descending order and select the best solutions needed to fill all population slots. The new population P_{t+1} of size N is now used for selection, crossover and mutation to create a new population Q_{t+1} of size N. It is important to note that we use a binary tournament selection operator but the selection criterion is now based on the crowded-comparison operator. Since this operator requires both the rank and crowded distance of each solution in the population, these quantities are calculated while forming the population P_{t+1}, as shown in Figure 3.4.

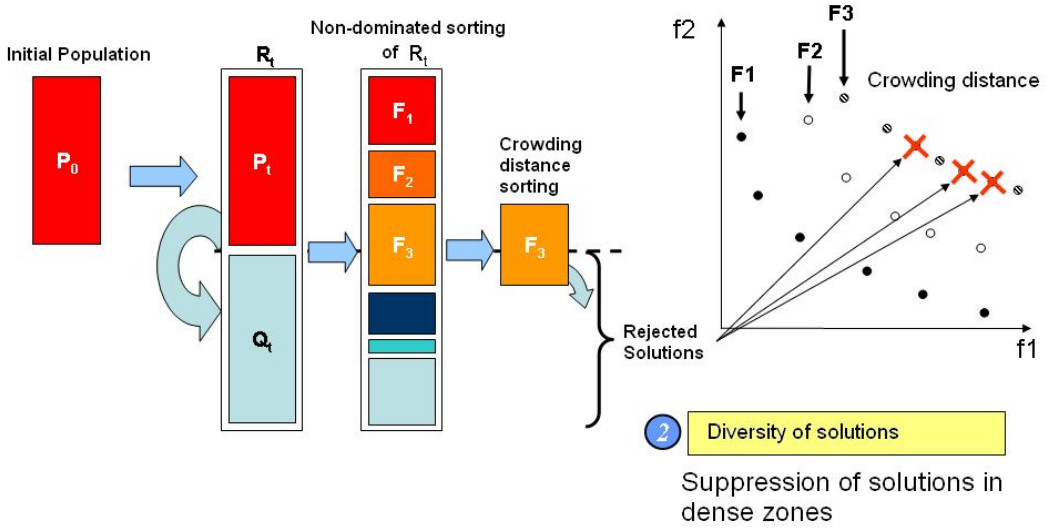

Figure 3.4: Operating principle of the *NSGA-II* (Part 3) [Gomez, 2008].

Because only continuous problems are considered in this work (n'' of discrete variables equals zero), the procedure *NSGA-IIb* of the *MULTIGEN* library has been retained. Compared with the well-known *NSGA-II* [Deb et al., 2002], new genetic operators are introduced for limiting clones creation. The classical crossover operator *SBX* has been modified to produce children different from parents. The objective is to prevent unnecessary calculations for clones of existing solutions: all the solutions generated by the reproduction and mutation procedures are statistically different. The *MULTIGEN* library is described in detail in Gomez et al. [2010].

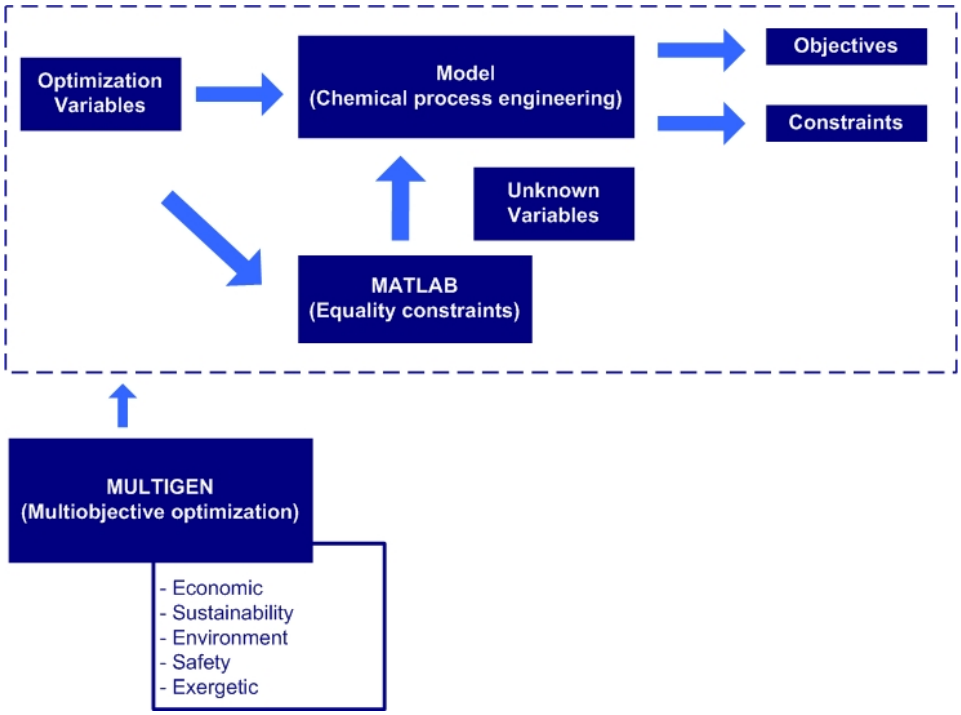

Figure 3.5: General algorithm coupling *NSGA-IIb*-MATLAB.

For a model (excluding the objective functions), involving n variables and m equality (linear or nonlinear) constraints ($m < n$), the analysis of degrees of freedom gives *(n-m)* independent variables. After scrutinizing the constraint set, these *(n-m)* decision variables can be chosen. For each evaluation of an objective function, the system of m equations must be solved. It is solved at each move of *NSGA-IIb* by the Newton-Raphson procedure *(fsolve)* of the MATLAB toolbox, and the squared accuracy is much lower than 10^{-6} (Figure 3.5). However the Newton-Raphson procedure must be correctly initialized, this is the reason why the time for finding the initial guess in the *GA* may be significant.

NSGA-IIb ALGORITHM

As already mentioned, the first algorithm coded in the *MULTIGEN* database is *NSGA-II* by Deb et al. [2002]. This elitist algorithm is based on a ranking procedure, where the rank of each solution is defined as the rank of the Pareto front to which it belongs. The diversity of non dominated solutions is guaranteed by using a crowding distance measurement, which is an estimation of the size of the largest cuboid enclosing a given solution without including any other.

This crowding sorting avoids the use of the sharing parameter as in the previous version of the *NSGA* algorithm.

Note that *NSGA-IIb*, which contains new genetic operators for clone creation limiting, implements the same algorithm than *NSGA-II*, with corrections on the crossover operator to avoid the creation of clones inherent of *SBX* original version. When the generated random number used to perform the crossover is greater than a given crossover probability, the crossover may produce two children identical to the parents: *SBX* crossover coded in *NSGA-IIb* includes a forced mutation of children when this event occurs.

4.3.2 Parameters of the algorithm

Concerning the interface developed, *MULTIGEN* uses a specific toolbar that is added to *Excel* default bars. There are three main phases in the process of optimizing a problem using *MULTIGEN*. The first step involves the generation of the interface that will encode the mathematical problem (Figure 3.6). The first column consists of the key arguments (green cells, Figure 3.6). These arguments are identified during the reading of the mathematical problem and allow *MULTIGEN* to identify necessary information. The set of instructions of *MULTIGEN* and their mode of use are detailed in Gomez [2008].

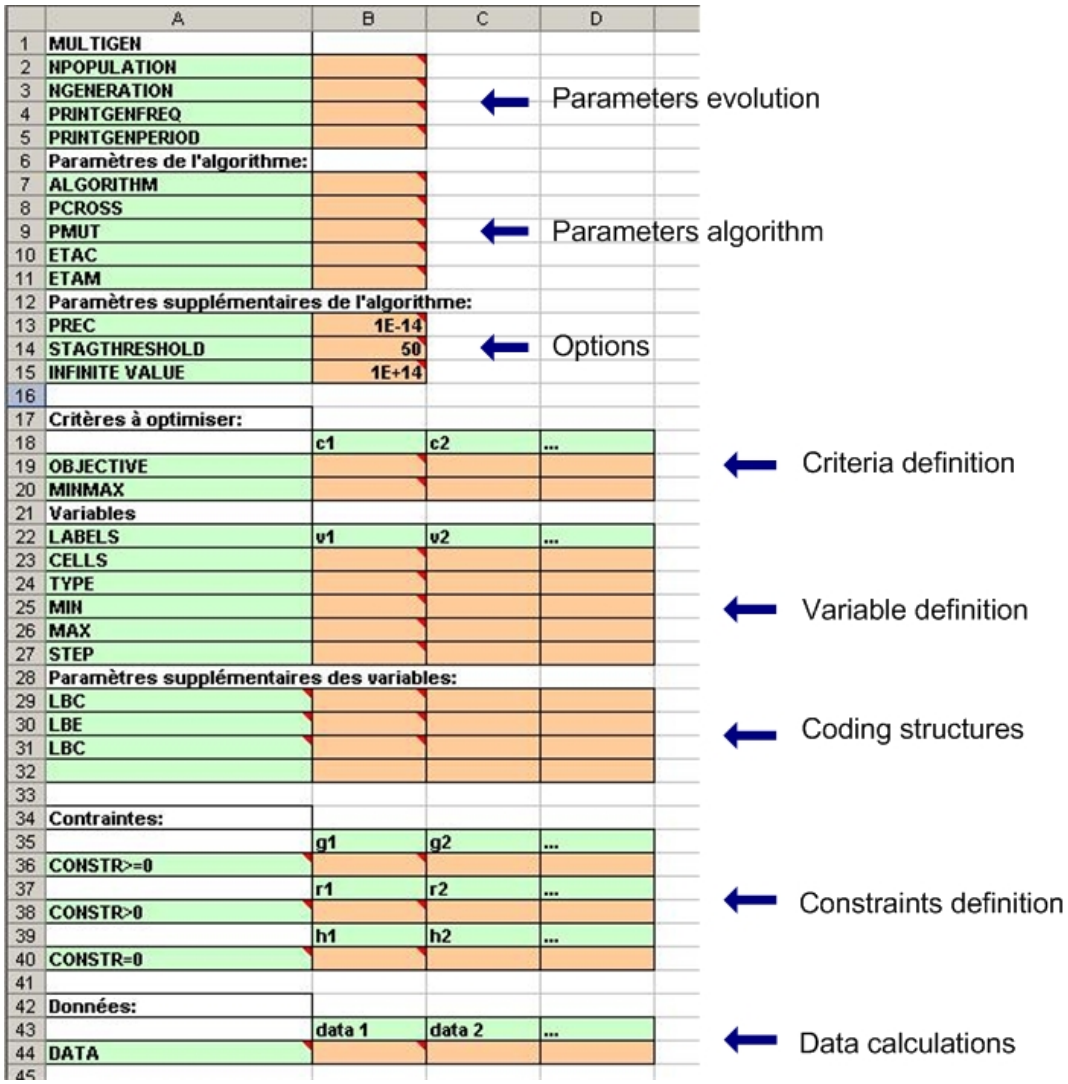

Figure 3.6: User interface in *MULTIGEN* (*Excel* sheet) [Gomez, 2008].

Once optimization is complete, the results are generated as well as the time calculation, the number of generations and individuals with the value of variables, criteria, constraints and data. The current values of the algorithm parameters are indicated in Table 3.8. These values include the tuning parameters of all the chemical engineering problems performed in Chapters 4 & 5. The tuning parameters description is performed in Gomez [2008].

Parameter	Value
NPOPULATION	100
NGENERATION	300
PRINTGENFREQ	10
PRINTGENPERIOD	300
ALGORITHM	3
PCROSS*	0.9
PMUT*	0.5

$*$ Proposed values by Gomez [2008]

Table 3.8: Tuning parameters values of the genetic algorithm: *NSGA-IIb*.

5 Mathematical examples

In this section the three procedures *AWS, AUGMECON* and *NSGA-IIb* are compared on two mathematical examples. All the computations were carried out on a processor *Intel Core Duo 2, 3 GHz, 2 GB of RAM*. The tolerances of the procedure *fmincon* of the MATLAB toolbox used in *AWS* and *AUGMECON* are fixed at their values per default, and 100 solutions are generated. The *GA* is implemented with 100 individuals per population, a crossover *SBX* with probability of 0.9, and a mutation probability of 0.5. As the *GA* is a random search randomly initialized, it is run 10 times for each problem. Among the generated Pareto fronts, that containing most points is retained.

5.1 Mavrotas problem

This linear problem was presented by Mavrotas [2009] for testing its implementation of the ε-*C* method.

$$Max\ f_1 = x_1 \tag{3.30}$$

$$Max\ f_2 = 3x_1 + 4x_2 \tag{3.31}$$

$$x_1 \leq 20 \tag{3.32}$$

$$x_2 \leq 40 \tag{3.33}$$

$$5x_1 + 4x_2 \leq 200 \tag{3.34}$$

In a first time, 60 generations were fixed in *NSGA-IIb*. As previously indicated, 100 solutions were generated with the three methods; the results are plotted in Figure 3.7, and the three fronts are plotted together in Figure 3.7(d). The problem being linear, the Pareto fronts must be linear; this is the case for *AUGMECON*, but not for the *GA* where only 12 solutions are found, nine of them being dominated by solutions of *AUGMECON*. This is probably due to a prema ture stopping of the search. The *AWS* method gives only the two extreme points of the Pareto front, which coincide with the extreme points of *AUGMECON*, any linear convex combination of these two points being a solution. This example shows that the *GA* provides slightly dominated solutions compared with *AUGMECON* and the Pareto front density is much better for *AUGMECON* than *AWS*. Furthermore, *AUGMECON* gives the same Pareto front as in Mavrotas [2009].

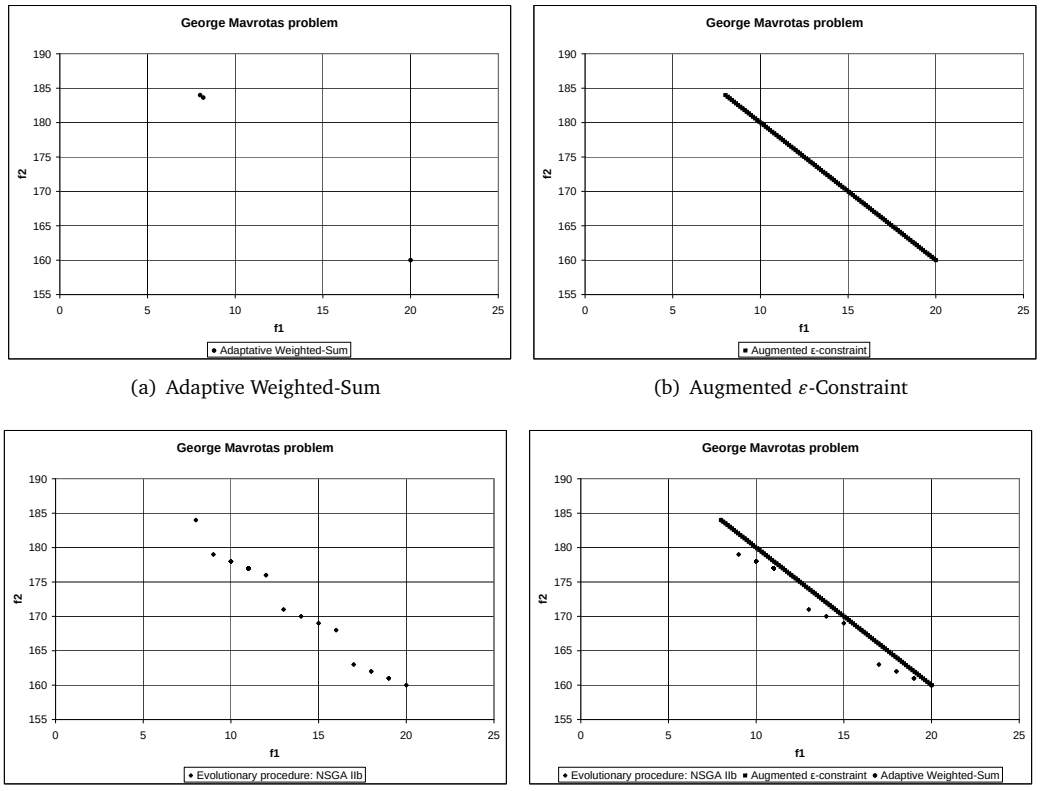

(a) Adaptive Weighted-Sum

(b) Augmented ε-Constraint

(c) Evolutionary procedure: NSGA-IIb

(d) Superimposed fronts

Figure 3.7: Solution of the Mavrotas problem.

Then the maximum number of generations in *NSGA-IIb* was increased up to 300, and the genetic algorithm gives the same Pareto front as *AUGMECON*. This numerical experiment shows that the maximum number of generations is a key parameter for the genetic algorithm. In the following example, as well as in Chapter 4, the maximum number of generations will be equal to 300.

5.2 TNK problem

This biobjective problem (two continuous variables and two inequality constraints) was first proposed in Tanaka et al. [1995], and involves discontinuities in the Pareto front. The problem is expressed as follows:

$$Min\ [f_1,\ f_2] \tag{3.35}$$

$$f_1(x_1, x_2) = x_1 \tag{3.36}$$

$$f_2(x_1, x_2) = x_2 \tag{3.37}$$

$$g_1(x_1, x_2) = -x_1^2 - x_2^2 + 0.1\ cos\left[16 \times arctan\left(\frac{x_1}{x_2}\right)\right] \leq 0 \tag{3.38}$$

$$g_2(x_1, x_2) = (x_1 - 0.5)^2 + (x_2 - 0.5)^2 \leq 0.5 \tag{3.39}$$

The Pareto fronts obtained from *AWS* and *GA* have similar shapes (Figure 3.8(a) and Figure 3.8(c)) than the one given in Tanaka et al. [1995], while the one from *AUGMECON* (Figure 3.8(b)) presents a gap at f_1 near 0.6 and f_2 near 0.8. Furthermore it involves fewer points than the two other fronts on the upper left side, but more points of the lower right side. *AUGMECON* method behaves as if it favours objective f_2 to the detriment of objective f_1. The three fronts are plotted together in Figure 3.8(d), where it can be observed that *AUGMECON* provides more points than the two other procedures at the end of the portions of curves.

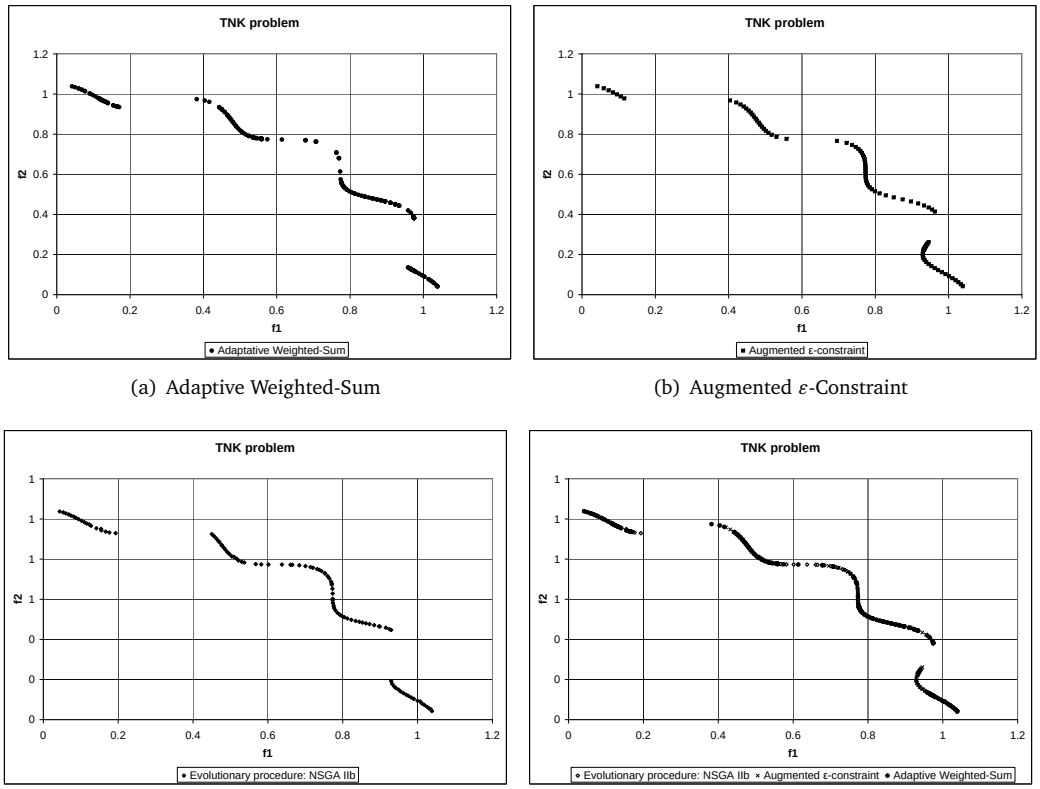

(a) Adaptive Weighted-Sum

(b) Augmented ε-Constraint

(c) Evolutionary procedure: NSGA-IIb

(d) Superimposed fronts

Figure 3.8: Solution of the TNK problem.

6 Conclusion

Three classical procedures for solving biobjective optimization problems were presented in this chapter. Two methods *(AWS and AUGMECON)* belong to the class of scalarization approach, and the third one *(NSGA-IIb)* is part of the evolutionary methods. From a popular classification, scalarization methods apply in well mathematically defined problems with explicit formulations of objectives and constraints, while genetic and evolutionary methods based on evolutionary strategies mainly apply in black-box problems, where objectives and/or constraints are returned by a computer code for each value of optimization variables. Besides the black-box problems, the possibility to mutate out of a local optimum and the ability to compute the entire Pareto front in one run, make also this type of methods attractive. However, these considerations do not al-

low choosing the most adequate method for solving the optimization problem related to natural gas networks.

From two small mathematical examples, it seems that *AUGMECON* and *NSGA-IIb* exhibit similar performances, while *AWS* is a little bit in the background. The only way for efficiently selecting the appropriate procedure is to carry on the trials on chemical engineering problems; this is the purpose of the following chapter.

Chemical process engineering test problems and choice of the solution procedure

4

Contents

1 Introduction

This chapter aims at studying the efficiency of classical multiobjective optimization methods in treating chemical engineering problems, in order to find the best class of method to solve multiobjective chemical engineering problems, often characterized by black-box formulations and/or large sets of nonlinear constraints. On the basis of four classical chemical engineering problems, this chapter gives a comparison of three methods: Weighed-sum *(WS)*, ε-constraint *(ε-C)* and an Evolutionary procedure implemented in a genetic algorithm *(GA)*, for solving multiobjective problems. The three methods were previously described in Chapter 3, where a literature analysis was carried out. This review is not intended to be comprehensive, but focuses on the most popular multiobjective methods. Let us note that, in the last years, a great attention was focused on monobjective optimization of chemical processes [Acevedo and Pistikopoulos, 1996; Kocis and Grossmann, 1987; Papalexandri and Dimkou, 1998], but few works were dedicated to multiobjective optimization of such processes.

The first example problem of the chapter is related to the classical Haber-Bosh process [Babu and Angira, 2005], where a nitrogen fixation reaction of nitrogen and hydrogen gases occur in a tubular reactor to produce ammonia, which is used for manufacturing fertilizers and explosives. The objectives to be maximized are both the annualized profit and safety by optimizing the reactor length and the inlet temperature of gases. The second one deals with the classical alkylation process [Rangaiah, 1985; Jones, 1995] wherein a light olefin reacts with isobutene to produce the alkylate which is used for blending with refinery products in order to increase their octane number. The problem consists in maximizing the profit while minimizing the isobutene recycle. The third illustration is the well-known Williams & Otto process [Williams and Otto, 1960], where the goal product (P) is produced into a continuous stirred tank reactor from two feeds in products A and B, followed by a separation step involving a decanter and a distillation column. For a given production capacity of product (P), the objectives are related to the minimization of the reactor volume and the minimization of the waste flow rate. The fourth example, known as Gas turbine cogeneration system *(GTCS)* problem, concerns the biobjective optimization of a thermal cogeneration system (electricity, saturated steam) made up of a gas turbine cycle with regeneration, and of a heat recovery steam generator for sa-

turated steam production [Valero et al., 1994; Lazzaretto and Toffolo, 2004]. The objectives are economic and exergetic ones.

An interesting question that one should keep in mind when comparing different procedures is related to the time spent in implementing the different methods before they are numerically compared. If a method is five percent faster than another one, but takes three times as long to implement and parameterize, it might not be worth the effort. Assuming that in all cases, the problem is already formulated in terms of objectives and constraints and that adequate solvers are available as well, the methods are compared in terms of both solution quality and resolution time, which embeds the following contributions:

- Tuning of solver parameters: this phase is often carried out by experience feedback gained by solver implementation and successive utilization,
- Searching for an adequate initial guess for the problem; as in the previous case, this step may require several executions of the solver,
- Time needed for fulfilling the solver input file(s) requiring the problem translation in the specific solver language (C, Fortran, Excel, MATLAB or another particular language as the one for example of the *GAMS* interface)
- *CPU* time

Obviously, excepted for *CPU* time, the other times given are unrefined estimations, they are there only to give general trends. In our knowledge, this type of study had never been reported in the field of multiobjective optimization in chemical engineering. The study of these times can seem of course debatable, because it heavily depends on the experience of the developer. The ideal situation would be to perform the study using several developers with different backgrounds, and to take the mean values, but it is out of the framework of this thesis. The only goal of this study is to draw some general trends, and not clear-cut conclusions.

In the following examples, all the computations were carried out on a processor *Intel Core Duo 2, 3 GHz, 2 GB of RAM*. The processor performances are about 15 *Mflops* either in MATLAB or in *VBA*, which can seem very low for such a processor; this value is very under the theoretical performances announced by *Intel*. However, our versions of *VBA* and MATLAB are interpreted languages,

and compared with compiled and optimized languages like *FORTRAN* or *C++*, the *CPU* times reported can seem to be excessively low.

In the scalarization methods, the tolerances of the procedure *fmincon* of the MATLAB toolbox used in *AWS* and *AUGMECON* are fixed at their values per default, and 100 solutions are generated for the Pareto fronts, so *AWS* and *AUGMECON* were run 100 times. On the other hand, the evolutionary method *(NSGA-IIb)* is implemented with 100 individuals per generation, 300 generations, a crossover *SBX* with probability of 0.9 and a mutation probability of 0.5. As the *GA* is a randomly initialized search, each problem is run 10 times for each problem. Among the Pareto fronts generated by the algorithm *NSGA-IIb*, that containing most points is retained (case 1). Indeed, sometimes the choice is quite difficult to perform. Another strategy would consist in merging the 10 fronts, and performing a Pareto sort on the final front (case 2). This strategy was implemented on each numerical example, and the same fronts as in the case 1 were found again.

Finally, some guidelines are given concerning the scalarization *(AWS, AUGMECON)* and evolutionary *(NSGA-IIb)* methods.

2 Ammonia synthesis reactor: Haber-Bosh process (HBP)

The synthesis reactor is treated as a separate unit with the aim of understanding its behavior and obtaining the key variables that lead to its stable and sustained optimum operation. We are interested mainly in predicting the reactor behavior when changes are made in the controllable variables and specifically in studying the variation of ammonia yield as a result of these changes. Thus, a mathematical model which predicts the trends of the reactor output and stability with reasonable accuracy, is required for the simulation.

Nomenclature

Symbol	Meaning
Cp	Heat capacity $(kcal/kg.K)$
fc	Catalyst activity
N	Flow rate $(kmol/h.m^2)$
p	Partial pressure
R	Ideal gas constant $(kcal/kmol.K)$
$S1$	Surface area of cooling tubes per unit length of reactor (m)
$S2$	Cross-sectional area of catalyst zone (m^2)
T	Temperature (K)
U	Overall heat transfer coefficient $(kcal/h.m^2.K)$
W	Total mass flow rate (kg/h)
x	Reactor length (m)
Greek letters	
κ	Rate constant
Others	
ΔH	Heat of reaction $(kcal/kmol\ \ N_2)$
$-\partial N_{N_2}/\partial x$	Reaction rate $(kmol\ \ N_2/h.m^3)$
Subscripts	
0	Reference
f	Feed gas
g	Reacting gas
H_2	Hydrogen
N_2	Nitrogen
NH_3	Ammonia
Superscripts	
0	Reference

Table 4.1: Nomenclature of the Ammonia synthesis reactor.

2.1 Ammonia synthesis reactor model

Ammonia is one of the most used chemical in industry for manufacturing a lot of products such as fertilizers, chemicals, explosives, fibers, plastics and cleaning products. It is produced from the reaction of hydrogen and nitrogen at high temperature and high pressures in a catalysed tubular reactor (Haber-Bosh process), according to the reaction shown in Equation 4.1. This exothermic reversible reaction is carried out in the ammonia synthesis tubular reactor.

$$N_2 + 3H_2 \Leftrightarrow 2NH_3 + \Delta H \ \ where: \ \ \Delta H = -92 \ \ kJ/mol \tag{4.1}$$

Any mathematical description of a chemical reactor basically relies on balance equations which express the general laws of conservation of mass and energy.

The model below can be derived by writing the Equations 4.2 to 4.9; all symbols used are listed in Table 4.1.

The energy balance for the feed gas is:

$$\frac{\partial T_f}{\partial x} = -\frac{US1}{WCp_f}\left(T_g - T_f\right) \tag{4.2}$$

The energy balance for the reacting gas is:

$$\frac{\partial T_g}{\partial x} = -\frac{US1}{WCp_g}\left(T_g - T_f\right) + \frac{(-\Delta H)S2}{WCp_g}\left(\frac{-\partial N_{N_2}}{\partial x}\right) \tag{4.3}$$

The balance for N_2 is:

$$\frac{\partial N_{N_2}}{\partial x} = -fc\left[\kappa_1 \frac{p_{N_2} p_{H_2}^{1.5}}{p_{NH_3}} - \kappa_2 \frac{p_{NH_3}}{p_{H_2}^{1.5}}\right] \tag{4.4}$$

$$\kappa_1 = 1.78954 \times 10^4 e^{(-20800/RT_g)} \tag{4.5}$$

$$\kappa_2 = 2.5714 \times 10^{16} e^{(-47400/RT_g)} \tag{4.6}$$

The partial pressures expressed in N_{N_2} are:

$$p_{H_2} = 3 \times p_{N_2} \tag{4.7}$$

$$p_{N_2} = 286\left[\frac{N_{N_2}}{2.598N_{N_2}^0 + 2N_{N_2}}\right] \tag{4.8}$$

$$p_{NH_3} = 286\left[\frac{2.23N_{N_2}^0 - 2N_{N_2}}{2.598N_{N_2}^0 + 2N_{N_2}}\right] \tag{4.9}$$

The boundary conditions are given by Equations 4.10 to 4.14:

$$T_f = T_0 \;\; at \;\; x = 0 \tag{4.10}$$

$$T_g = T_0 \;\; at \;\; x = 0 \tag{4.11}$$

$$N_{N_2} = 701.2 \ \ at \ \ x = 0 \tag{4.12}$$

$$1 \leq x \leq 15 \tag{4.13}$$

$$600 \leq T_0 \leq 675 \tag{4.14}$$

Symbol	Value
fc	1
Cp_f	0.707
Cp_g	0.719
$N^0_{N_2}$	701.2
R	1.987
$S1$	10
$S2$	0.78
U	500
W	26,400
ΔH	-26,000

Table 4.2: Fixed parameters of the Ammonia synthesis reactor.

2.2 Problem formulation

In the monobjective case (Equation 4.15), the function f to be maximized is based on the difference between the value of the produced gas (heating value and economic value) and the amortization of reactor capital cost. In this equation, x represents the reactor length and constitutes the decision variable for a given top temperature, T_0.

$$\begin{aligned} f(x, N_{N_2}, T_f, T_g) \ = \ & 1.33563 \times 10^7 - 1.70843 \times 10^4 N_{N_2} + 704.09(T_g - T_0) \\ & -699.27(T_f - T_0) - [3.45663 \times 10^7 + 1.98365 \times 10^9 x]^{\frac{1}{2}} \end{aligned} \tag{4.15}$$

This problem was extensively studied in the literature [Murase et al., 1970; Edgar and Himmelblau, 1970; Upreti and Deb, 1996; Babu and Angira, 2005], but all these papers contained typos on formulae. In this work, the recent formulation of Ksasy et al. [2010] is implemented. The three ordinary differential

equations (Equations 4.2 to 4.4) resulting from heat and mass balances and, giving T_f, T_g and N_{N_2} are solved by the module *ODE45* of the MATLAB toolbox.

By optimizing the reactor cost for four reactor top temperatures T_0 (580 K, 694 K, 706 K and 820 K), Ksasy et al. [2010] showed the existence of an optimum versus T_0. This study led us to consider the problem under a multiobjective optimization one. So, the biobjective problem (Max f, Min T_0) is studied in the following section.

2.3 Problem solution

The results are plotted in Figure 4.1(a) to Figure 4.1(c), where it can be observed that the three Pareto fronts given by *AWS*, *AUGMECON* and *NSGA-IIb* have very similar shapes, and are perfectly superimposed in Figure 4.1(d). The temperature (T_0) lies in the range [600, 675] K and the ammonia profit is between 2 $M\$/y$ and 5 $M\$/y$. The results improve the ones of Ksasy et al. [2010]; namely, the ammonia maximum profit is 5.66 $M\$/y$ at the optimal temperature (T_0) equal to 695 K.

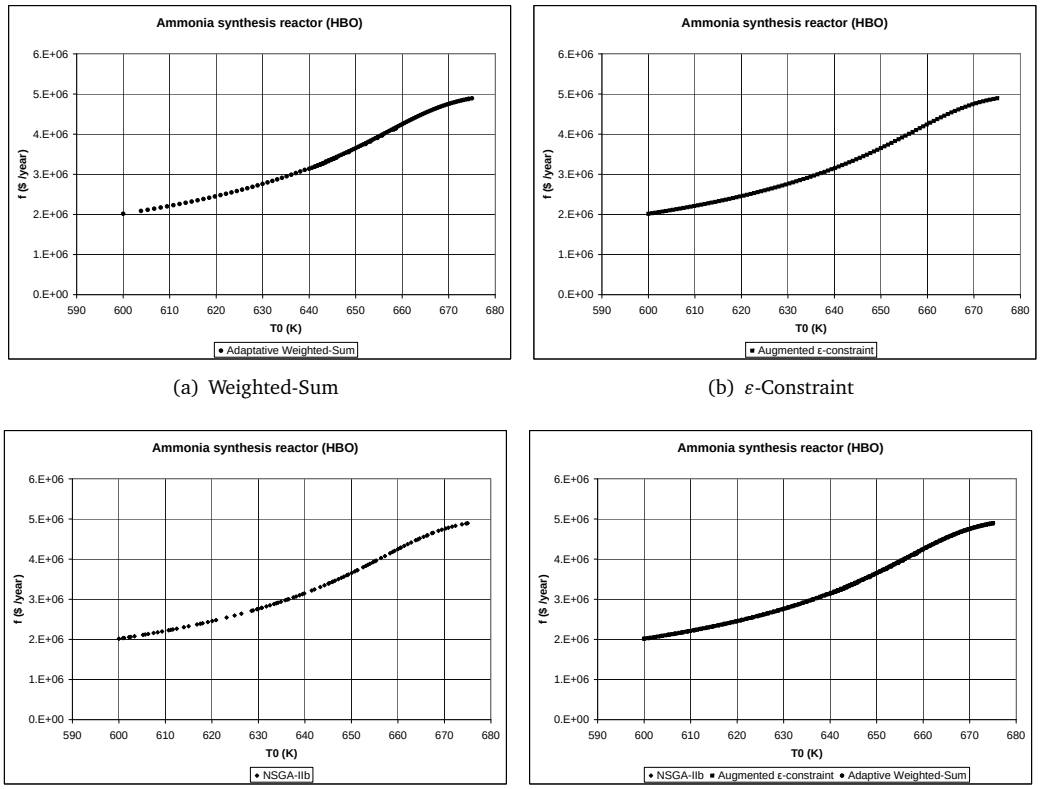

(a) Weighted-Sum (b) ε-Constraint

(c) Genetic algorithm (d) Superimposed fronts

Figure 4.1: Solution of the Ammonia synthesis reactor.

3 Alkylation process (AP)

An important process in petroleum refining is the alkylation process, wherein a light olefin such as propene, butene or pentene reacts with isobutane in the presence of a strong sulfuric acid catalyst to produce the alkylate product (e.g., 2,2,4 tri-methyl pentane from butene and isobutane). The alkylate product is used for blending with refinery products, such as gasoline and aviation fuel, in order to increase their octane number. Jones [1995] provides a comprehensive overview of the alkylation process, its chemistry, design and operational aspects. Sauer et al. [1964] developed a nonlinear model for the alkylation process and used it for optimization via linear programming methods. Since then, many researchers (e.g., [Bracken et al., 1968; Luus and Jaakola, 1973; Rangaiah, 1985]) employed this model in their optimization studies. Also, the alkylation process optimization is a classic example included in the text-book on optimiza-

tion by Edgar et al. [2001]. In our knowledge, only Luus [1978] reported alkylation process optimization for multiple objectives by the ε-constraint method.

Nomenclature

Symbol	Meaning
P	Profit ($\$/day$)
x_1	Olefin Feed ($barrels/day$)
x_2	Isobutane Recycle ($barrels/day$)
x_3	Acid Addition Rate ($thousand\ pounds/day$)
x_4	Alkylate Production Rate ($barrels/day$)
x_5	Isobutane Feed ($barrels/day$)
x_6	Spent Acid Strength ($weight\ percent$)
x_7	Octane Number
x_8	Isobutane to Olefin Ratio
x_9	Acid Dilution Factor
x_{10}	F-4 Performance Number
α	Alkylate product value ($\$/octane\text{-}barrel$)
β	Olefin feed cost ($\$/barrel$)
ϑ	Isobutane recycle cost ($\$/barrel$)
κ	Fresh acid cost ($\$/thousand\ pounds$)
ξ	Isobutane feed cost ($\$/barrel$)

Table 4.3: Nomenclature of the Alkylation process.

3.1 Alkylation process model

A simplified process flow diagram of the alkylation process is shown in Figure 4.2. The process involves a reactor with olefin feed, isobutane makeup and isobutane recycle as the inlet streams. Fresh acid is added to catalyze the reaction and spent acid is withdrawn. The exothermic reactions between olefins and isobutane occur at around room temperature, and excess isobutane is used. The hydrocarbon outlet stream from the reactor is fed into a fractionator from where isobutane is recovered at the top and recycled back to the rector, and the alkylate product is withdrawn from the bottom.

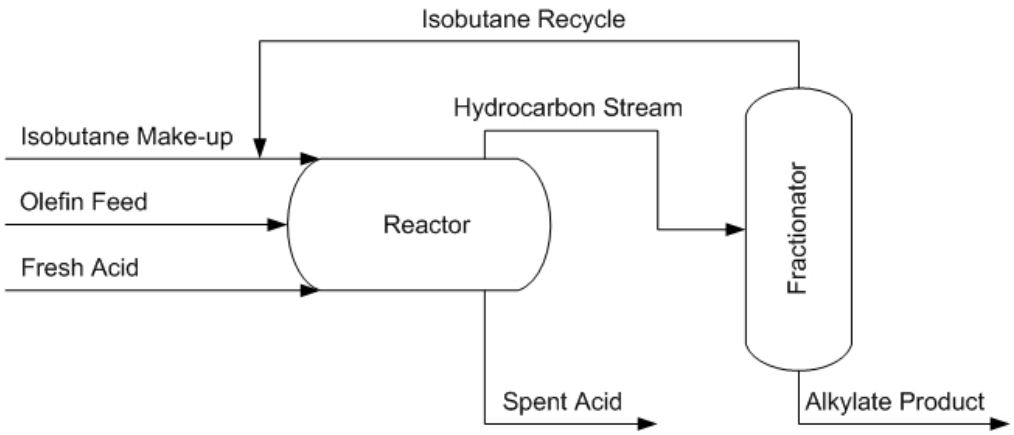

Figure 4.2: Flowsheet of the Alkylation process.

Sauer et al. [1964] developed a model for this process based on a combination of the first principle, empirical equations and a number of simplifying assumptions. The resulting model has 10 variables, x_i, (Table 4.3) and seven equality constraints (Equations 4.20 to 4.26). Bracken et al. [1968] have presented this model and the optimization problem in a different way. After noting that the four equality constraints derived by regression analysis do not need to be satisfied exactly, they converted them into eight inequality constraints. This optimization problem and its solution are concisely described by Edgar et al. [2001]. Rangaiah [1985] studied both problems: the original one with seven equality constraints and the modified one with both equality and inequality constraints. Variables involved in the alkylation process model of Sauer et al. [1964] and their bounds are summarized in Table 4.5. The *SOO* (Single Objective Optimization) problem of this process is described by Equation 4.16 to Equation 4.26. The cost coefficients used for computing the profit (α, β, ϑ, κ, ξ) are listed in Table 4.4.

$$P = \alpha_1(x_4 x_7) - \beta_2(x_1) - \vartheta_3(x_2) - \kappa_4(x_3) - \xi_5(x_5) \tag{4.16}$$

$$0 \leq x_1 \leq 2000 \tag{4.17}$$

$$90 \leq x_7 \leq 95 \tag{4.18}$$

$$3 \leq x_8 \leq 12 \tag{4.19}$$

$$0 \leq [x_4 \equiv x_1(1.12 + 0.13167x_8 - 0.006667x_8^2)] \leq 5000 \tag{4.20}$$

$$0 \leq [x_5 \equiv 1.22x_4 - x_1] \leq 2000 \tag{4.21}$$

$$12000 \leq [x_2 \equiv x_1x_8 - x_5] \leq 17500 \tag{4.22}$$

$$85 \leq [x_6 \equiv 89 + \frac{x_7 - (86.35 + 1.098x_8 - 0.038x_8^2)}{0.325}] \leq 93 \tag{4.23}$$

$$145 \leq [x_{10} \equiv -133 + 3x_7] \leq 162 \tag{4.24}$$

$$1.2 \leq [x_9 \equiv 35.82 - 0.222x_{10}] \leq 4 \tag{4.25}$$

$$0 \leq [x_3 \equiv 0.001\frac{x_4x_6x_9}{98 - x_6}] \leq 120 \tag{4.26}$$

Symbol	Value
α	0.063
β	5.04
ϑ	0.035
κ	10
ξ	3.36

Table 4.4: Cost coefficients of the Alkylation process.

Symbol	Lower bound	Upper bound
x_1	0	2,000
x_2	12,0000	17,500
x_3	0	120
x_4	0	5,000
x_5	0	2,000
x_6	85	93
x_7	90	95
x_8	3	12
x_9	1.2	4
x_{10}	145	162

Table 4.5: Variables and bound values in the Alkylation process.

3.2 Problem formulation

This biobjective optimization problem was already presented in the book of Rangaiah [2009]. It consists in maximizing the profit (P) expressed as a nonlinear function of the alkylate production rate, octane number, olefin feed, isobutene recycle, acid addition rate, isobutene feed, and minimizing the isobutene recycle. The set of decision variables is reduced to olefin feed, octane number and isobutene to olefin ratio. Other variables such as spent acid strength, isobutene to olefin ratio, acid dilution factor and F-4 performance number can be deduced by using the seven constraints (three linear and four nonlinear) of the problem.

3.3 Problem solution

The results are plotted in Figures 4.3(a) to 4.3(c), where it can be observed that the three procedures give similar Pareto fronts, perfectly superimposed in Figure 4.3(d). The profit lies in the range [900, 1200] $\$/day$ and the isobutene recycle is between 12,000 $barrels/day$ and 17,500 $barrels/day$. These results are in the same order of magnitude that the ones of Rangaiah [2009]. Namely, the optimal profit increases from about 900 to 1,200 $\$/day$ as the isobutene recycle (x_2) increases from 12,000 to 17,500 $barrels/day$.

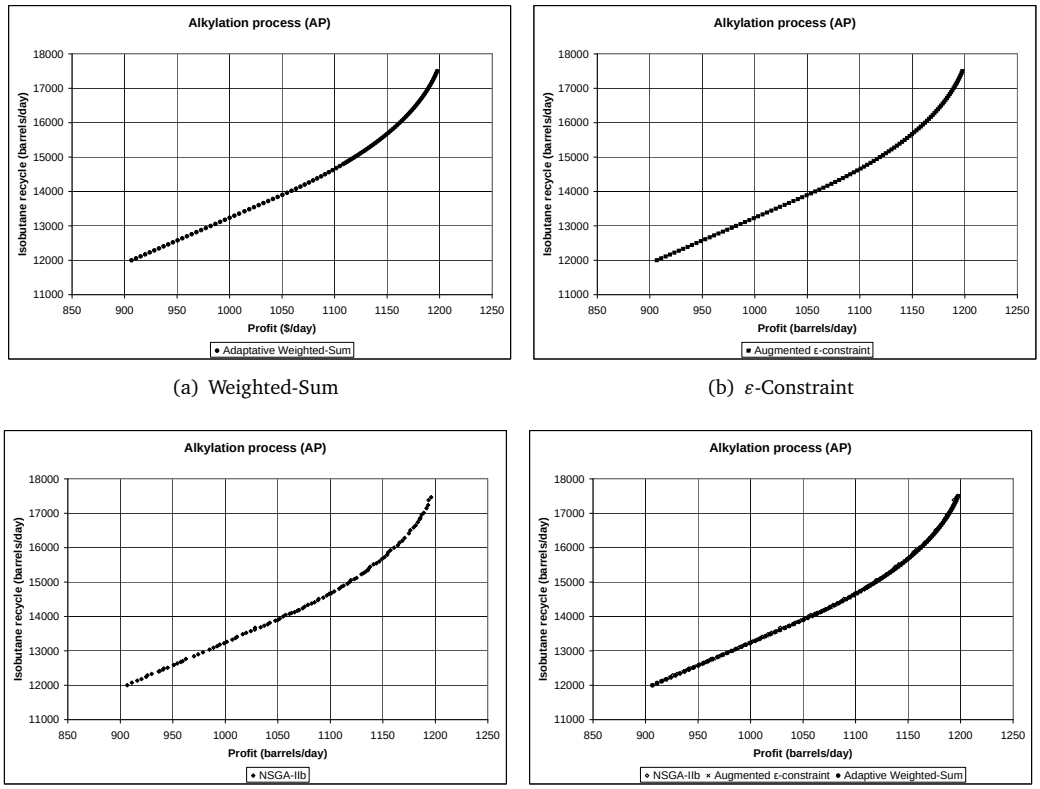

(a) Weighted-Sum (b) ε-Constraint

(c) Genetic algorithm (d) Superimposed fronts

Figure 4.3: Solution of the Alkylation process.

4 Williams & Otto chemical plant (WOP)

This engineering problem was first proposed by Williams and Otto [1960] and used by many workers as a benchmark for *NLP* studies. This fictitious process contains many of the characteristics of a typical chemical plant while being realistic enough. The plant is to manufacture 40 million pounds of chemical (P) per year; it consists of a perfectly stirred reactor, a heat exchanger, a decanter and a distillation column in series (Figure 4.4). There is a recycle from the column reboiler to the reactor, where three second-order irreversible reactions occur. Reactants A and B are fed separately to the reactor in pure form; components C and E are intermediate products (with no sale values); component G is a heavy oil considered as a waste material; the reaction coefficients are expressed in the Arrhenius form as shown in the Equation 4.30.

In addition, the rate of reaction is negligible below $120^{\circ}F$ ($\approx 48.88^{\circ}C$) and undesirable decomposition occurs above $220^{\circ}F$ ($\approx 104.44^{\circ}C$). So, the reactor temperature must be bounded.

Nomenclature

Symbol	Meaning
A	Component A
B	Component B
C	Component C
E	Component E
F	Flow rate (lb/hr)
G	Waste
k	Reaction coefficient
$M_{B,C,E,G,P}$	Molecular weight of B, C, E, G, P $(Molecular\ weight)$
P	Product
T	Reactor temperature $(^{\circ}R)$
V	Reactor volume $(cu.ft)$
α_i	Pre-exponential factor in the Arrhenius rate equation for the ith reaction $(/hr., wt.fraction)$
β_i	Exponential factor in the Arrhenius rate equation for the ith reaction $(^{\circ}R)$
ρ	Density of reactor solution $(lb/cu.ft)$
Subscripts	
A	Of reactant A to reactor
B	Of reactant B to reactor
D	Of column bottoms returned as plant fuel
G	Of G from decanter (to waste)
P	Of Product P from column
R	From reactor
RA	Of A from reactor
RB	Of B from reactor
RC	Of C from reactor
RE	Of E from reactor
RP	Of Product P from reactor

Table 4.6: Nomenclature of the Williams & Otto chemical plant.

4.1 The Williams & Otto chemical plant model

As outlined in the earlier work of Ray and Szekely [1973], the production of P is assumed to involve three second order irreversible chemical reactions:

$$A + B \xrightarrow{k_1} C \tag{4.27}$$

$$C + B \xrightarrow{k_2} P + E \tag{4.28}$$

$$P + C \xrightarrow{k_3} G \tag{4.29}$$

In these chemical reactions, the rate constants change with temperature, following the Arrhenius relationship [Di Bella and Stevens, 1965]:

$$k_i = \alpha_i exp(-\frac{\beta_i}{T}) \tag{4.30}$$

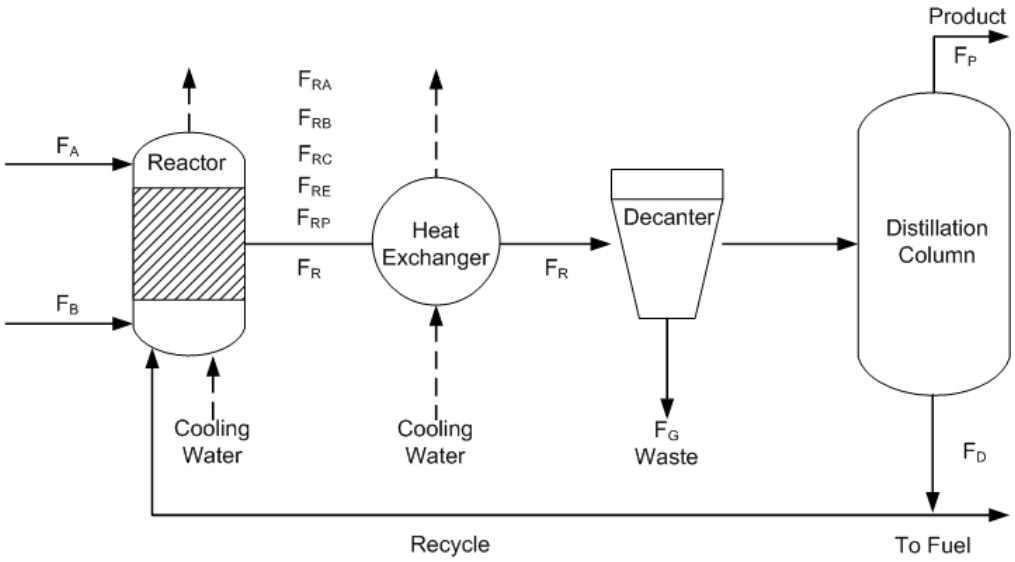

Figure 4.4: A schematic representation of the Williams & Otto chemical plant [Williams and Otto, 1960].

The problem involves numerous constraints [Ray and Szekely, 1973], which are listed below. These following constraint equations are derived by making independent material balances across the system, with two supplementary constraints related to the separation efficiency in the distillation column, and the definition of F_R:

Overall material balance:

$$F_A + F_B - F_G - F_P - F_D = 0 \tag{4.31}$$

Restriction related to separation efficiency of the distillation column and the azeotrope formation gives:

$$F_{RP} - 0.1F_{RE} - F_P = 0 \tag{4.32}$$

Material balance on component E:

$$\left(\frac{M_E}{M_B}\right)\frac{k_2 F_{RB} F_{RC} V\rho}{F_R^2} - F_D\left[\frac{F_{RE}}{F_R - F_G - F_P}\right] = 0 \tag{4.33}$$

Material balance on component P:

$$\left[k_2 F_{RB} F_{RC} - \left(\frac{M_P}{M_C}\right) k_3 F_{RC} F_{RP}\right]\frac{V\rho}{F_R^2} - F_D\frac{F_{RP} - F_P}{F_R - F_G - F_P} - F_P = 0 \tag{4.34}$$

Material balance on component A:

$$(-k_1 F_{RA} F_{RB})\frac{V\rho}{F_R^2} - F_D\left[\frac{F_{RA}}{F_R - F_G - F_P}\right] + F_A = 0 \tag{4.35}$$

Material balance on component B:

$$(-k_1 F_{RA} F_{RB} - k_2 F_{RB} F_{RC})\frac{V\rho}{F_R^2} - F_D\left[\frac{F_{RB}}{F_R - F_G - F_P}\right] + F_B = 0 \tag{4.36}$$

Material balance on component C:

$$\left[\left(\frac{M_C}{M_B}\right) k_1 F_{RA} F_{RB} - \left(\frac{M_C}{M_B}\right) k_2 F_{RB} F_{RC} - k_3 F_{RC} F_{RP}\right]\frac{V\rho}{F_R^2} - \frac{F_D F_{RC}}{F_R - F_G - F_P} = 0 \tag{4.37}$$

Material balance on component G:

$$\left(\frac{M_G}{M_C}\right)\frac{k_3 F_{RC} F_{RP} V\rho}{F_R^2} - F_G = 0 \tag{4.38}$$

And finally, by utilizing the definition of F_R, the last constraint is obtained as:

$$F_{RA} + F_{RB} + F_{RC} + F_{RP} + F_G - F_R + F_{RE} = 0 \tag{4.39}$$

4.2 Problem formulation

The problem data is displayed in Table 4.6, where the units of Williams and Otto [1960] have been conserved. The objective is to minimize the reactor volume (V), while minimizing the waste flow rate (F_G). The optimization variables are the two flow rates F_A, F_B and T lying in the range $[580, 680]^\circ R$ ($\approx [49.07, 104.62]^\circ C$). Due to mass balances, the problem is submitted to nine (linear, nonlinear) equality constraints, some of them involving the molecular weights and the solution density, given in Table 4.7. These values are provided by previous studies [Chakraborti et al., 2006; Di Bella and Stevens, 1965].

Symbol	Value
α_i	$\alpha_1 = 5.9755 \times 10^9$
	$\alpha_2 = 2.5962 \times 10^{12}$
	$\alpha_3 = 9.6283 \times 10^{15}$
β_i	$\beta_1 = 12,000$ (based on A or B)
	$\beta_2 = 15,000$ (based on B)
	$\beta_3 = 20,000$ (based on C)
M_i	$M_B = 100$
	$M_C = 200$
	$M_E = 200$
	$M_G = 300$
	$M_P = 100$
F_P	4763
ρ	50

Table 4.7: Fixed parameters of the Williams & Otto chemical plant.

4.3 Problem solution

The results are plotted in Figures 4.5(a) to 4.5(c), where it can be observed that the Pareto front given by *AWS* is much more restricted than the two other ones, which have very similar shapes. In Figure 4.5(d), the three fronts are perfectly superimposed. For example, for a reactor volume (V) of 60 $cu.ft$ ($\approx$ 1.69 m^3), the waste flow rate (F_G) is equal to 2,400 lb/hr ($\approx$ 1 088.62 kg/h). In Di Bella and Stevens [1965], where only the reactor volume was optimized, the authors found a volume (V) of 60 $cu.ft$ ($\approx$ 1.69 m^3) and a flow rate (F_G) equal to 3,600 lb/hr ($\approx$ 1 632.93 kg/h). In a more recent work [Chakraborti et al., 2006], where a biobjective problem involving the return of investment and the constraint squared sum is solved for a fixed reactor volume (V) of 60 $cu.ft$ ($\approx$ 1.69 m^3), a value of waste flow rate (F_G) of 2,610 lb/hr ($\approx$ 1 183.87

kg/h) is found; the minimal value of the squared sum of constraints is in the order of magnitude of 10^{-6}. Let us recall that the nine linear-nonlinear equality constraints due to the mass balance equations are solved at each move of *NSGA-IIb* by the Newton-Raphson procedure *(fsolve)* of the MATLAB toolbox, and the squared accuracy is much lower than 10^{-6}.

The biobjective optimization of the Williams & Otto chemical plant was recently carried out by Rangaiah [2009] under economic objectives: Max *[NPV* or *PBT]* and Min *[PBB]*, where *NPV* is the Net Present Value of the plant; *PBT*, the Profit Before Taxes and *PBP*, the PayBack Period. They used the *NSGA-II JG* algorithm [Agrawal et al., 2006], with the solver *DNEGQBF* of *IMSL* embedded in the objective function evaluation to solve the system of nonlinear equality constraints. The jumping gene adaptation of *NSGA-II* seems to be an attractive approach for studying chemical processes [Ramteke and Gupta, 2009]. On a *Pentium M* (123 *Mflops* for *Fortran*), 8 minutes *CPU* were required for performing 1,000 generations with populations of 200 individuals. They assumed a similar production of 2,160 kg/h of chemical (P), for the first problem a good solution from the Pareto front is a reactor volume (V) of 4.41 m^3, and for the second the volume (V) is 3.1 m^3. On the Pareto fronts displayed below a good solution for the volume is $V \in [100, 120]\ cu.ft$, that is to say $V \in [2.8, 3.5]\ m^3$; a similar order of magnitude for the reactor volume is obtained.

Concerning the *CPU* time, 1.5 hours were needed for performing $10 \times 300 = 3{,}000$ generations, that is to say 30 minutes for 1,000 generations (with a population of 100 individuals) with 15 *Mflops*. Note that 70% of the *CPU* time is spent in MATLAB for solving the set on nonlinear constraints. If the time (8 minutes) of Rangaiah [2009] is multiplied by the ratios of *Mflops* (123/15) and of population sizes (1/2), we obtain for their work an equivalent *CPU* time of 32.8 minutes. The two *CPU* times are in the same order of magnitude. Finally from an engineering point of view, the biobjective optimization performed in this work provides better results concerning both the reactor volume (directly linked to the return on investment) and the waste flow rate, than previously published works.

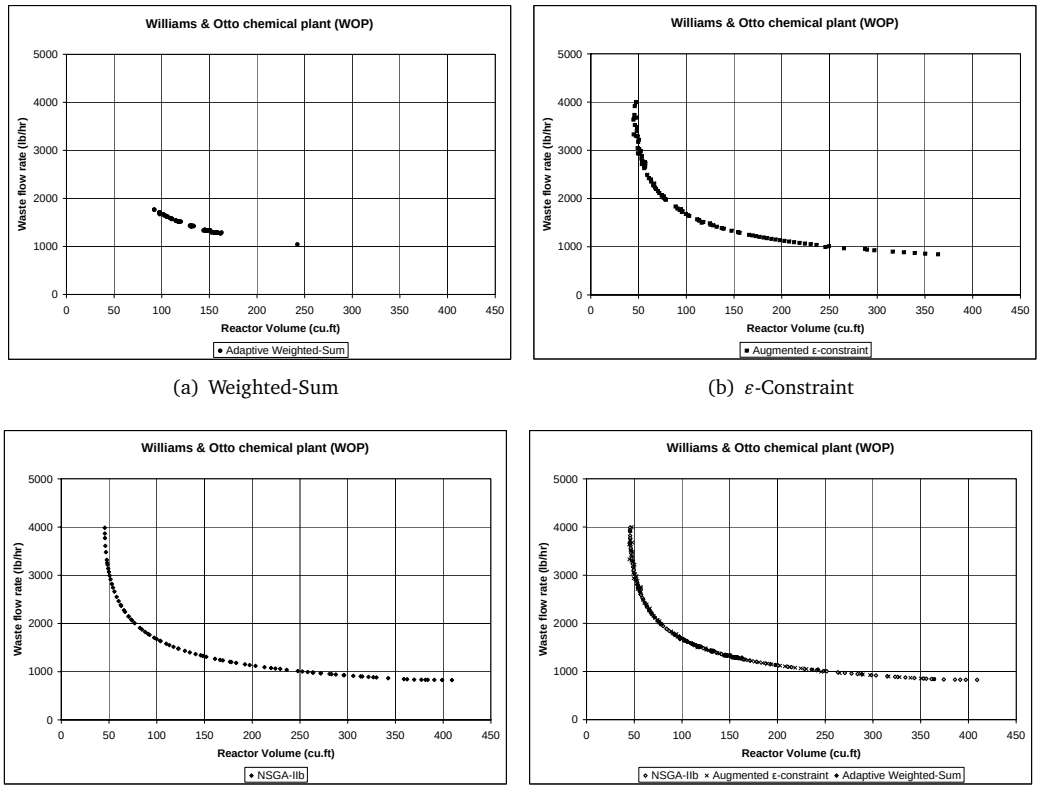

(a) Weighted-Sum (b) ε-Constraint

(c) Genetic algorithm (d) Superimposed fronts

Figure 4.5: Solution of the Williams & Otto chemical plant.

5 Gas turbine cogeneration system (GTCS)

In 1990, a group of concerned specialists in the field (C. Francopoulos, G. Tsatsanoris, A. Valero and M. von Spakovsky) decide to define the problem *CGAM* (from the first initials of the participants) to compare methodologies for designing efficient and cost-effective energy systems [Valero et al., 1994]. The objective of the problem, also called Gas Turbine Co-generation System *(GTCS)*, is to show how the methodologies can be applied, what concepts are used and what numbers are required and what numerical values are obtained in a simple and specific problem. Indeed, the aim of the *GTCS* problem is the unification of thermo-economic methodologies.

In the definition of the problem shown in the following sub-sections, the equations that describe the behavior of the system (physical model), the equations for calculating the capital costs of the components (economic model) and

the equations of state used to compute the thermodynamic properties (thermodynamic model) are considered. To simplify these models without loss of methodological generality, some assumptions are made.

Nomenclature

Symbol	Meaning
c	Cost per unit of energy
$\dot{C}$	Cost rate ($\$/s$)
Cp	Specific heat at constant pressure ($kJ/kg.K$)
CRF	Annual capital recovery factor
e	Specific exergy (kJ/kg)
h	Enthalpy (kJ/kg)
LH	Lattent heat (kJ/kg)
LHV	Low Heat Value (kJ/kg)
$\dot{m}$	Mass flow rate (kg/s)
N	Plant operation per year (h/y)
$\dot{Q}$	Heat transfer rate (kJ/s)
P	Pressure (MPa)
Pr	Expansion ratio
R	Universal constant ($kJ/kg.K$)
T	Temperature (K)
U	Heat transfer coefficient ($kW/m^2.K$)
W	Power (kW)
Z	Capital cost ($)
$\dot{Z}$	Cost rate ($\$/s$)
γ	Specific heat ratio
ζ	Exergetic objective
η	Efficiency
φ	Maintenance factor
ΔP	Pressure variation (MPa)
ΔT	Temperature variation (K)
ΔTLM	Log Mean Temperature (K)
Subscripts	
a	Air
AC	Air compressor
APH	Air Pre-Heater
CC	Combustion chamber
EV	Evaporator
f	Fuel
g	Combustion gases
GEN	Electric generator
GT	Gas turbine
$HRSG$	Heat-Recovery Steam Generator
IS	Isentropic
MST	Steam turbine mechanical
PH	Pre-Heater
NET	Net
REG	Regenerator
ss	Saturated steam
T	Total
w	Water

Table 4.8: Nomenclature of the Gas turbine cogeneration system.

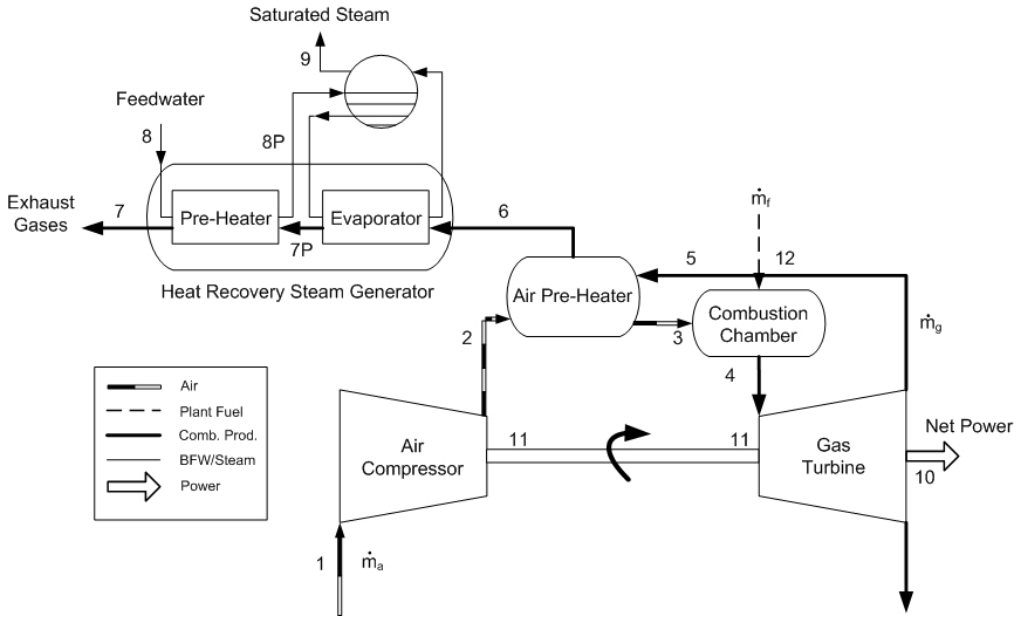

Figure 4.6: Gas turbine cogeneration system [Valero et al., 1994].

5.1 Gas turbine cogeneration system model

5.1.1 Physical model

The model is given by the mass and energy balances for each component of the plant.

AIR COMPRESSOR:

$$P_1 = P_0 \tag{4.40}$$

$$T_1 = T_0 \tag{4.41}$$

$$T_2 = T_1 \left[1 + \frac{1}{\eta_{IS_{AC}}} \left[\left(\frac{P_2}{P_1} \right)^{\frac{\gamma_a - 1}{\gamma_a}} - 1 \right] \right] \tag{4.42}$$

$$W_{AC} = \dot{m}_a \int_{T_1}^{T_2} Cp_a\{T\} dt \tag{4.43}$$

COMBUSTION CHAMBER:

$$P_4 = P_3(1 - \Delta P_{CC}) \tag{4.44}$$

$$\dot{m}_g = \dot{m}_a + \dot{m}_f \tag{4.45}$$

$$\dot{m}_f = \frac{\dot{m}_g(h_4 - h_3)}{LHV(\eta_{CC}) - h_3} \tag{4.46}$$

$$T_4 = \frac{T_5}{\left[1 - \eta_{IS_{GT}}\left[1 - \left(\frac{P_4}{P_5}\right)^{\frac{1-\gamma_g}{\gamma_g}}\right]\right]} \tag{4.47}$$

Air Pre-Heater:

$$P_3 = P_2(1 - \Delta P_{a,APH}) \tag{4.48}$$

$$P_6 = P_5(1 - \Delta P_{g,APH}) \tag{4.49}$$

$$T_3 = T_2 + \eta_{REG}(T_5 - T_2) \tag{4.50}$$

$$T_6 = \frac{\dot{m}_g Cp_g T_5 - \dot{m}_a(h_3 - h_2)}{\dot{m}_g Cp_g} \tag{4.51}$$

Gas Turbine:

$$Pr = \frac{P_4}{P_5} \tag{4.52}$$

$$W_{GT} = \dot{m}_g Cp_g(T_4 - T_5) \tag{4.53}$$

$$W_{NET} = W_{GT} - W_{AC} \tag{4.54}$$

Heat-Recovery Steam Generator:

$$T_{8P} = T_9 - \Delta T \tag{4.55}$$

$$T_7 = T_6 - \frac{\dot{m}_{ss}(h_9 - h_8)}{\dot{m}_g Cp_g} \tag{4.56}$$

$$\dot{m}_g Cp_g(T_6 - T_{7P}) = \dot{m}_{ss}(h_9 - h_{8P}) \tag{4.57}$$

$$\Delta T_{Pinch} = T_{7P} - T_9 \tag{4.58}$$

$$P_0 = P_6(1 - \Delta P_{HRSG}) \tag{4.59}$$

$$P_7 = P_6(1 - \Delta P_{HRSG}) \tag{4.60}$$

GENERAL EQUATIONS:

$$\gamma_{a,g} = \frac{1}{1 - \frac{R_{a,g}}{Cp_{a,g}}} \tag{4.61}$$

$$h_{a,g} = Cp_{a,g}(T - T_0) \tag{4.62}$$

5.1.2 Thermodynamic model

The thermodynamic model proposed in Valero et al. [1994] is very straightforward, yet complex enough to highlight the role played by the most important variables and to obtain significant results. The following assumptions are made to simplify the problem:

1. The air and the combustion gases behave as ideal gases with constant specific heats;
2. For combustion calculations, the fuel is taken to be pure methane (CH_4). The real gas composition is displayed in Table 4.9;
3. All components, except the Combustion chamber are adiabatic;
4. Fixed values for all thermodynamic quantities on the steam side of the Heat-Recovery Steam Generator are given in Table 4.10;
5. Environmental conditions of the air at the inlet are $P_0 = 1.013\ bar$ and $T_0 = 25°C$. These values are also used as the reference in enthalpy and exergy calculations (Table 4.10)

Component	Mass (%)	LHV
CH_4	80.92	50,000
C_2H_6	13.64	47,525
C_3H_8	1.94	46,390
C_4H_{10}	0.23	45,775
C_5H_{12}	0.04	45,400
CO_2	1.20	-
N_2	2.03	-
Total	**100.00**	**47,966**

Table 4.9: Natural gas composition for the Gas turbine cogeneration system.

Symbol	Value
c_f	0.004
Cp_a	1.004
Cp_g	1.17
Cp_w	4.5541
CRF	0.182
$(e_9 - e_8)$	910
e_f	51,850
$(h_9 - h_8)$	2,690
$(h_9 - h_{8P})$	1,956
LH	1,888.65
LHV	50,000
$\dot{m}_{ss,8,9}$	14
N	8,000
$P_{0,1}$	0.101325
$P_{8,9}$	2
R_a	0.287
R_g	0.290
$T_{0,1,8}$	298.15
T_9	485.52
W_{NET}	30,000
$\Delta P_{a,APH}$	0.05
$\Delta P_{g,APH}$	0.03
ΔP_{CC}	0.05
ΔP_{HRSG}	0.05
ΔT	15
η_{CC}	0.98
$\eta_{IS_{AC}}$	0.8468
$\eta_{IS_{GT}}$	0.8786
φ	1.06

Table 4.10: Fixed parameters of the Gas turbine cogeneration system.

5.1.3 Economic model

When evaluating the cost of a plant, it is necessary to consider the annual cost of fuel and the annual cost associated with purchasing and operating each plant component. The expressions for obtaining the purchase cost of the components, Z_i, are presented in this section. Based on these costs, the general equation for the cost rate, $\dot{Z}_i$, associated with capital investment and the maintenance costs for the *ith* component is:

$$\dot{Z}_i = \frac{(Z_i)(CRF)(\varphi)}{(N)(3600)} \tag{4.63}$$

The cost rate associated with fuel is obtained from:

$$\dot{C}_f = (c_f)(\dot{m}_f)(LHV) \tag{4.64}$$

The total cost rate of operation for the installation is obtained as follows:

$$\dot{C}_T = (c_f)(\dot{m}_f)(LHV) + \sum_{i=1}^{5} \dot{Z}_i \tag{4.65}$$

The expressions for obtaining the Capital cost of the components (Z_i) are given by:

AIR COMPRESSOR:

$$Z_{AC} = \left(\frac{c_{11}\dot{m}_a}{c_{12} - \eta_{IS_{AC}}}\right)\left(\frac{P_2}{P_1}\right) ln\left(\frac{P_2}{P_1}\right) \tag{4.66}$$

COMBUSTION CHAMBER:

$$Z_{CC} = \left(\frac{c_{21}\dot{m}_a}{c_{22} - \frac{P_4}{P_3}}\right)[1 + exp^{(c_{23}T_4 - c_{24})}] \tag{4.67}$$

GAS TURBINE:

$$Z_{GT} = \left(\frac{c_{31}\dot{m}_g}{c_{32} - \eta_{GT}}\right) ln\left(\frac{P_4}{P_5}\right)[1 + exp^{(c_{33}T_4 - c_{34})}] \tag{4.68}$$

AIR PRE-HEATER:

$$Z_{APH} = c_{41}\left(\frac{\dot{m}_g(h_5 - h_6)}{(U)\Delta TLM}\right)^{0.6} \tag{4.69}$$

$$(\Delta TLM)_{APH} = \frac{(T_5 - T_3) - (T_6 - T_2)}{ln\left(\frac{T_5 - T_3}{T_6 - T_2}\right)} \tag{4.70}$$

HEAT-RECOVERY STEAM GENERATOR:

$$Z_{HRSG} = c_{51}\left[\left(\frac{\dot{Q}_{PH}}{(\Delta TLM)_{PH}}\right)^{0.8} + (\frac{\dot{Q}_{EV}}{(\Delta TLM)_{EV}})^{0.8}\right] + c_{52}\dot{m}_{ss} + c_{53}\dot{m}_g^{1.2} \tag{4.71}$$

$$\dot{Q}_{PH} = Cp_w(T_{8P} - T_8)\dot{m}_{ss} \tag{4.72}$$

$$(\Delta TLM)_{PH} = \frac{(T_7 - T_8) - (T_{7P} - T_{8P})}{ln\left(\frac{T_7 - T_8}{T_{7P} - T_{8P}}\right)} \tag{4.73}$$

$$\dot{Q}_{EV} = (Cp_w(T_9 - T_{8P}) + LH)\dot{m}_{ss} \tag{4.74}$$

$$(\Delta TLM)_{EV} = \frac{(T_6 - T_9) - (T_{7P} - T_{8P})}{ln\left(\frac{T_6 - T_9}{T_{7P} - T_{8P}}\right)} \tag{4.75}$$

The values of constant cost (c_{ij}) used in Equation 4.66 to 4.71 are indicated in Table 4.11.

Component	Constant cost	
Compressor	$c_{11} = 39.5$ \$/(kg/s)	$c_{12} = 0.9$
Combustion Chamber	$c_{21} = 25.6$ \$/(kg/s)	$c_{22} = 0.995$
	$c_{23} = 0.018\ K^{-1}$	$c_{24} = 26.4$
Gas Turbine	$c_{31} = 266.3$ \$/(kg/s)	$c_{32} = 0.92$
	$c_{33} = 0.036\ K^{-1}$	$c_{34} = 54.4$
Air Pre-Heater	$c_{41} = 2{,}290$ \$/$(m^{1.2})$	$U = 0.018$
Heat-Recovery Steam Generator	$c_{51} = 4{,}745$ \$/$(kW/K)^{0.8}$	$c_{52} = 11{,}820$ \$/(kg/s)
	$c_{53} = 658$ \$/$(kg/s)^{1.2}$	

Table 4.11: Constant costs used for the purchase cost of the components.

5.2 Problem formulation

The *GTCS* problem refers to a cogeneration plant which delivers at least 30 MW of electrical power and 14 kg/s of saturated steam at 20 $bars$. The fuel of the plant is natural gas (considered as methane) with a low heating value equal to 50,000 kJ/kg.

5.2.1 Definition of the objectives

The two considered objectives are the exergetic efficiency of the cogeneration plant (to be maximized) and the total cost rate of operation (to be minimized) without pollution damage costs. The mathematical formulation of the two objectives is the following:

EXERGETIC:

$$\zeta = \frac{W_{NET} + \dot{m}_{ss}(e_9 - e_8)}{(\dot{m}_f)(e_f)} \tag{4.76}$$

ECONOMIC:

$$\dot{C}_T = \dot{C}_f + \sum_{i=1}^{5} \dot{Z}_i \tag{4.77}$$

5.2.2 Choice of decision variables

The decision variables (design parameters) in this study are the compressor pressure ratio ($Pr = P4/P5$), the mass flow rate of combustion gases ($\dot{m}_g$), the gas turbine outlet temperature (T_5) and the regenerator efficiency (η_{REG}). The bounds on the four variables are listed in Table 4.12.

Symbol	Value
Pr	[1,20]
$\dot{m}_g$	[20,100]
T_5	[700,1550]
η_{REG}	[0.001,0.95]

Table 4.12: Bounds on decision variables.

5.2.3 Physical constraints

The heat exchange between hot and cold streams in the Air Pre-Heater and in the Heat-Recovery Steam Generator must satisfy the following feasibility constraints:

COMBUSTION CHAMBER:

$$T_4 \leq 1550 \tag{4.78}$$

AIR PRE-HEATER:

$$T_5 \geq T_3 \tag{4.79}$$

$$T_6 \geq T_2 \tag{4.80}$$

HEAT-RECOVERY STEAM GENERATOR:

$$\Delta T_{Pinch} = T_{7P} - T_9 \geq 0 \tag{4.81}$$

$$T_6 \geq T_9 + \Delta T_{Pinch} \tag{4.82}$$

$$T_7 \geq T_8 + \Delta T_{Pinch} \tag{4.83}$$

An additional constraint with respect to the original *CGAM* problem [Valero et al., 1994], is imposed on the exhaust gases temperature, which must not fall below 400 K:

$$T_7 \geq 400^{\circ}K \tag{4.84}$$

Finally, the electrical power delivery of the cogeneration plant is lower-bounded as:

$$W_{NET} \geq 30\ MW \tag{4.85}$$

5.3 Problem solution

As is it shown in Figure 4.7 the three methods give the same fronts.

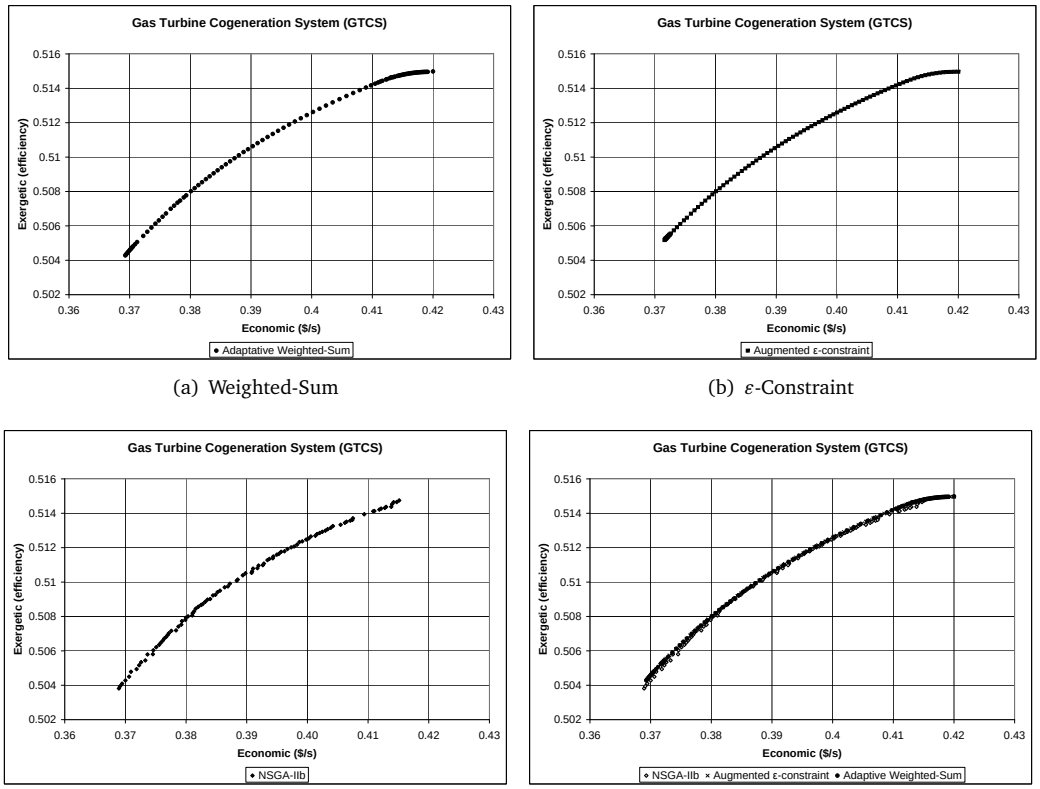

(a) Weighted-Sum

(b) ε-Constraint

(c) Genetic algorithm

(d) Superimposed fronts

Figure 4.7: Solution of the Gas Turbine Cogeneration System.

6 Resolution time

Let us recall that the *CPU* times reported in Tables 4.13 to 4.15 correspond to 100 runs of *AWS* and *AUGMECON*, and 10 runs of the *NSGA-IIb* with 100 individuals per generation and 300 generations. As indicated in the Introduction of this chapter, excepted for *CPU* time, the other times given are unrefined estimations and they are reported only to give general trends. The times are expressed in hours. Tables 4.13 to 4.15 contain the intermediate times (tuning parameters, fulfilling files, initial guess, *CPU*). The total times (resolution times) are gathered in Table 4.16. The dimensions of problems in terms of independent variables and number of equality constraints are recalled in Table 4.17.

Concerning the resolution time, the *NSGA-IIb* is ranked first, followed by *AUGMECON* and *AWS*. Except for the *NSGA-IIb* and for problems involving a significant number of equality constraints (*WOP* and *NGTN* cases), the *CPU* time

represents a very small proportion of the total time. It is necessary to point out that, from an economic point of view, the *CPU* time is only a masked time little expensive because it requires no human intervention.

Problem	Tuning parameters	Fulfilling input file	Finding the initial guess	CPU time
HBP	4	5	3	0.1
AP	8	10	5	0.05
WOP	11	21	8	0.5
GTCS	18	32	12	0.14

Table 4.13: Various times (h) for *AWS*.

Problem	Tuning parameters	Fulfilling input file	Finding the initial guess	CPU time
HBP	5	6	2	0.05
AP	7	9	4	0.01
WOP	10	18	5	0.1
GTCS	12	25	8	0.03

Table 4.14: Various times (h) for *AUGMECON*.

Problem	Tuning parameters	Fulfilling input file	Finding the initial guess	CPU time
HBP	1	2	1	0.6
AP	3	5	2	0.2
WOP	7	11	4	1.5
GTCS	8	18	6	1.39

Table 4.15: Various times (h) for *NSGA-IIb*.

Problem	AWS	AUGMECON	NSGA-IIb
HBP	12.1	23.05	4.6
AP	23.05	20.01	10.2
WOP	40.5	33.1	23.5
GTCS	62.14	45.03	33.39

Table 4.16: Resolution times (h) for the four problems.

Problem	HBP	AP	WOP	GTCS
Independent variables	2	3	3	4
Equality constraints	3	7	9	0

Table 4.17: Problem dimensions.

7 Conclusion

7.1 Numerical efficiency

The numerical study carried in this chapter allows to reject the *WS* method because, on the one hand, many process engineering problems are locally non-convex and, on the other hand, *WS* gives restricted Pareto fronts.

From a strict numerical point of view, *NSGA-IIb* and *AUGMECON* give similar results, while *AWS* may produce restricted Pareto fronts, due to non convexities in problem formulations. Nevertheless, the solutions are well superimposed. The main advantages of *AUGMECON* versus *NSGA-IIb* are listed below:

1. Convergence conditions are well established, contrary to *NSGA-IIb* where the stopping criterion very commonly used is a maximum number of generations;
2. When an unfeasible path method is implemented, i.e. *fmincon*, the handling of crisp equality constraints is easier than in a *NSGA-IIb*, where an external solver has to be run at each move of the algorithm.

The main features of a *NSGA-IIb* concern:

1. The ease of implementation;
2. The ability for solving black-box problems, where objectives and/or constraints are returned by a computer code for each value of optimization variables, which are frequently encountered in chemical engineering;
3. The possibility to mutate out of a local optimum and the ability to compute the entire Pareto front in one run.

These conclusions can be often found in the literature which also applies to process engineering problems. According to the numerical efficiency, let us note that in many engineering fields, like chemical, electrical, mechanical, very precise solutions are not required, as the goal is often to improve some process characteristics. However, in some particular fields, very crisp solutions are needed for avoiding serious troubles often in low *CPU* times; as for example aerospace or ballistic areas. So, from this point of view, *GAs* are the best common engineering solution. Nevertheless, many process engineering problems involve

nonlinear equality constraints, due to mass balance equations, that have to be solved with a lot of accuracy. From this point of view, efficient constrained *NLP* solvers *(GRG, SQP)* used in the ε-constraint method can constitute an advantage for this method.

7.2 Resolution time

Another point which pleads in favour of *GAs* is the resolution time, defined as the time including all steps from data entry to tuning and final solution. Obviously, except for *CPU* time, the other times are measurable with difficulty and are only unrefined estimations. However the general trend remains the same for all the treated examples: the *GA* is the most efficient procedure. Furthermore, from Tables 4.16 & 4.17, it can be observed that the gap between ε-*C* and *GA* is reduced when the problem complexity increases. Considering the resolution time, for explicit problems with high numbers of nonlinear equality constraints, we can think that both methods will have similar performances.

These conclusions are to be taken with care, because to have reasonable evaluations of the resolution times, it would have been necessary that several developers with different backgrounds solve the test problems.

7.3 Choice of the method

According to the above discussion, the ε-*C* and *GA* methods will be used in the following chapter. A last test to decide between them will be carried out on the biobjective optimization of a natural gas transportation network *(NGTN)*. Then, the selected procedure will be implemented for solving a triobjective optimization problem related to hydrogen injection in a natural gas transportation network.

Optimization of a natural gas transmission network

5

Contents

1 Introduction

Natural Gas *(NG)* is an important source of energy for reducing pollution and maintaining a clean and healthy environment. In addition to being a domestically abundant and secure source of energy, the use of *NG* also offers a number of environmental benefits over other sources of energy, particularly other fossil fuels.

The transport of large quantities of *NG* is carried out by pipeline network systems across long distances. Pipeline network systems include one or several compressor stations which compensate for pressure drops. A typical network today might consist of thousands of pipes, dozens of stations, and many other devices, such as valves and regulators. Inside each station, there can be several groups of compressor units of various vintages that were installed as the capacity of the system expanded. The compressor stations typically consume about 3 to 5% of the transported gas [Suming et al., 2000]. Thus, efficient operation of compressor stations is of major importance for enhancing the performance of the pipeline network. It is estimated that the global optimization of operations can save considerably the fuel consumed by the stations. Hence, the problem of minimizing fuel cost is of great importance.

This chapter performs the gas transportation model presented previously (Chapter 2) on a particular example with the aim at optimizing the network performances [Abbaspour et al., 2005]. Firstly, a monobjective case, where a classical deterministic optimization procedure based either on the nonlinear programming tool *CONOPT3* of the *GAMS*, *(General Algebraic Modelling System)* library or on the code *fmincon* of the MATLAB toolbox, is implemented; the goal is the fuel minimization problem in the compressor stations for fixed gas mass flow delivery. In the second case, the genetic algorithm *(NSGA-IIb)* [Gomez, 2008] coupled with a Newton-Raphson method and the ε-*C* procedure *(AUGMECON)* are used to solve a biobjective problem, constituted by the simultaneous maximization of the gas mass flow delivery and the minimization of the fuel consumption in the compression stations. At the conclusion of this example, the choice of the best procedure (namely *NSGA-IIb*) is carried out. Finally, considering hydrogen injection in the network, a triobjective problem related to the maximization of the gas mass flow delivery, the minimization of the fuel

consumption in the compression stations together with the maximization of the percentage of injected hydrogen is performed.

In each case, the study of carbon dioxide CO_2 emissions by the compression stations is carried out [Rodriguez et al., 2010]. In the multiobjective problems, the choice of the best solution is made by using *MCDM (Multiple Choice Decision Making)* tools: *TOPSIS* [Ren et al., 2007] and *FUCA* [Moralez-Mendoza et al., 2011].

2 Problem presentation and modelling equations

2.1 Problem presentation

This example is directly connected to the subject of the thesis which concerns the natural gas transportation networks *(NGTN)*. The modelling of gas pipeline networks has already been presented in Chapter 2, which proposes a general framework able to embed several formulations from design to operational purposes for steady-state problems. So, in this section, only the network characteristics are described.

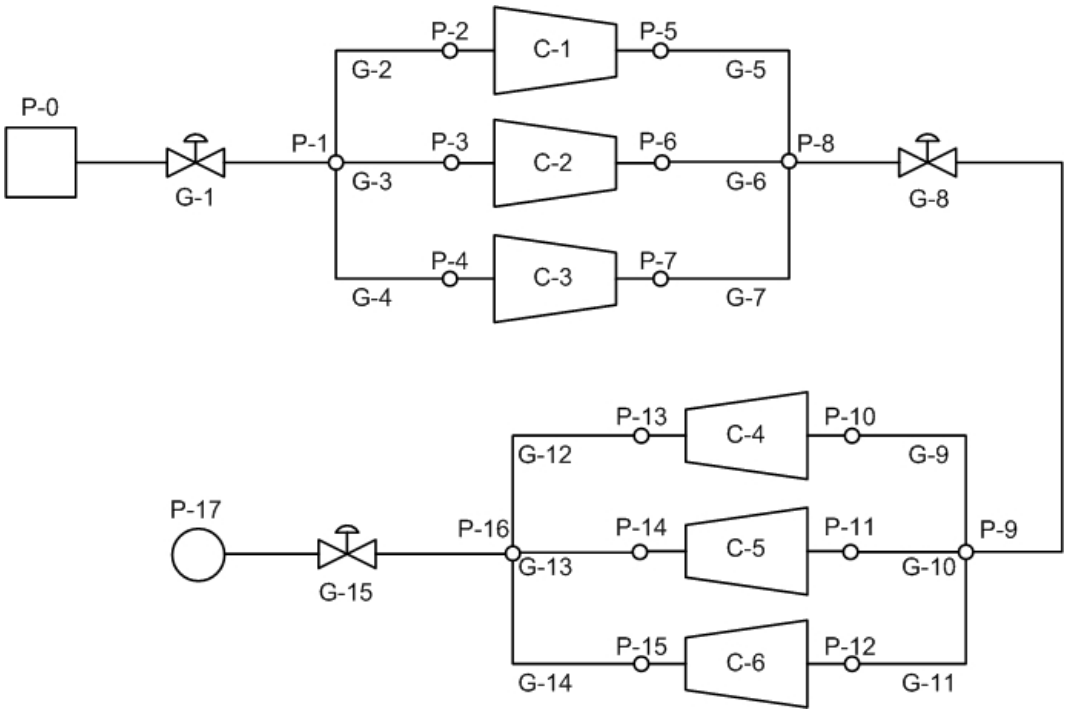

Figure 5.1: Schema of the considered pipeline network.

This didactic example is inspired from the work of Abbaspour et al. [2005]. The network consists of three long pipelines of 100 kilometers. There are two compressor stations that operate to compensate for pressure drop in the pipelines. Each compressor station includes three parallel centrifugal compressors. In each station, there are six short pipe segments of about a hundred meters linked to the entrances and outlets of the compressors (Figure 5.1). Although the length and the diameter of these pipes are lower than those of the three major pipelines, their role in the pressure change through the network may not be negligible and may even sometimes become bottleneck of the system. Therefore, these pipelines are also considered in the model. The technical features (expressed in meters) of the pipeline system corresponding to Figure 5.1, considered as fixed parameters for the optimization problem, are proposed in Table 5.1.

Pipeline tag	**G-1**	**G-2**	**G-3**	**G-4**	**G-5**
Diameter (m)	0.787	0.330	0.381	0.330	0.330
Length (m)	100000	200	300	100	200
Pipeline tag	**G-6**	**G-7**	**G-8**	**G-9**	**G-10**
Diameter (m)	0.330	0.330	0.838	0.381	0.330
Length (m)	100	200	100000	100	100
Pipeline tag	**G-11**	**G-12**	**G-13**	**G-14**	**G-15**
Diameter (m)	0.432	0.330	0.330	0.330	0.889
Length (m)	100	100	400	100	100000

Table 5.1: Technical features of the pipeline network.

2.2 Network modelling

The pressure is considered to be equal to 60 bar with a margin of $\pm$ 2% at the entrance point of the network, *P-0*, as well as the delivery pressure, *P-17*. In other words, the lower bound is 58.8 bar and the upper one is 61.2 bar. The gas flows from *P-0* towards *P-17*, and there is no input or output in the other nodes. The network includes 18 nodes, 15 pipes-arcs and 6 compressor-arcs. As for each compressor unit, there is a stream that carries fuel to it (Figure 2.2 of Chapter 2); there are 6 fuel streams which have not been shown in Figure 5.1 to avoid complexity. For each compressor, this stream originates from suction node (Figure 2.3 of Chapter 2). A flow direction is assigned to each pipe, so the gas flows from *P-0* to *P-17*. The nomenclature description is presented in Table 2.2 of Chapter 2.

The problem is modelled (gas pipeline equations, maximum allowable operational pressure, critical velocities, compressor characteristics) in Chapter 2. Here, Equations 2.4 to 2.8, Equations 2.11 & 2.12, 2.18, Equations 2.20 to 2.39 constitute the modelling set.

Component	**Methane**	**Ethane**	**Propane**
Mole fraction $(Decimal)$	0.70	0.25	0.05
Molecular mass (kg/mol)	0.01604	0.03007	0.0441
Critical temperature (K)	190.60	305.40	369.80
Critical pressure (bar)	46.00	48.80	42.50
Lower Heating Value (J/kg)	$50{,}009\times10^3$	$47{,}794\times10^3$	$46{,}357\times10^3$
Heat capacity $(J/kmol.K)$	35.6635	52.848	74.916

Table 5.2: Thermodynamic properties of the components of gas flowing in the pipelines.

The typical composition of *NG* considered in the numerical runs is presented in Table 5.2 together with the thermodynamic properties of gas components.

Roughness of inner surface of the pipes is considered to be equal to 4.6×10^{-5} (traditional value reported for stainless steel). The temperature is assumed to be isothermal and equal to 330 K all over the system. The adiabatic efficiency, η_{IS}, is defined by Equation 2.34; the mechanical efficiency, η_m, and driver efficiency, η_{dr}, for the compressors are assumed to be 0.90 and 0.35 respectively, according to values proposed in the dedicated literature [Menon, 2005]. The compressors within the compressor stations are modelled using compressor map-based polynomial equations. The set of polynomial equations uses constant coefficients (b_i) shown in Table 5.3.

Coefficient	Value	Unit
b_1	3.8113×10^{-4}	m^2
b_2	3.849×10^{-6}	m^{-1}
b_3	-6.3985×10^{-9}	m^{-4}
b_4	17.269	-
b_5	0.3237	m^{-3}
b_6	-4.1789×10^{-4}	m^{-6}

Table 5.3: Coefficients of the $h_i/\bar{\omega}^2$ and η_{IS} compressor equations.

3 Degrees-of-freedom analysis

A Degree-of-freedom *(DOF)* analysis is a powerful tool for systematic analysis of block flow diagrams. However, it is important to choose only the variables for which the values can be directly controlled while operating the actual network. At the same time, the set of optimization variables must be large enough to perform a consistent optimization search. With these considerations in mind, *(n-1)* compressor rotational speeds have been selected to be the independent optimization variables. The selection of *(n-1)* compressor rotational speeds is due to a *DOF* analysis, which (1) provides a rapid means for determining if the information available is sufficient and, (2) provides a structured method for determining the set of constraints that has to be solved, and in which order to solve them. Concerning the criteria, there are several possible objective functions that can be used as, fuel consumption minimization, amount of added hydrogen and transmitted power maximization.

In both monobjective and multiobjective optimizations, the variables are: 16 pressure variables governing the nodes, 21 flow rate variables (including fuel

streams) corresponding to pipes and compressors and 6 rotational speeds of the compressors. Besides variables, the equality constraints consist of 11 mass balances around nodes, 15 equations of motion for the pipe-arcs (Equation 2.18), 6 relationships between rotational speed, suction volumetric flow rate and head of each compressor (Equation 2.33) and 6 equations to calculate isentropic efficiency according to Equation 2.34. Altogether, there are 43 continuous variables and 38 equality constraints. So, the analysis of *DOF* gives five rotational speeds as independent variables.

4 Monobjective optimization

4.1 Problem formulation

The considered objective function is the total fuel consumption in the compressor stations. For each compressor, fuel consumption flow rate is obtained by using Equation 2.31. The variables and equality constraints are the same as described above. Obviously, some inequality constraints constitute the total formulation problem (76 inequality constraints). The set of inequality constraints is constituted by a lower bound for delivery flow rate (flow rate in arc *G-15*) equal to 150 kg/s, an upper bound as well as a lower bound for the pressures of the nodes (*MAOP* as an upper bound and atmosphere pressure as a lower bound; the following values were chosen for computing the *MAOP:* φ_F*=0.72,* φ_E*=1,* φ_T*=1)*, sonic velocity and erosional velocity in the role of upper bounds of the velocities through pipes, lower and upper bounds on the rotation speed of all compressors (166.7 and 250 rps respectively), a lower bound on compressor throughput in order to avoid pumping phenomenon, an upper bound on compressor throughput to prevent from chocking phenomenon.

4.2 Problem solution

As indicated above, in this monobjective case, the solver *CONOPT3* of the *GAMS* package has been used for solving the problem. The initialization of the variables is performed directly through the software *CONOPT3* under the condition that the problem is well-scaled and that bounds are assigned adequately. For bounded variables, *CONOPT3* takes as the initial values the average of the

bounds. Several other initial points were randomly selected (inside the bounds, for bounded variables) and the same solution was obtained. Strictly considering the non-convexity feature, the example is not so strongly non-convex.

The options used for implementing *CONOPT3* are the following: optimality tolerance $= 10^{-8}$, maximum feasibility tolerance $= 10^{-5}$, number of iterations=100. The resolution takes about 0.5 *s CPU* on a *PC* (processor *Intel Core 2 Duo*, 2.99 *GHz*, *RAM* 1.96 *GB*). With the same tolerances, *fmincon* of MATLAB gives identical results, the *CPU* time is yet higher (a few seconds). Table 5.4 presents the results relative to pressure values at each node. It must be observed that at *P-0* (i.e., supply node), the algorithm found the maximum possible pressure (61.2 bar) whereas the minimum possible value (58.8 bar) was obtained at *P-17* (i.e., delivery node).

Node	**Pressure** (bar)	**Node**	**Pressure** (bar)
P-0	61.2	*P-9*	58.3
P-1	47.4	*P-10*	58.3
P-2	47.0	*P-11*	58.2
P-3	47.1	*P-12*	58.3
P-4	47.2	*P-13*	65.1
P-5	67.0	*P-14*	65.5
P-6	66.9	*P-15*	65.1
P-7	67.0	*P-16*	65.0
P-8	66.8	*P-17*	58.8

Table 5.4: Pressure at all nodes of the pipeline network.

The value of objective function, that is the total fuel consumption in the compressor stations, is equal to 0.749 kg/s (sum of individual compressor consumptions, see Table 5.5, bold line), it leads to a significant reduction of 13% from the initial solution (0.863 kg/s for initial values between their bounds). Other results are listed in Table 5.5. The optimum percentage of the input gas that is consumed in the stations can thus be calculated and is found equal to 0.499%. For each compressor, consumption ratio is defined as the fuel consumption divided by the input mass flow rate. Let us mention in this example that the compressors involved in the second station work at their minimum rotational speeds, whereas the compressors of the first station work close to their maximum speeds. Finally, the transmitted power of the pipeline, that is the product of the pipeline delivery throughput (150 kg/s) and the lower heating

value *(LHV)* of the *NG* (48,830 kJ/kg) is found to be equal to 7,324 MW at this optimal point.

Compressor	**C-1**	**C-2**	**C-3**	**C-4**	**C-5**	**C-6**
Discharge flow rate (kg/s)	49.186	50.450	50.559	50.200	49.521	50.279
Rotational speed (rps)	244.3	246.5	246.6	166.7	166.7	166.7
Fuel consumption (kg/s)	**0.182**	**0.186**	**0.187**	**0.064**	**0.066**	**0.064**
Consumption ratio (%)	0.369	0.367	0.369	0.127	0.133	0.127
Isentropic head (kJ/kg)	42.592	42.188	42.201	12.664	13.367	12.607
Isentropic efficiency (%)	74.917	74.215	74.207	64.195	65.331	64.101

Table 5.5: Optimal values for the compressor units of the network.

4.3 Post-optimal analysis

The Lagrange multipliers obtained at the solver convergence can be used to carry out a sensitivity analysis. All these parameters are null or quasi-null except for the supply pressure at *P-0* (value=-0.047) and the delivery pressure at *P-17* (value 0.017). This means for example that, if the supply pressure is increased of 1 bar, the total fuel consumption will be decreased of 0.047 kg/s. In the same way, if the delivery pressure is decreased of 1 bar, the total fuel consumption will be decreased of 0.017 kg/s.

4.4 Carbon dioxide emissions

Chemically, when the reaction between methane (CH_4) and oxygen O_2 takes place, the result is carbon dioxide (CO_2), water (H2O), and a great deal of energy. Chemists would write the following to represent the combustion of methane:

$$CH_4[g] + 20_2[g] \rightarrow C0_2[g] + 2H_2O[l] + 891kJ \tag{5.1}$$

The total fuel consumption in the compressor stations is found equal to 0.749 kg/s, that is to say 23 640 $ton/year$. Thereby, taking into account a complete reaction of methane (Equation 5.1), an approximation of the carbon dioxide emissions can be obtained for ethane and propane. The combustion reaction of one molecule of methane (molar mass=16 g) produces one molecule of CO_2 (molar mass=44 g). One molecule of ethane (molar mass=30 g) gives two molecules of CO_2, and for one molecule of propane (molar mass=44 g), three molecules of CO_2 are obtained.

The results are summarized in Table 5.6. The carbon dioxide emissions are 66 332 $ton/year$. Let us recall that the *NG* delivery is 150 kg/s, that is to say 4 730 400 $ton/year$. The carbon dioxide emissions represent only 1.4% of the delivery gas, which is very acceptable.

Component	**Fuel consumption** $(ton/year)$	CO_2 **emissions** $(ton/year)$
Methane (70%)	16,534	45,468
Ethane (25%)	5,905	17,321
Propane (5%)	1,181	3,543
Total	**23,620**	**66,332**

Table 5.6: Carbon dioxide emissions.

5 Biobjective optimization

5.1 Problem formulation

In the previous section, the fuel consumption in the compressor stations was minimized for a given gas mass flow delivery. However, for a *NG* delivery company, the demand may vary according to climatic conditions or industrial requirements. So the problem which arises is to determine, for a given supply at the network entrance nodes, the minimal and maximal network capacities in terms of *NG* mass flow delivery and fuel consumption in compressor stations. This problem can be formulated as a biobjective optimization problem.

In fact, this does not refer to a problem of decision making strictly speaking, as far as the practical problem formulates as follows. For a *NG* delivery company, the total mass flow delivery is imposed on a given period, and the problem is to operate the compressor stations so as to minimize the fuel consumption in the stations. When performing the biobjective optimization, the largest Pareto front (Figure 5.2(b)) provides an easy way for:

1. Identifying the minimum and maximum network capacities in terms of mass flow delivery and fuel consumption;

2. For a given mass flow delivery between the above extreme values, the minimal fuel consumption, and thus the minimal carbon dioxide emission, can be deduced.

Concerning the optimization variables and constraints, the problem is identical to the previous one, but here the *NG* mass flow delivery is not fixed at 150 kg/s. The goal is to simultaneously minimize the total fuel consumption (this objective is noted f_1) in the compressor stations, while maximizing the *NG* delivery mass flow at *P-17* (objective denoted f_2).

Moreover, the set of constraints involves mass and momentum balances on the one hand and compressor equations on the other hand. The numerical solution of this set of equations must be performed carefully, making sure that the equality system of equations captures all the relevant aspects of the associated network problem. To solve efficiently this set of nonlinear equations, adequate variable bounds and initial values have to be applied at each node of the network. These values are taken from Tabkhi [2007].

5.2 Problem solution

As abovementioned, the solver *NSGA-IIb* of the *MULTIGEN* library, coupled with a Newton-Raphson procedure, was implemented for solving the multiobjective problem. The options used for implementing *NSGA-IIb* are: population size=100, maximum number of generations=300. The *GA* was run 10 times with different initial values for the rotational speeds (randomly generated); the Pareto front reported on Figure 5.2(b) has been obtained five times. The resolution of one *GA* takes an average time of 4 hours *CPU* on the same *PC* as above.

Relevant information lies in the two extreme points of the front, insofar as they represent the minimum (133 kg/s) and maximum capacities (157 kg/s) of the network in terms of *NG* delivery and fuel consumption. These solutions were verified by performing monobjective optimizations of the fuel consumption for a *NG* mass flow delivery of 133 kg/s and then of 157 kg/s; the same solutions for the fuel consumption were found again. Conversely, the *NG* mass flow delivery was computed with compressor rotational speeds given at the two extreme points, the mass flow delivery of 133 kg/s and of 157 kg/s were obtained again.

It can be observed on the Pareto front, that for *NG* mass flow delivery of 150 kg/s, the same value (0.749 kg/s) of the total fuel consumption as in the monobjective case is found again. The values of pressures, discharge flow rates, rotational speeds, fuel consumptions, isentropic head and isentropic efficiency

for the compressors are the same as the ones listed in Tables 5.4 & 5.5. The carbon dioxide emissions for the two extreme points are given in Tables 5.7 & 5.8.

An additional verification was carried out by implementing the *AUGMECON* method. The obtained front is given on Figure 5.2(a). The two fronts obtained from genetic algorithm and *AUGMECON* are superimposed (Figure 5.2(c)), but the front of *AUGMECON* is much more restricted than the one of genetic algorithm, due to local non convexities in the problem formulation. From these checks, we can assume that the Pareto front given by the *NSGA-IIb* is correct, and brings more information since it is more extended than the one of *AUGMECON*.

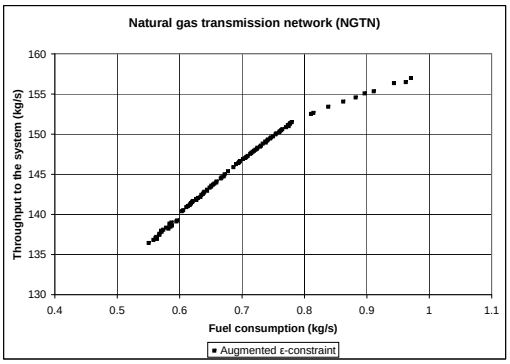

(a) ε-Constraint

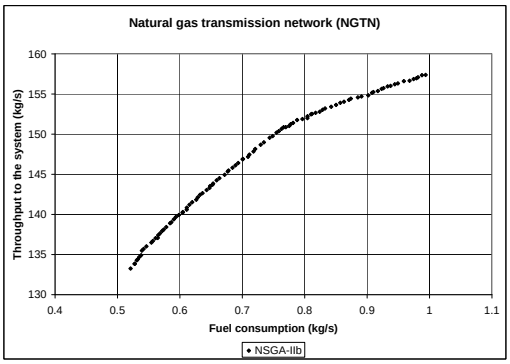

(b) Genetic algorithm

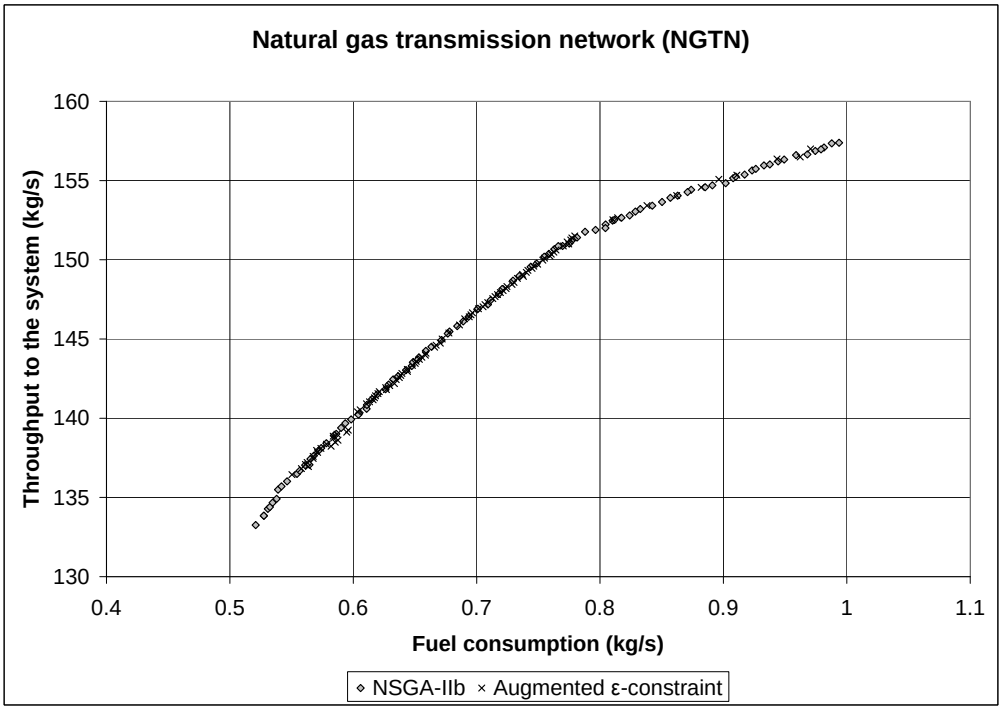

(c) Superimposed fronts

Figure 5.2: Solution of the Natural Gas transmission network.

5.3 Carbon dioxide emissions

For the pair (f_1=0.749 kg/s, f_2=150 kg/s), the results are already reported in Table 5.6. Two new studies for the extreme solutions (case 1: f_1=0.540 kg/s, f_2=133 kg/s) and (case 2: f_1=0.980 kg/s, f_2=157 kg/s) are carried out, the results are indicated in Tables 5.7 & 5.8.

CASE 1:

The carbon dioxide emissions are 47,823 $ton/year$ (Table 5.7). The *NG* delivery is 133 kg/s, that is to say 4,194, 288 $ton/year$. The carbon dioxide emissions represent 1.1% of the delivery gas.

Component	**Fuel consumption** $(ton/year)$	CO_2 **emissions** $(ton/year)$
Methane (70%)	11,920	32,780
Ethane (25%)	4,257	12,487
Propane (5%)	852	2,556
Total	**17,029**	**47,823**

Table 5.7: Carbon dioxide emissions (case 1).

CASE 2:

The carbon dioxide emissions are 86,794 $ton/year$ (Table 5.8). The *NG* delivery is 157 kg/s, that is to say 4,951, 152 $ton/year$. The carbon dioxide emissions represent 1.8% of the delivery gas.

Component	**Fuel consumption** $(ton/year)$	CO_2 **emissions** $(ton/year)$
Methane (70%)	21,635	59,496
Ethane (25%)	7,726	22,663
Propane (5%)	1,545	4,635
Total	**30,905**	**86,794**

Table 5.8: Carbon dioxide emissions (case 2).

DISCUSSION:

Along the Pareto front, the carbon dioxide emissions vary from 1.1% to 1.8% of the *NG* mass flow delivery. These values are lower than those usually admitted; indeed as mentioned in the Introduction section, it is estimated that the compressor stations typically consume about 3 to 5% of the transported gas [Suming et al., 2000]. So the optimization of compression operations yields significant savings for the fuel consumed in the stations.

5.4 Resolution time

Let us recall that the *CPU* times reported in Table 5.9 correspond to 100 runs of *AUGMECON*, and 10 runs of the *NSGA-IIb* with 100 individuals per generation and 300 generations. Except for *CPU* times, the other values must be taken with all the precautions expressed in Chapter 4. The times are expressed in hours.

Concerning the *CPU* time, *NSGA-IIb* is not ranked first, since it involves a significant number of equality constraints. However, the *CPU* time represents a very small proportion of the total time. It is necessary to notice that, from an economic point of view, the *CPU* time is only a masked time little expensive because, it requires no human intervention.

Problem	**Tuning parameters**	**Fulfilling input file**	**Finding the initial guess**	**CPU time**	**Resolution time**
AUGMECON	55	60	40	1	156
NSGA-IIb	10	25	8	40	83

Table 5.9: Various times (h) for the *NGTN* (*AUGMECON* and *NSGA-IIb*).

5.5 Choice of the method

From a numerical point of view, the Pareto front given by the genetic algorithm brings more information than the one of ε-*C*. Since it is more extended, the computational time of *NSGA-IIb* represents half of that of *AUGMECOM*. These are the reasons why only the genetic algorithm was used for performing the triobjective optimization of the following section.

5.6 Choice of the best solutions

As already mentioned, although the biobjective problem is not strictly speaking a *MCDM* one, the determination of a *good* solution for the biobjective optimization problem, would provide relevant information for the practitioner. After the complete set of solutions of the biobjective optimization problem (i.e. the Pareto front or set of efficient solutions) is found, the next step consists in identifying the best ones. This *Multiple Choice Decision Making (MCDM)* question is also a complex problem, mainly because of its more subjective nature, more than the multiobjective optimization problem itself. Some generic tools, like the knee method [Branke et al., 2004] or the *TOPSIS* and *FUCA* procedures, can be used for choosing a restricted set of good solutions on the Pareto front. However, for industrial problems, the practitioner may make his final decision according to some specific internal features of his company.

5.6.1 *MCDM* methods: *TOPSIS* and *FUCA*

TOPSIS is one of the most commonly used method in *Process Systems Engineering*. The fundamental concept of this method [Opricovic and Tzeng, 2004; Ren et al., 2007; Chen et al., 2009] is the comparison of Euclidian distances to choose the best alternative. *TOPSIS* is a synthetic evaluation method, where the distance between available solutions and *the optimized ideal reference point* is calculated. The optimized ideal reference point is a theoretical point where objectives are at their minimal values (in the case of minimization problems); it may be the origin of the Euclidian space.

The method calculates the distance between the ideal reference at each point of the Pareto curve and ranks them by increasing order of distances. The method starts with a decision matrix that contains all the alternatives ordered by the criteria and a weight vector is defined. The next step is to calculate the normalized decision matrix, after the positive and negative ideal solutions are defined from the standardized matrix. Then, the separation measures of each alternative are calculated and, finally, a ratio for each alternative is estimated. The alternatives are ranked according to their ratio.

On the other hand, *FUCA* is the French acronym for *Faire Un Choix Adéquat*: Make An Adequate Choice. This simple method, developed in our research group, is based on individual rankings of objectives; for a given criterion, the rank one is assigned to its best value and the rank n (n being the number of points of the Pareto front) to the worst one. Then, for each point of the front, a weighted summation (the weights representing the preferences) of ranks is performed, and the choice is carried out according to the lowest values of the sum. In a recent paper [Moralez-Mendoza et al., 2011], the *FUCA* method was compared with classical *MCDM* procedures on a tricriteria problem related to the portfolio management in a pharmaceutical industry. For each solution found by *ELECTRE* [Teixeiro de Almeida et al., 2004], *PROMETHEE* [Zhaoxu and Min, 2010] and *TOPSIS* [Chen et al., 2009], the *FUCA* ranking is also reported. A very good agreement between the three classical *MCDM* methods and *FUCA* can be observed, showing the efficiency of the *FUCA* procedure.

However, the *FUCA* procedure cannot be implemented on biobjective problems. Let us consider for example a biobjective minimization problem, with a Pareto front involving n points. One of the extreme point corresponds to the

best value of one objective (individual rank=1) and the worst value for the second objective (individual rank=n); so the sum of ranks is *(n+1)*. For the other extreme point, the best value of one objective becomes the worst, and for the second objective, the worst value becomes the best one; the sum of ranks is also *(n+1)*. Indeed, *FUCA* cannot distinguish the points of the Pareto front for a biobjective optimization problem.

5.6.2 Choice of the best solution by using *TOPSIS*

The *TOPSIS* procedure was implemented for determining the three best solutions of the biobjective optimization problem. They are indicated by: *TS1, TS2* and *TS3* in Figure 5.3 and Table 5.10. The goal is now to identify the best solution among the three proposed ones. The chosen criterion selection is to minimize the distances between criteria f_1 and f_2 of the monobjective and the biobjective solutions.

The selected solution will be the one which degrades the least possible the values obtained in the monobjective case. Let us note that *TOPSIS* is implemented by using the same weight on both objectives. The euclidian norm of distances between monobjective and biobjective solutions is given in Table 5.11, where it can be noted that *TS3* is the best solution. For solution *TS3*, the corresponding values of pressures in the network are indicated in Table 5.12. Other values are listed in Table 5.13.

Obviously, in the three best solutions provided by *TOPSIS*, the throughput flow rate is decreased, compared to the imposed value of 150 kg/s of the monobjective case, and consequently, the fuel consumption value decreases. Like in many biobjective optimization cases, *TOPSIS* tends to identify solutions near one extremity of the Pareto front, when the same weight is affected to the objectives. We could correct it by assigning different weights to the objectives, but the problem of the arbitrary choice of the weighting factors would raise then. For this reason, we did not assign different weights to the two objectives.

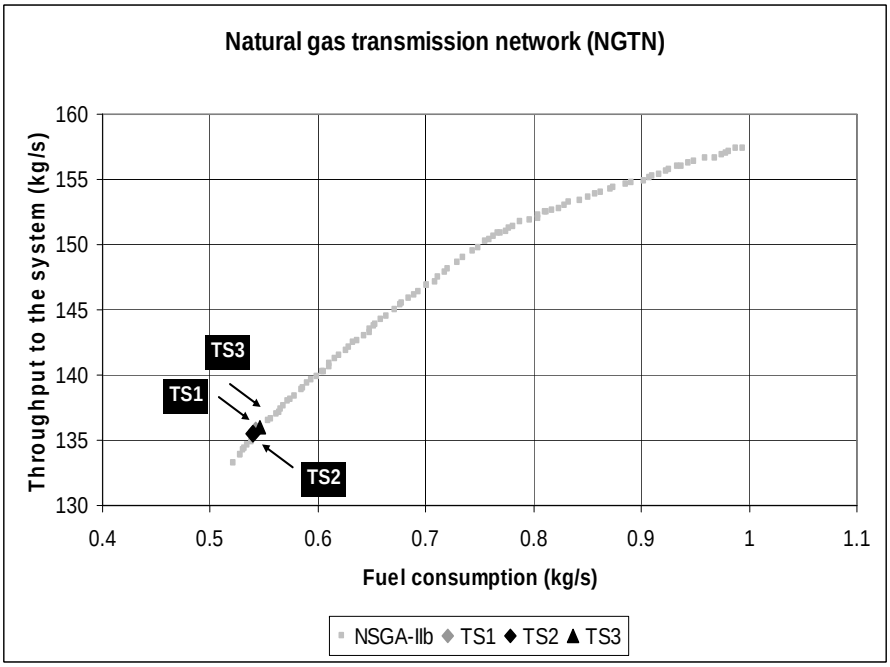

Figure 5.3: Graphical representation of the best solutions found by *TOPSIS*.

Objective / **Solution**	**Fuel consumption** $f_1 = 0.749\ (kg/s)$	**Throughput to the system** $*f_2 = 150\ (kg/s)$
TS1	0.541	135.698
TS2	0.539	135.490
TS3	0.546	136.019

$*$ Imposed by the monobjective case

Table 5.10: Best solutions found by using *TOPSIS*.

Solution	**Euclidian norm**
TS1	14.30
TS2	14.51
TS3	13.98

Table 5.11: Selection of the best solution for the biobjective case.

Node	**Pressure** (bar)	**Node**	**Pressure** (bar)
P-0	61.200	*P-9*	56.029
P-1	50.144	*P-10*	55.977
P-2	49.860	*P-11*	55.921
P-3	50.016	*P-12*	56.002
P-4	49.994	*P-13*	64.102
P-5	63.574	*P-14*	64.377
P-6	63.427	*P-15*	64.103
P-7	63.587	*P-16*	64.007
P-8	63.359	*P-17*	58.800

Table 5.12: Pipeline network pressures (the best solution *TS3* by using *TOPSIS*).

Compressor	**C-1**	**C-2**	**C-3**	**C-4**	**C-5**	**C-6**
Discharge flow rate (kg/s)	48.196	38.373	49.652	45.372	44.979	45.669
Rotational speed (rps)	212.163	189.230	214.796	166.797	167.326	167.308
Fuel consumption (kg/s)	**0.125**	**0.090**	**0.129**	**0.067**	**0.068**	**0.067**
Consumption ratio (%)	0.258	0.235	0.259	0.147	0.151	0.147
Isentropic head (kJ/kg)	28.699	28.028	28.389	15.572	16.191	15.522
Isentropic efficiency (%)	72.002	77.286	71.100	68.772	69.560	68.549

Table 5.13: Optimal values for the compressor units (best solution *TS3* by using *TOPSIS*).

6 Triobjective optimization for hydrogen injection

6.1 Why injecting hydrogen in existing natural gas transportation networks?

Hydrogen (H_2) is foreseen as an important energy carrier in the future sustainable energy society. The transition towards the situation in which H_2 will become little by little an important energy carrier will be lengthy (decades), costly and needs a significant effort for *R&D*. Preliminary studies have shown that the transport of a mixture of *NG*-H_2 is possible through the existing *NG* networks without pipeline modification as long as the mass fraction of H_2 remains sufficiently low [Castello et al., 2005]. This problem is the aim of the present section. Defining the conditions under which H_2 can be added to *NG* constitutes a key point of this investigation as well as how much H_2 can be injected into the existing pipeline network, while minimizing fuel consumption and maximizing the pipeline throughput (mass flow rate). The main hydraulic limiting factor for H_2 introduction in an existing pipeline is that H_2 specific volume is greater than this corresponding to *NG*, which results in a strong decrease pipeline throughput and consequently in the transmitted energy. However, a part of the reduction in

transmitted energy is compensated by LHV of H_2, that is higher than the value corresponding to *NG*. Consequently, an examination of the potential of using the existing *NG* pipeline system for the transmission and distribution of H_2 is a logical first step. Hence, this study presents in Chapter 2 a generalized mathematical formulation for modelling and evaluating *NG* pipeline networks under H_2 injection.

As abovementioned, the transition towards the situation in which H_2 will become an important energy carrier, will need decades but worldwide great efforts are made nowadays in the field of H_2 production, delivery, storage and utilization. In this view, an analysis of the potential of using the actual *NG* pipeline systems for the delivery of H_2 is a valid argument.

6.2 Differences between the properties of natural gas and hydrogen

The physical and chemical properties of H_2 differ significantly from those of *NG*. Table 5.14 shows some indicative values of relevant properties for the gas chain from source to end-user. As a result of these contrasting properties, a system designed for *NG* cannot be used without appropriate modifications for pure H_2, and vice versa. Even the addition of a certain percentage of H_2 to *NG* will have a direct impact on the combustion properties, on the diffusion into materials and on the behaviour of the gas mixture in air. These aspects are considered further below.

The addition of H_2 to the *NG* modifies its transport and calorific properties [Schouten et al., 2004]. Besides, a gas with higher H_2 content can have an impact on the safety of the *transmission-distribution-utilization chain*, the durability and the reliability of the gas pipeline and the utilization performances for the end-user.

Component	**Hydrogen**	**Methane**	**Unit**
Molecular mass	2.02	16.04	g/mol
Critical temperature	33.2	190.65	K
Critical pressure	13.15	45.4	bar
Heat capacity at constant pressure ($25°C$)	28.8	35.5	$J/mol.K$
Lower Heating Value (weight basis)	120	48	MJ/kg
Higher Heating Value (weight basis)	142	53	MJ/kg

Table 5.14: Physical properties of hydrogen and methane as the principal constituent of *NG*.

6.3 The impact of hydrogen on the natural gas system

In principle, H_2 can be added to *NG* in the high-pressure grid, in the medium pressure grid, or in the low pressure distribution grid; but it must be remembered that the existing system was designed and constructed specifically for *NG* and, as explained above, the physical and chemical properties of H_2 differ significantly from those of *NG*. In particular, the addition of H_2 to *NG* may have an impact on the following aspects:

- **Safety related to the transmission, distribution and use of gas**
  Aspects of pipeline systems, such as location, materials, wall thickness, safety devices, etc., are designed on the basis of risk assessments. For instance, the design criteria for a pipeline in a populated area differ from the criteria for a pipeline in the countryside. As H_2 is added, it will change the gas properties and, as a consequence, the related risks will change. An additional safety risk of using a *NG* system for H_2 may arise from the fact that the potential leakage rate of H_2 is much larger than that of *NG* through the same sized leak.

- **Integrity of pipelines**
  H_2 may diffuse into materials and change their mechanical properties. For example, H_2 embrittlement of steel, leading to an accelerated growth of micro cracks, is a well recognized phenomenon. H_2 may also diffuse through polymers, thus resulting in a significant loss of H_2. This may affect the integrity of the system and could also have an impact on safety. A related issue concerns condition monitoring and repair techniques of the delivery system.

- **Gas quality management**
  It should be ensured that end-users will remain supplied with gas that meets the contractual specific cautions in order to guarantee their safety, performance of end-user appliances and billing accuracy. Moreover, this is an issue if H_2 is extracted from the mixture, and the remaining gas is supplied to end-users further downstream.

- **The performance of end-user appliances**
  As the combustion properties change when H_2 is added to *NG*, this may also affect the performance of end-user appliances.

- **The energy capacity of the delivery system**
  The *NG* system is designed for the maximum capacity that may be required. As energy demand shows a pattern over the day, over the seasons and over the year, dynamic simulations are routinely used to optimize the layout and the dimensions of the systems. The delivery system not only moves gas from production to end-user, but it also adapts to the different patterns of supply and demand, and it must be capable of coping with fluctuations in composition of the gases entering the system. *Capacity* is the key issue of a *NG* system to ensure a sufficiently high level of security of supply, both volume and gas quality. If an existing pipeline system could be switched from *NG* to H_2 and still be operated at the same maximum pressure, its maximum capacity (measured in energy terms) would be approximately one third less with H_2 than with *NG* (the calorific value of H_2 in volume basis is about 1/3 of the value for *NG*, but H_2 can be transported with lesser friction resistance than *NG*). For the same reason, it is anticipated that the addition of H_2 to *NG* will reduce the capacity of a pipeline. Pipelines are usually not continuously loaded up to their full capacity and so, for most of the time, there will be, in principle, room for the addition of H_2, without limiting the energy transmission and distribution capacity of the delivery system.

- **Gas and energy losses**
  During the transmission, storage and distribution, the permeability of the walls of underground storages and of pipeline materials, etc., is higher for H_2 than for *NG*. In addition, leakage from small leaks will be increased. Next to feasible safety aspects, these losses also have economic and environmental aspects.

Some authors have examined H_2 transport by pipeline and a few reports discuss the use of existing *NG* pipelines to transport H_2 or *NG*-H_2 blends. These are also the main objectives of the *NATURALHY* project (supported by the European Commission within a Thematic Priority on Sustainable Energy Systems of the Sixth Framework Program) which investigates the conditions under which H_2 can be added to *NG* with acceptable consequences for safety, life cycle and socioeconomic aspects, durability of the system, gas quality management and performance of end-user appliances [Florisson et al., 2006].

Among the recent works, the influence of H_2 on the pressure drop in the pipelines has been calculated by [Schouten et al., 2004]. In Parker [2004], the construction costs of *NG* transmission pipelines have been analyzed and the impact of H_2 in the global cost has been studied. From an economic viewpoint, the cost of *NG* pipelines is a function of pipe diameter and the cost of a H_2 pipeline can be 50%-80% higher than that of a *NG* pipeline of the same size [Veziroglu and Barbir, 1998]. Regional transportation costs could be as much as five times higher than *NG*, primarily because of the lower volumetric energy density of H_2 [Whaley and Long, 2001]. Besides, H_2 embrittlement of the steel under the high pressures environment of H_2 constitutes a major concern: consequently, the transportation of a H_2-rich gas requires a great attention since H_2 embrittlement is characterized by a loss of ductility of the steel [Sherif et al., 2005].

Obviously, this section has not the ambition to give an answer to all questions that may arise, but may help to approach the potential challenges of the exploitation of H_2 as an energy carrier using current pipeline systems. The possibility of low amounts of H_2 injection into *NG* pipelines will be analyzed from a process engineering viewpoint in what follows.

6.4 Modelling extension to natural gas-hydrogen mixtures

A mathematical modelling of the gas transportation problem in networks was presented in Chapter 2. The model is general enough to take into account various gases: methane, ethane, propane and hydrogen. Note that a constraint concerning the fraction of hydrogen injected has been considered (Equation 5.2). Natural gas is composed by 70% methane, 25% ethane and 5% propane (Table 5.2). The material balance and equations of momentum conservation on the basic elements of the network, as well as the other governing equations presented in Chapter 2, constitute the modelling core of the gas pipeline hydraulics. It is assumed that the compressor performances represented by classical characteristic curves are compatible with the case of *NG*-H_2 (Equations 2.33 & 2.34).

$$0 < \Phi_{H_2} < 0.15 \tag{5.2}$$

The influence of the presence of hydrogen on the pipeline hydraulic is reflected in molecular weight and compressibility factor in Equation 2.5. Note

that the effect of the former is more significant than the latter. Since the presence of hydrogen reduces the molecular weight of the gas mixture (Equation 2.18), gas transportation by a fixed mass flow rate demands a higher pressure difference. For this reason, the pipelines transporting hydrogen require higher pressures.

Additional problems related to the optimization of the operating conditions can be treated with the same formulation by only changing the objective function. For instance, delivery pressure optimization for different hydrogen fractions in *NG*-H_2 mixtures is another interesting problem. This point will not be treated in this study.

6.5 Case study: Injecting hydrogen in a natural gas transportation network

6.5.1 Problem formulation

Hydrogen addition is examined in this section for the pipeline network showed in Figure 5.1. This example, used as a test bench, is enough representative of the elements that may take place in a real gas transportation network. Technical features of the *NG* transmission network are shown in Table 5.1. The composition of the *NG* is the same as the reference problem presented above (Table 5.2).

The *DOF* analysis gives 44 variables: 16 pressure variables governing the nodes, 21 flow rate variables (including fuel streams) corresponding to pipes and compressors, 6 rotational speeds of the compressors and the percentage of hydrogen injection), and 38 independent equations: 11 mass balances around nodes, 15 equations of motion for the pipe-arcs (Equation 2.18), 6 relationships between rotational speed, suction volumetric flow rate and head of each compressor (Equation 2.33) and 6 equations to calculate isentropic efficiency according to Equation 2.34. So the number of *DOF* is six, five rotational speeds and the percentage of hydrogen injection have been chosen as independent variables.

6.5.2 Problem solution

Three objectives have to be simultaneously optimized: minimizing the fuel consumption in compressor stations, maximizing the network throughput and maxi-

mizing the percentage of added hydrogen at the network entrance. The genetic algorithm *NSGA-IIb* coupled with a Newton-Raphson procedure of the MATLAB toolbox is implemented. As in the previous case, the genetic algorithm was run 10 times, requiring a total *CPU* time of 45 hours. The *3-D* Pareto front is displayed in Figure 5.4.

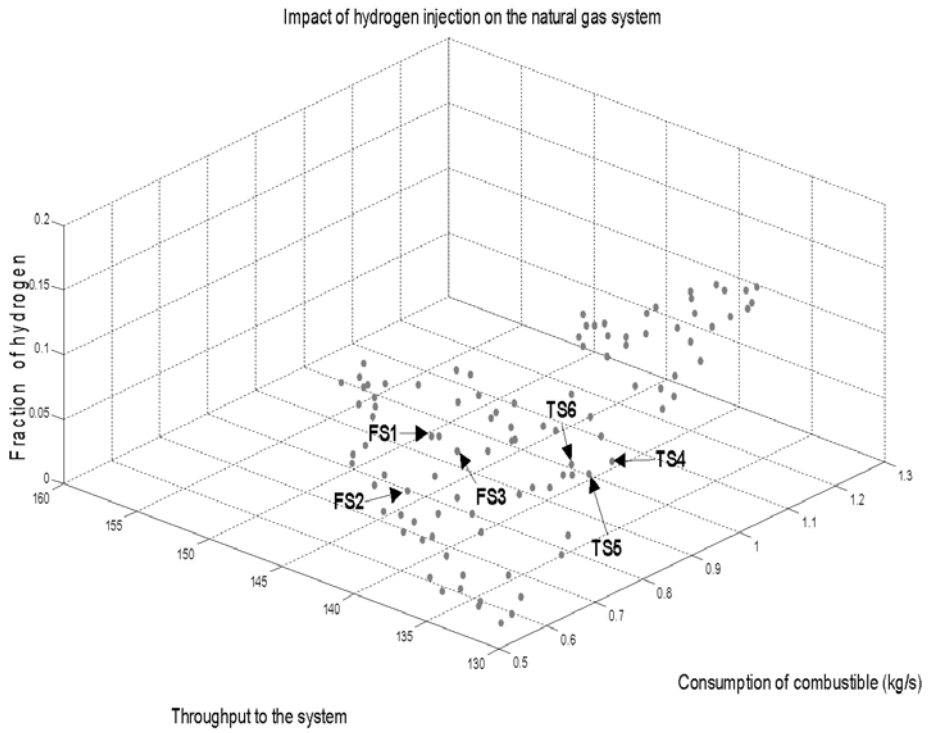

Figure 5.4: Graphical representation of the best solutions found by *TOPSIS* and *FUCA*.

6.6 Choice of the best solution

The *TOPSIS* and *FUCA* procedures were implemented for determining the three best solutions of the triobjective optimization problem. As in the biobjective case, the same weight has been assigned to the three objectives, either in *TOPSIS* and *FUCA*. They are denoted respectively: *TS4, TS5* and *TS6* for *TOPSIS* and *FS1, FS2* and *FS3* for *FUCA* in Figure 5.4. The goal is now to identify the best solution among the three proposed ones of each procedure. The results are displayed in Table 5.15. As in the biobjective optimization case, the chosen criterion is to minimize the euclidian norm of the distances between criteria $f_1 = 0.749\ kg/s$

and $f_2 = 150\ kg/s$ of the monobjective and the triobjective solutions (Table 5.16). So the selected solution is *FS1*, for which the corresponding values of pressures in the network are indicated in Table 5.17. Other values are listed in Table 5.18.

Objective	Fuel consumption $*f_1 = 0.749\ kg/s$	Throughput to the system $*f_2 = 150\ kg/s$	Percentage of hydrogen
TS4	0.783	131.619	0.087
TS5	0.745	131.984	0.083
TS6	0.763	133.748	0.079
FS1	0.844	146.096	0.033
FS2	0.737	144.165	0.019
FS3	0.811	143.245	0.041

$*$ Imposed by the monobjective case

Table 5.15: Best solutions found by using *TOPSIS* and *FUCA*.

Solution	Euclidian norm
TS4	18.38
TS5	18.01
TS6	16.25
FS1	3.905
FS2	5.835
FS3	6.755

Table 5.16: Selection of the best solution for the triobjective case.

Node	Pressure (bar)	Node	Pressure (bar)
P-0	61.200	*P-9*	54.839
P-1	47.475	*P-10*	54.783
P-2	47.146	*P-11*	54.680
P-3	47.251	*P-12*	54.806
P-4	47.310	*P-13*	65.113
P-5	63.981	*P-14*	65.535
P-6	63.861	*P-15*	65.126
P-7	63.982	*P-16*	65.017
P-8	63.749	*P-17*	58.800

Table 5.17: Pipeline network pressures for the best solution *FS1*.

Compressor	**C-1**	**C-2**	**C-3**	**C-4**	**C-5**	**C-6**
Discharge flow rate (kg/s)	49.095	48.115	49.195	45.229	52.598	48.269
Rotational speed (rps)	245.059	241.375	244.068	185.180	204.805	192.100
Fuel consumption (kg/s)	**0.181**	**0.174**	**0.180**	**0.091**	**0.118**	**0.100**
Consumption ratio (%)	0.368	0.360	0.364	0.202	0.224	0.207
Isentropic head (kJ/kg)	40.195	39.601	39.686	21.496	22.593	21.467
Isentropic efficiency (%)	73.256	73.656	73.135	71.570	67.865	69.705

Table 5.18: Optimal values for the compressor units for the best solution *FS1*.

6.7 Discussion

When going from monobjective to the best solution of biobjective optimization, the pressures in the network do not vary a lot, while the discharge flow rate, the rotational speeds and consequently the fuel consumption decrease.

Contradictory when going now to triobjective case, since the pipeline throughput has a similar value to the monobjective case, only a little injected fraction of hydrogen causes an increase in the pressures of the network, the discharge flow rate, the rotational speeds and consequently in the fuel consumption. As abovementioned, the principal hydraulic limiting factor for H_2 introduction in an existing pipeline is that H_2 specific volume is higher than this corresponding to *NG* which results in a strong decrease pipeline throughput and consequently in the transmitted energy. However, a part of the reduction in transmitted energy is compensated by the LHV of H_2 that is higher than the value corresponding to *NG*.

According to this study, an adaptation of the current networks of transmission of natural gas to the transport of hydrogen seems yet possible until low values that can be quantified with optimization tools, such as the network model proposed. More precisely, the quantitative amount of hydrogen that can be added to natural gas can be determined without neglecting the energy capability of the natural gas system.

Typical quantitative results are presented, showing that the addition of hydrogen to natural gas decreases significantly the transmitted power: the maximum fraction of hydrogen that can be added to natural gas is around 3% for this example. The observed reduction in the transmitted energy by the pipeline (7%) can be mainly attributed to the low molecular weight of hydrogen, i.e., about 10% of the value of *NG* (Table 5.14 and the role of molecular weight

in the equation of motion). Since the mass basis LHV of hydrogen is about 2.5 times of the corresponding value for NG, it reduces the impact of the low molecular weight of hydrogen on the reduction of the transmitted energy by the pipeline. Other parameters, such as compressibility factor, play a relatively minor role. Yet, it must be also that the diameters of the pipelines existing in the compressor stations are so small; so the gas average velocity tends to its upper limits (erosional velocity), when the amount of hydrogen increases. Consequently, the mass flow rate can not increase any more.

7 Conclusion

A mathematical modelling framework for gas pipeline networks was proposed in this study showing that efficient operation of compressor stations is of major importance for enhancing the performances of pipeline networks. In this chapter, a pipeline network system including two compressor stations is optimized. Some interesting results of the natural gas network under different operating conditions are presented by implementing two strategies of optimization: monobjective and multiobjective. Both procedures are devoted to the consideration of gas mass flow delivery maximization, fuel consumption minimization and amount of hydrogen injected maximization. In the monobjective case, a deterministic optimization procedure is used. In the biobjective case, a genetic algorithm and a ε-constraint method are implemented. From a comparative study, the genetic algorithm seems to be the most adequate method. So the genetic algorithm is used for solving a triobjective problem concerning hydrogen injection in the network.

In the monobjective study, the objective function is the total fuel consumption in the compressor stations to be minimized for a fixed gas delivery mass flow, since the reduction of the energy used in pipeline operations will have a significant economical impact. Typical results are analyzed and the characteristic values of some key parameters, like isentropic head and isentropic efficiency, are computed. The numerical results show that numerical optimization is an efficient tool for optimizing compressor rotational speeds, and can yield significant reductions in fuel consumption. The carbon dioxide emissions evaluated

at the optimal solution represent only 1.4% of the delivery gas, which is very acceptable.

For the biobjective study, the goal consists in simultaneously minimizing the total fuel consumption while maximizing the gas mass flow delivery. The problem is solved by means of a genetic algorithm and a ε-constraint procedure. Both methods give superimposed Pareto fronts, but the one from genetic algorithm is much larger than the one from ε-constraint. So the genetic algorithm is used in the last part of the chapter related to hydrogen injection in the gas transportation network. Along the Pareto front provided by the genetic algorithm, the carbon dioxide emissions vary from 1.1% to 1.8% of the *NG* mass flow delivery. So the optimization of compression operations yields significant savings for the fuel consumed in the stations, and thus has a real environmental impact. For instance, in the *NGTN* problem, the Pareto front supplies two significant information. First, bounds on the network capacity in terms of mass flow delivery and CO_2 emissions can be directly obtained from the curve. Second, for an imposed mass flow delivery that corresponds to practical case for a *NG* delivery company, the minimal fuel consumption directly linked to CO_2 emissions can be obtained by tuning compressor stations (particularly rotational speeds of compressors) at values provided by the optimizer.

Finally, a major interest of this work is to take into account the amount of hydrogen that can be added to the pipeline network traditionally devoted to the transportation of natural gas, without any modification in the system. Defining the conditions under which hydrogen can be added to natural gas constitutes a key point of this investigation as well as how much hydrogen can be injected into the existing pipeline network while minimizing fuel consumption and maximizing the pipeline throughput. The resolution of this triobjective optimization problem shows that the maximum achievable fraction of hydrogen that can be added to natural gas is around 3% mass for the studied example. However, addition of hydrogen to natural gas decreases the transmitted power significantly (of about 7%). According to this study, an adaptation of the current network of *NG* transmission to the transport of hydrogen seems yet possible.

In the multiobjective cases, some generic *MCDM* tools, like the *TOPSIS* and *FUCA* procedures, are used for choosing the best solution among the ones provided by the Pareto fronts. For the biobjective optimization case, *TOPSIS* is implemented for identifying the three best solutions of the Pareto front. Then,

by computing the euclidian norm of distances between these solutions and the one of the monobjective case, the best biobjective solution can be identified. A similar strategy is implemented in the triobjective problem. *TOPSIS* and *FUCA* are used for identifying the six best solutions on the *3-D* Pareto front and the distance between these six solutions and the monobjective one allows to find the best solution of the triobjective case.

A perspective of this work is now to treat more complex systems, including the conditions under which hydrogen can be added to natural gas with acceptable consequences for safety, durability of the system, gas quality management and performance of the end-user appliances, in the design and operation phase. In that context, the use of multiobjective optimization techniques, as it was strongly demonstrated in this work, still constitutes a natural way and stochastic algorithms, such as genetic algorithms, appear as serious candidates.

Conclusions and perspectives

6

Contents

The optimization of a *NG* transportation network *NGTN* is typically a multi-objective optimization problem, involving for instance energy consumption minimization at the compressor stations and gas delivery maximization. However, very few works concerning multiobjective optimization of *NGTN* are reported in the literature. The main goal of this study is to provide a general framework of formulation and resolution of multiobjective optimization problems related to *NGTN*. Moreover, this work attempts to provide a general methodology in a manner useful to both the scientist/engineer engaged in process development or design for finding the most appropriate operating conditions, while optimizing some objective function(s). Various multiobjective optimization techniques belonging to two main classes, scalarization and evolutionary techniques, can be used for engineering purposes. In that context, this work illustrates their application on a series of case studies covering a range of significant chemical process engineering problems. The idea is to implement, for a given mathematical model, a numerical method that meets the multi-criteria aspect which embeds both solution quality and resolution time. Of course, the variables and objective functions may differ, according to the problem which is considered; however, the nature of variables is always continuous in all treated cases.

From this comparative study, the choice of a stochastic procedure, namely a genetic algorithm, is performed since it is generally recognized that this kind of methods is particularly well-fitted to take into account the multi-criteria aspect, despite the important number of constraints that are likely to be involved in an engineering problem formulation. Adequate solvers of the MATLAB toolbox are used *(fmincon, fsolve)*, since this optimization tool is often considered as a standard for the solution of *Process Systems Engineering* problems.

Finally, a didactic natural gas transportation network is considered for mono, bi and triobjective optimization studies. An interesting topic concerning multi-objective optimization arises with the determination of a *good* solution on the Pareto front or set of efficient solutions. So, after the optimization phase, the next step consists in identifying the best one. It is a problem of *Multiple Choice Decision Making (MCDM)*, which is also a complex problem, mainly because of its more subjective nature, than the multiobjective optimization problem itself. Some generic tools are implemented for choosing the best solution on the Pareto front. The selected solution will be the one which degrades the least possible the values obtained in the monobjective optimization case. However, for indus-

trial problems, the practitioner may make his final decision according to some specific internal features of his company.

1 Modelling natural gas pipeline networks

A gas transportation modelling approach, that serves as a methodology framework, takes into account the elements of the network under steady-state conditions. This general framework contains some typical aspects:

- Mass and transportation equations;
- Compressor characteristics modelling through characteristic curves;
- Several constraints such as: maximum allowable operational pressure, critical velocity, erosional velocity, etc.

In this work, compressor stations, which consist of several identical centrifugal compressor units in parallel, are considered, since this type of station is very common in today's gas industry, and having an understanding of this type of station is fundamental for modelling more complex station configurations. Note that the model can take into account various compositions of gas mixtures.

Complementing the modelling core, various objectives can be considered to improve the operating conditions of a gas network system. Three types of objective functions are chosen for illustration purposes: fuel consumption minimization, pipeline throughput maximization and injected hydrogen maximization.

The use of the proposed strategy can help the gas network manager to answer these recurrent questions:

- Knowing that I need to deliver a certain volume of gas at certain key points, how do I utilize the compressors at my disposal most efficiently to reduce fuel gas consumption?
- How do I set the consequent pressures and flow rates?

Let us mention that characteristic values for compressor stations of some key parameters that may be useful for the practitioner (isentropic head, isentropic efficiency) are systematically computed. The results obtained show that numerical optimization is an effective tool for optimizing compressor speeds, and can

yield significant reductions in the fuel consumption. Finally, the global framework can help decision making for optimizing the operating conditions of gas networks, anticipating the changes that may occur (i.e. gas quality, variation in supply sources availability and consequences in maintenance) and quantifying CO_2 emissions.

A natural extension of this methodology is now to treat more complex systems. For instance, multi-supply multi-delivery transmission grids, which may be highly meshed. Hereby, a mixed integer nonlinear programming approach is recommended with binary variables representing flow directions. In that context, genetic algorithms appear as serious candidates.

1.1 Fuel consumption minimization

In the monobjective case, when the fuel consumption has to be minimized, natural gas transportation networks usually involves continuous variables, i.e., pressures at nodes and flow rates through pipes. When the flow directions can be easily predicted, the formulation is based on a nonlinear-programming procedure. In this case, compressor modelling occurs through the use of characteristic curves, as previously mentioned, and the search for their optimal operating conditions is carried out in the feasible operating domain for the unit. Using this objective function is particularly interesting, since reduction of the energy used in pipeline operations will not only have a beneficial economical impact, but also an environmental one: the more efficient the use of compressors stations is, the less greenhouse emissions are dissipated in the atmosphere.

1.2 Pipeline throughput maximization

In the monobjective methodology, the fuel consumption in the compressor stations was minimized for a given gas mass flow delivery. However, for a *NG* delivery company, the demand may vary, according to climatic conditions or industrial requirements. So, an interesting study which arises is to determine, for a given supply at the network entrance nodes, the minimal and maximal network capacities, in terms of *NG* mass flow delivery and fuel consumption in compressor stations.

1.3 Injected hydrogen maximization

The general framework approach applied to natural gas was easily extended to the case of Natural gas-Hydrogen mixture. The hydrogen properties are taken into account in the model: for instance, the compressibility factor is calculated from appropriate equations of state. Addition of hydrogen to natural gas decreases the pipeline throughput significantly. According to this study, an adaptation of the current networks of transmission of natural gas to the transport of hydrogen seems to be possible, until an upper limit on the percentage of injected hydrogen.

However, a major concern is now to include the conditions under which hydrogen can be added to natural gas with acceptable consequences for safety, durability of the system, gas quality management and performance of the end-user appliances, in the design and operation phase. In that context, the use of multiobjective optimization techniques, as it was strongly demonstrated in this work, still constitutes a natural way.

2 Optimization strategies: from monobjective to multiobjective optimization

Nowadays, most of optimization studies in process engineering have to be performed within a multiobjective framework, where some objectives related to environmental impacts, security, etc, must be simultaneously optimized with classical economic or technical criteria. In natural gas network optimization problems, a lack of published works on multiobjective optimization can be observed, and this thesis aims at filling this gap.

2.1 Monobjective methodology

In the monobjective case, where the fuel consumption at compression stations has to be minimized, classical *NLP* solvers of the *GAMS* package and the MATLAB toolbox are used. They give the same results, but *GAMS* is faster than MATLAB, which is an interpreted language. The genetic algorithm was not implemented, because it has been developed only for multiobjective optimization problems.

2.2 Multiobjective methodology

Among the most commonly used approaches in multiobjective optimization - scalarization and evolutionary procedures-, a deeply study was carried out. Three specific algorithms: Weighted-sum, ε-constraint and Genetic algorithm are detailed. For Weighted-sum and ε-constraint, some improvements concerning the density of the Pareto fronts are carried out. Indeed, among the diversity of optimization methods, the choice of the relevant technique for the treatment of a given problem keeps being a delicate issue. A comparative study in the biobjective case is on the basis of two mathematical problems, four process engineering examples and the gas transportation network. So, due to the resolution time as well as the aspects related to the quantity and quality of results, a genetic algorithm has been used.

Optimal solutions to one objective may contradict optimal solutions of the other ones; therefore, a solution to the problem will entail mutual sacrifice (trade-off) of objectives. The choice of the *best* solution among the ones displayed on the Pareto front is a typical *Multiple Choice Decision Making* problem. In the biobjective case, the generic method *TOPSIS* is used, and in the triobjective study, *TOPSIS* on the one hand, and *FUCA* on the other hand, a new procedure recently developed in the research group, are implemented.

3 Future works

3.1 Resolution time

Except for *CPU* time, the conclusions about resolution times are to be taken carefully, because the only developer was the thesis author. To obtain reasonable evaluations of the resolution times, it would have been necessary that several developers with different backgrounds solve the test problems.

3.2 Flow directions in the network

A natural extension of the developed methodology is to treat more complex systems. For instance, multi-supply multi-delivery transmission grids which may be highly meshed. Hereby, a mixed integer nonlinear programming approach is recommended with binary variables representing flow directions.

3.3 Environmental impacts

Carbon dioxide emissions are studied a posteriori, after the problem solutions are obtained. A better way would consist in introducing environmental impacts, like for example *GWP* (Global Warming Potential), in the set of objectives of the multiobjective optimization problem.

3.4 Uncertainty modelling

Another extension that could increase the realism of the model is to consider uncertainty in the demand. The most common approaches treated in the dedicated literature represent the demand uncertainty with a probabilistic frame by means of Gaussian distributions. Yet, this assumption does not seem to be a reliable representation of the reality, since in practice the parameters are interdependent, leading to very hard computations of conditional probabilities.

Fuzzy concepts and arithmetic constitute an alternative to describe the imprecise nature on product demands. This reinforces the interest of using genetic algorithms, since similar problems were treated previously by extension of a multiobjective genetic algorithm [Lasserre, 2006; Pérez Escobedo, 2010] to fuzzy objectives.

3.5 Other evolutionary methods

Other evolutionary procedures, like particle swarms, colonies of social insects (ants, bees) should be tested for solving multiobjective optimization problems related to *NGTN*.

Conclusions et perspectives

L'optimisation de réseaux de transport de gaz naturel *(RTGN)* est typiquement un problème multiobjectif où, par exemple, la consommation d'énergie dans les stations de compression doit être minimisée et le débit de gaz livré maximisé. Toutefois, peu de travaux concernant l'optimisation multiobjectif de *RTGN* sont décrits dans la littérature. L'objectif de cette étude est d'établir un cadre général de formulation et de résolution des problèmes multiobjectif relatifs aux *RTGN*. De plus, ce travail fournit des résultats utiles sur le plan scientifique et de l'ingénierie, en déterminant les conditions optimales d'exploitation d'un réseau de façon à optimiser certaines fonctions objectif. Plusieurs techniques d'optimisation relevant des deux principales classes, scalarisation et évolutionnaire, peuvent être mises en œuvre en ingénierie. Ce travail illustre leur application sur plusieurs cas d'étude, couvrant un certain nombre de problèmes de génie des procédés. L'objectif est de choisir, pour une modélisation donnée d'un problème, la méthode numérique qui fournit une solution de qualité, en un temps de résolution raisonnable. Bien sûr, les variables et les fonctions objectifs diffèrent selon les problèmes mais, dans tous les cas, les variables sont continues dans ce mémoire.

Cette étude comparative conduit à retenir une procédure stochastique, plus précisément un algorithme génétique, dont l'adéquation au traitement de problèmes multiobjectif est unanimement reconnue, bien que les problèmes d'ingénierie puissent faire apparaître un nombre conséquent de contraintes, ce qui peut pénaliser ce type de procédure. Des solveurs adéquats de la boîte à

outils MATLAB *(fmincon, fsolve)*, qui est reconnue comme un standard pour la résolution de problèmes de *Process Systems Engineering*, sont utilisés.

Enfin, un exemple didactique de *RTGN* est considéré pour une optimisation mono, bi et triobjectif. Un problème majeur soulevé par l'optimisation multiobjectif est la détermination d'une bonne solution, parmi toutes celles figurant sur un front de Pareto. Ainsi, après la phase d'optimisation, vient celle d'aide à la décision, en présence de choix multiples. De par sa nature subjective, ce problème peut être aussi complexe que l'optimisation multiobjectif elle-même. Certains outils génériques d'aide à la décision sont mis en œuvre pour déterminer la *meilleure* solution sur un front de Pareto. La solution retenue sera celle qui dégrade le moins possible les valeurs fournies par l'optimisation monobjectif. Bien évidemment, le praticien industriel pourra prendre la décision finale, en considérant de plus des aspects internes à sa compagnie.

1 Modélisation des réseaux de transport de gaz naturel

La modélisation des réseaux de transport de gaz naturel est effectuée en se plaçant en régime stationnaire. Les principaux aspects intervenant dans cette modélisation concernent :

- Les équations de bilan matière et de transport ;
- Les propriétés des compresseurs exprimées par des courbes caractéristiques ;
- Des contraintes, telles que la pression opératoire maximale autorisée, la vitesse critique, la vitesse d'érosion, etc.

Dans ce travail, on considère des stations de compression composées de plusieurs compresseurs centrifuges en parallèle, dans la mesure où ce type de station est très répandu actuellement dans l'industrie gazière. Définir un modèle précis pour ce type de station est fondamental pour déterminer les modèles de stations encore plus complexes. Il convient de remarquer que le modèle s'adapte à différentes compositions du gaz naturel.

En complément de la modélisation mathématique, plusieurs fonctions objectifs et problèmes d'optimisation peuvent être considérés, de façon à améliorer les conditions opératoires du réseau. Trois types de problèmes ont été abordés :

la minimisation de la consommation de fuel dans les stations de compression, la maximisation du débit de gaz en sortie du réseau et la maximisation du pourcentage d'hydrogène injecté dans le réseau.

La stratégie proposée peut aider l'exploitant du réseau de gaz à répondre aux questions récurrentes suivantes :

- Connaissant la quantité de gaz à livrer à des points donnés du réseau, comment dois-je utiliser les compresseurs dont je dispose pour réduire la consommation d'énergie?
- En conséquent, comment dois-je fixer les pressions et les débits dans le réseau?

Il convient de remarquer que les valeurs de certains paramètres clés utiles au praticien (hauteur et efficacité isentropique) sont systématiquement reportées après la phase d'optimisation. Les résultats obtenus montrent que l'optimisation est un outil puissant pour déterminer les vitesses de rotation des compresseurs, et conduit à des réductions significatives de la consommation de fuel. Enfin, ce cadre de modélisation, qui conduit à l'optimisation des conditions opératoires d'un réseau, peut également aider à anticiper des variations qui peuvent survenir dans la composition du gaz, dans les débits de livraison et donc sur les conditions de maintenance, et permet aussi de quantifier les émissions de CO_2.

1.1 Minimisation de la consommation de fuel

Dans le cas monobjectif, où la consommation de fuel doit être minimisée, lorsque les directions des flux sont spécifiées, les *RTGN* ne comportent que des variables continues, associées aux pressions et aux débits dans les tuyaux. Le problème est de type *NLP (NonLinear Programming)*. L'utilisation des courbes caractéristiques issues de la modélisation des compresseurs permet de déterminer le domaine acceptable pour chaque compresseur, ce qui définit l'espace de recherche dans lequel les conditions opératoires optimales seront déterminées. Considérer la consommation de fuel est un point particulièrement intéressant, car la réduction de la consommation d'énergie dans le réseau a un impact non seulement économique, mais également environnemental : une utilisation plus efficace des stations de compression s'accompagne d'une diminution des rejets de gaz à effet de serre dans l'atmosphère.

1.2 Maximisation du débit de livraison

Dans le cas monobjectif, la consommation de fuel dans les stations de compression est minimisée pour un débit de livraison de gaz naturel donné. Cependant, pour une compagnie assurant la distribution de gaz, la demande peut varier en fonction des conditions climatiques ou des besoins industriels. Ainsi, une question intéressante est de déterminer, pour une capacité d'approvisionnement donnée, les capacités minimale et maximale du réseau, en termes de livraison de gaz et de consommation de fuel dans les stations de compression.

1.3 Maximisation du pourcentage d'hydrogène injecté dans le réseau

Le cadre général relatif au gaz naturel peut être étendu au cas de mélanges de gaz naturel et d'hydrogène. Les propriétés de l'hydrogène peuvent aisément être prises en compte par le modèle, par exemple le facteur de compressibilité est calculé à partir d'équations d'état appropriées. L'addition d'hydrogène a pour effet de réduire significativement le débit de sortie du réseau. Toutefois, cette étude montre que l'adaptation de *RTGN* existants au transport d'hydrogène semble possible, jusqu'à une limite supérieure du pourcentage d'hydrogène injecté.

Cependant, la préoccupation majeure est de tenir compte des conditions sous lesquelles l'hydrogène peut être ajouté au gaz naturel, avec des conséquences acceptables pour la sécurité, la durabilité du réseau, la gestion de la qualité du gaz, et les performances attendues par les utilisateurs. Dans ce contexte, les techniques d'optimisation multiobjectif constituent une voie naturelle d'approche du problème.

2 Stratégies d'optimisation : du cas monobjectif à l'optimisation multiobjectif

De nos jours, la plupart des études d'optimisation en génie des procédés doivent être effectuées dans un cadre multiobjectif, où certains critères relatifs aux impacts environnementaux, à la sécurité, etc., doivent être simultanément optimisés avec les critères techniques ou économiques classiques. Toutefois, en ce qui concerne les *RTGN*, les travaux publiés en optimisation multiobjectif sont rares, et cette thèse vise à combler cette déficience.

2.1 Optimisation monobjectif

Dans le cas monobjectif, où la consommation de fuel dans les stations de compression doit être minimisée, des solveurs *NLP* classiques de la bibliothèque *GAMS* ou de la boîte à outils MATLAB sont utilisés. Les deux types de procédures donnent les mêmes résultats, mais *GAMS* est plus rapide que MATLAB, qui est un langage interprété. L'algorithme génétique n'a pas été mis en œuvre, car il a été développé uniquement pour des applications multiobjectif.

2.2 Optimisation multiobjectif

Parmi les méthodes les plus couramment utilisées en optimisation multiobjectif : scalarisation et techniques évolutionnaires, une étude a été menée en profondeur. Trois procédures spécifiques : somme pondérée, ε-contrainte et algorithme génétique sont détaillées. Pour les méthodes de somme pondérée et ε-contrainte, des améliorations concernant la densité du front de Pareto ont été apportées. Toutefois, le choix de la procédure la plus appropriée au traitement d'un problème particulier est une tâche délicate. Une étude comparative sur des problèmes biobjectif a été menée sur la base de deux exemples mathématiques, quatre problèmes de génie des procédés et un *RTGN*. En raison du temps de résolution, aussi bien que la qualité et la quantité des résultats fournis, un algorithme génétique a été retenu.

Une bonne solution, selon l'un des critères, peut être très mauvaise vis-à-vis des autres, donc le choix de la solution globale d'un problème multiobjectif nécessite de faire des compromis. La sélection de la meilleure solution, parmi toutes celles du front de Pareto, est typiquement un problème d'aide à la décision, en présence de choix multiples. Dans le cas de problèmes biobjectif, la méthode générique *TOPSIS* est mise en œvre, et pour les problèmes triobjectif, la méthode *TOPSIS* d'une part, et la procédure *FUCA* récemment développée dans le groupe de recherche, sont implémentées.

3 Perspectives

3.1 Temps de résolution

Mis à part les temps *CPU*, les conclusions au sujet des temps de résolution doivent être prises avec beaucoup de précaution, parce que le seul développeur a été l'auteur de la présente thèse. Pour avoir des estimations plus fiables des temps de résolution, il faudrait faire intervenir plusieurs développeurs ayant des formations différentes.

3.2 Directions des écoulements dans le réseau

Une extension naturelle de la méthodologie développée ici est de traiter des systèmes plus complexes, avec plusieurs points d'alimentation et plusieurs points de livraison, et où la direction des écoulements n'est pas fixée a priori. Il s'agit là d'un problème *MINLP (Mixed-Integer NonLinear Programming)* dans lequel les variables binaires sont associées aux directions des flux.

3.3 Impacts environnementaux

Les émissions de dioxyde de carbone ont été étudiées a posteriori, après avoir obtenu la solution du problème. Une procédure plus efficace pourrait consister à introduire des impacts environnementaux, comme par exemple le *GWP (Global Warming Potential)* dans l'ensemble des critères à optimiser.

3.4 Prise en compte des incertitudes

Une autre extension, qui pourrait conférer au modèle un caractère plus réaliste, est de considérer des incertitudes sur la demande. Une méthode que l'on retrouve souvent dans la littérature est l'utilisation de lois de distribution de probabilité, souvent gaussiennes, pour modéliser l'incertitude. Mais cette approche est délicate à mettre en œvre dans la pratique, car de nombreux paramètres sont interdépendants, conduisant à des calculs très complexes pour les probabilités conditionnelles.

Les concepts et l'arithmétique flous constituent une alternative intéressante pour aborder l'imprécision. Ce-ci renforce l'intérêt d'utiliser des algorithmes génétiques, dans la mesure où des problèmes de ce type ont déjà été traités dans

notre groupe de recherche, par extension d'algorithmes génétiques multiobjectif au cas de critères flous [Lasserre, 2006; Pérez Escobedo, 2010].

3.5 Autres procédures évolutionnaires

Enfin, d'autres procédures évolutionnaires, telles que par exemple les essaims de particules ou les colonies d'insectes sociaux, pourraient être testées, pour traiter des problèmes relatifs aux *RTGN*.

Bibliography

Abbaspour, M., K. Chapman, and P. Krishnaswami (2005). Nonisothermal compressor station optimization. *Journal of Energy Resources Technology 127*, 131–141.

Acevedo, J. and E. Pistikopoulos (1996). A parametric MINLP algorithm for process synthesis problems under uncertainty. *Industrial & engineering chemistry research 35*(1), 147–158.

Agrawal, N., G. Rangaiah, A. Ray, and S. Gupta (2006). Multi-objective optimization of the operation of an industrial low-density polyethylene tubular reactor using genetic algorithm and its jumping gene adaptations. *Ind. Eng. Chem. Res 45*(9), 3182–3199.

André, J. (2010). *Optimisation des investissements sur les réseaux de gaz*. Ph. D. thesis, Université Lille Nord de France.

André, J., F. Bonnans, and L. Cornibert (2006). Planning reinforcement on gas transportation networks with optimization methods. In *Operational Research Models and Methods in the Energy Sector (ORMMES 2006)*.

Ang, J., C. Goh, E. Teoh, and A. Mamun (2007). Multi-objective evolutionary Recurrent Neural Networks for system identification. In *Evolutionary Computation, 2007. CEC 2007. IEEE Congress*, pp. 1586–1592. IEEE.

Babonneau, F., Y. Nesterov, and J. Vial (2009). Design and operations of gas transmission networks. *CORE Discussion Papers 1*, 1–31.

Babu, B. and R. Angira (2005). Optimal design of an auto-thermal ammonia synthesis reactor. *Computers & chemical engineering 29*(5), 1041–1045.

Bandyopadhyay, S., S. Saha, U. Maulik, and K. Deb (2008). A simulated annealing-based multiobjective optimization algorithm: AMOSA. *Evolutionary Computation, IEEE Transactions 12*(3), 269–283.

Berard, G. and B. Eliason (1978). An improved gas transmission system simulator. *Old SPE Journal 18*(6), 389–398.

Biegler, L. and I. Grossmann (2004). Retrospective on optimization. *Computers & Chemical Engineering 28*(8), 1169–1192.

Botros, K. (1989). Dynamic simulation of compressor station installations including control systems. In *PSIG Annual Meeting*.

Botros, K. (1990). Thermodynamic aspects of gas recycling during compressor surge control. In *Pipeline Engineering Symposium 1990- Presented at the Thirteenth Annual Energy-Sources Technology Conference and Exhibition, New Orleans, LO, USA, 01/14-18/90*, pp. 57–65.

Botros, K. (1994). Transient phenomena in compressor stations during surge. *Journal of engineering for gas turbines and power 116*, 133–143.

Botros, K., P. Campbell, and D. Mah (1991). Dynamic simulation of compressor station operation including centrifugal compressor and gas turbine. *Journal of Engineering for Gas Turbines and Power 113*, 1–23.

Bracken, J., G. McCormick, and R. A. C. M. VA. (1968). *Selected applications of nonlinear programming*. Wiley New York.

Branke, J., K. Deb, H. Dierolf, and M. Osswald (2004). Finding knees in multiobjective optimization. In *Parallel Problem Solving from Nature-PPSN VIII*, pp. 722–731. Springer.

Bryant, M. (1997). Complex compressor station modeling. In *PSIG Annual Meeting*.

Cameron, I. (1999). Using an excel-based model for steady state and transient simulation. In *31st Annual Meeting Pipeline Simulation Interest Group (PSIG)*, pp. 20–22.

Carter, R. (1996). Compressor station optimization: Computational accuracy and speed. In *28th Annual Meeting, Pipeline Simulation Interest Group*.

Castello, P., E. Tzimas, P. Moretto, and S. Peteves (2005). Techno-economic assessment of hydrogen transmission & distribution systems in europe in the medium and long term. *European Commission, Joint Research Center 1*, 1–20.

Chafekar, D., L. Shi, K. Rasheed, and J. Xuan (2005). Multiobjective GA optimization using reduced models. *Systems, Man, and Cybernetics, Part C: Applications and Reviews, IEEE Transactions 35*(2), 261–265.

Chakraborti, N., P. Mishra, A. Aggarwal, A. Banerjee, and S. Mukherjee (2006). The Williams and Otto Chemical Plant re-evaluated using a Pareto-optimal formulation aided by Genetic Algorithms. *Applied Soft Computing 6*(2), 189–197.

Chankong, V. and Y. Haimes (1983). *Multiobjective decision making: theory and methodology*. North-Holland, New York.

Chauvelier-Alario, C., B. Mathieu, and C. Toussaint (2006). Decision making software for Gaz de France distribution network operators: CARPATHE. In *Proc. of 23rd World Gas Conference, Amsterdam, The Netherlands*.

Chen, Y., K. Li, H. Xu, and S. Liu (2009). A DEA-TOPSIS method for multiple criteria decision analysis in emergency management. *Journal of Systems Science and Systems Engineering 18*(4), 489–507.

Cobos-Zaleta, D. and R. Ríos-Mercado (2002). A MINLP model for minimizing fuel consumption on natural gas pipeline networks. In *Proceedings of the XI Latin-Ibero-American Conference on Operations Research*.

Coello, C. and R. Becerra (2009). Evolutionary Multiobjective Optimization in Materials Science and Engineering. *Materials and Manufacturing Processes 24*(2), 119–129.

Coello Coello, C. A. (2009, February). List of References on Evolutionary Multiobjective Optimization. www.lania.mx/ ccoello/EMOO/EMOObib.html.

Collette, Y. and P. Siarry (2002). *Optimisation multiobjectif*. Eyrolles.

Costa, A., J. Medeiros, and F. Pessoa (1998). STEADY-STATE modeling and simulation of pipeline networks for compressible fluids. *Brazilian Journal of Chemical Engineering 15*(4), 344–357.

De Weck, O. (2004). Multiobjective optimization: History and promise. In *China-Japan-Korea Joint Symposium on Optimization of Structural and Mechanical Systems*, pp. 1–14.

De Wolf, D. (1992). *Optimisation de réseaux de transport de gaz avec considération des pertes de charge dans le gazoducs*. Ph. D. thesis, Université Catholique de Louvain.

Deb, K. (2001). *Multi-objective optimization using evolutionary algorithms*. Wiley.

Deb, K., A. Pratap, S. Agarwal, and T. Meyarivan (2002). A fast and elitist multiobjective genetic algorithm: NSGA-II. *Evolutionary Computation, IEEE Transactions 6*(2), 182–197.

Di Bella, C. and W. Stevens (1965). Process optimization by nonlinear programming. *Industrial & Engineering Chemistry Process Design and Development 4*(1), 16–20.

Ding, Y., S. Gregov, O. Grodzevich, I. Halevy, Z. Kavazovic, O. Romanko, T. Seeman, R. Shioda, and F. Youbissi (2006). Discussions on Normalization and Other Topics in Multi-Objective Optimization. Technical report, Algorithmics Group, Fields Industrial Problem Solving Workshop.

Doonan, A., I. Fletcher, C. Cox, and W. Arden (1998). Evaluation of a remote boundary pressure control strategy using simulink. In *Control'98. UKACC International Conference on (Conf. Publ. No. 455)*, Volume 1, pp. 129–134. IET.

Dorigo, M. (1992). *Optimization, learning and natural algorithms*. Ph. D. thesis, Politecnico di Milano, Italy.

Droste, S., T. Jansen, and I. Wegener (2002). Optimization with randomized search heuristics–the (a)nfl theorem, realistic scenarios, and difficult functions. *Theoretical Computer Science 287*(1), 131 – 144.

Edgar, T. and D. Himmelblau (1970). *Optimization of chemical processes*. McGraw-Hill Book Company.

Edgar, T. F., D. M. Himmelblau, and L. S. Lasdon (2001). *Optimization of Chemical Processes*. McGraw-Hill, New York.

Ehrgott, M. and S. Ruzika (2008). Improved ε-constraint method for multiobjective programming. *Journal of Optimization Theory and Applications 138*(3), 375–396.

Engau, A. and M. Wiecek (2007). Generating ε-efficient solutions in multiobjective programming. *European Journal of Operational Research 177*(3), 1566–1579.

Farmer, J., N. Packard, and A. Perelson (1986). The immune system, adaptation, and machine learning. *Physica D: Nonlinear Phenomena 22*(1-3), 187–204.

Fauer, D. (2002). The making of a useful pipeline simulation model. In *PSIG Annual Meeting*.

Figueira, J., S. Greco, and M. Ehrgott (2005). *Multiple criteria decision analysis: state of the art surveys*. Springer Verlag.

Florisson, O., I. Alliat, B. Lowesmith, and G. Hankinson (2006). The value of the existing natural gas system for hydrogen, the sustainable future energy carrier (progress obtained in the naturalhy-project). In *23rd World Gas Conference, Amsterdam*.

Fonseca, C. and P. Fleming (1998). Multiobjective optimization and multiple constraint handling with evolutionary algorithms. I. A unified formulation. *Systems, Man and Cybernetics, Part A: Systems and Humans, IEEE Transactions 28*(1), 26–37.

Fonseca, C., P. Fleming, et al. (1993). Genetic algorithms for multiobjective optimization: Formulation, discussion and generalization. In *Proceedings of the fifth international conference on genetic algorithms*, Volume 423, pp. 416–423. Citeseer.

Gomez, A. (2008). *Optimisation technico-économique multiobjectif de systèmes de conversion d'énergie: cogénération électricité-hydrogène à partir d'un réacteur nucléaire de IVème génération.* Ph. D. thesis, Université de Toulouse.

Gomez, A., L. Pibouleau, C. Azzaro-Pantel, S. Domenech, C. Latgé, and D. Haubensack (2010). Multiobjective genetic algorithm strategies for electricity production from generation IV nuclear technology. *Energy Conversion and Management 51*(4), 859–871.

Gorla, R. and A. Khan (2003). *Turbomachinery: design and theory*. Taylor & Francis Group.

Greyvenstein, G. and D. Laurie (1994). A segregated cfd approach to pipe network analysis. *International journal for numerical methods in engineering 37*(21), 3685–3705.

Griffiths, E. J. and P. Orponen (2005). Optimization, block designs and no free lunch theorems. *Information Processing Letters 94*(2), 55 – 61.

Grigson, C. (1992). Drag losses of new ships caused by hull finish. *Journal of ship research 36*(2), 182–196.

Grossmann, I. (2002). Review of nonlinear mixed–integer and disjunctive programming techniques. *Optimization and Engineering 3*(3), 227–252.

Hao, J., P. Galinier, and M. Habib (1999). Metaheuristiques pour l'optimisation combinatoire et l'affectation sous contraintes. *Revue d'Intelligence Artificielle 13*(2), 283–324.

Hoeven, T. (1992). Some mathematical aspects of gas network simulation. In *PSIG Annual Meeting*.

Holland, J. (1975). Adaptation in natural and artificial systems. *Ann Arbor: University of Michigan Press 134*, 1–30.

Horn, J., N. Nafpliotis, and D. Goldberg (1994). A niched Pareto genetic algorithm for multiobjective optimization. In *Evolutionary Computation, 1994. IEEE World Congress on Computational Intelligence., Proceedings of the First IEEE Conference*, pp. 82–87.

Isermann, R. E. et al. (1988). Computational experience concerning payoff tables and minimum criterion values over the efficient set. *European Journal of Operational Research 33*(1), 91–97.

Jenicek, T. and J. Kralik (1995). Optimized control of generalized compressor station. In *PSIG Annual Meeting*.

Jin, Y., M. Olhofer, and B. Sendhoff (2001). Dynamic weighted aggregation for evolutionary multi-objective optimization: Why does it work and how. In *Proceedings of the Genetic and Evolutionary Computation Conference (GECCO 2001)*, pp. 1042–1049. Citeseer.

Jones, D. (1995). *Elements of petroleum processing*. Wiley.

Kennedy, J. and R. Eberhart (1995). Particle swarm optimization. In *Neural Networks, 1995. Proceedings., IEEE International Conference*, Volume 4, pp. 1942–1948.

Kim, I. and O. de Weck (2005). Adaptive weighted sum method for bi-objective optimization: Pareto front generation. *Structural and Multidisciplinary Optimization 29*(1), 149–158.

Kim, I. and O. de Weck (2006). Adaptive weighted sum method for multiobjective optimization: a new method for Pareto front generation. *Structural and Multidisciplinary Optimization 31*(2), 105–116.

Kim, J., S. Park, and I. Lee (1997). Multiobjective optimization of structures using modified e-Constraint approach. Technical report.

Kirkpatrick, S., D. Jr., and M. Vecchi (1983). Optimization by simulated annealing. *science 220*(4598), 671–680.

Kocis, G. and I. Grossmann (1987). Relaxation strategy for the structural optimization of process flow sheets. *Industrial & engineering chemistry research 26*(9), 1869–1880.

Konak, A., D. Coit, and A. Smith (2006). Multi-objective optimization using genetic algorithms: A tutorial. *Reliability Engineering & System Safety 91*(9), 992–1007.

Kruse, B., S. Grinna, and C. Buch (2002). Hydrogen statu sog muligneter. Technical report, Bellona Foundation, Oslo, Norway.

Ksasy, M. S. M., F. Areed, S. Saraya, and M. Khalik (2010). Optimal reactor length of an auto-thermal ammonia synthesis reactor. *International Journal of Electrical & Computer Sciences 10*(3), 6–15.

Lasserre, A. A. (2006). *Approche multicritére pour la conception d'ateliers discontinus dans un environnement incertain*. Ph. D. thesis, Institut National Polytechnique de Toulouse.

Lazzaretto, A. and A. Toffolo (2004). Energy, economy and environment as objectives in multi-criterion optimization of thermal systems design. *Energy 29*(8), 1139–1157.

Letniowski, F. (1993). Compressor station modeling in networks. In *25th Annual Meeting of Pipeline Simulation Interest Group (PSIG), Pittsburgh, Pennsylvania*.

Li, W. and M. Guangwen (1990). Application of multi-objective programming with analytical hierarchy process to river water quality management. *The Hydrological Basis for Water Resources Management 1*(197), 193–198.

Luus, R. (1978). Optimization of systems with multiple objective functions. In *European Federation of Chemical Engineering*.

Luus, R. and T. Jaakola (1973). Optimization by direct search and systematic reduction of the size of search region. *AIChE Journal 19*(4), 760–766.

Mansouri, S., S. Hendizadeh, and N. Salmasi (2007). Bicriteria two-machine flowshop scheduling using metaheuristics. In *Proceedings of the 9th annual conference on Genetic and evolutionary computation*, pp. 909–909. ACM.

Mavrotas, G. (2006). Generation of efficient solutions in Multiobjective Mathematical Programming problems using GAMS. Effective implementation of the ε-constraint method. Technical report, Citeseer.

Mavrotas, G. (2009). Effective implementation of the [epsilon]-constraint method in Multi-Objective Mathematical Programming problems. *Applied Mathematics and Computation 213*(2), 455–465.

Menon, E. (2005). *Gas pipeline hydraulics*. Taylor & Francis Group.

Metcalf, J. (2000). Effects of compressor valves on reciprocating compressor performance. In *Proceedings of the 2000 Gas Machinery Conference*.

Miettinen, K. (1999). *Nonlinear multiobjective optimization*. Springer.

Mintz, M., S. Folga, J. Gillette, and J. Molburg (2002). Hydrogen: On the horizon or just a mirage? *Society of Automotive Engineers, Inc. 1*, 1–11.

Mohitpour, M., W. Thompson, and B. Asante (1996). The importance of dynamic simulation on the design and optimization of pipeline transmission systems. In *Proceedings of the International Pipeline Conference*, pp. 1183–1188.

Mohring, J., J. Hoffmann, T. Halfmann, A. Zemitis, G. Basso, and P. Lagoni (2004). Automated model reduction of complex gas pipeline networks. In *Proceedings of the 36th Annual Meeting of Pipeline Simulation Interest Group, Palm Springs, California*.

Mora, T. and M. Ulieru (2005). Minimization of energy use in pipeline operations-an application to natural gas transmission system. In *Industrial Electronics Society, 2005. IECON 2005. 31st Annual Conference of IEEE*, pp. 2190–2197.

Moralez-Mendoza, L., J. Perez-Escobedo, A. Aguilar-Lasserre, C. Azzaro-Pantel, L. Pibouleau, and S. Domenech (2011). Selecting the best alternative based on a hybrid Multiobjective GA-MCDM approach for New Product Development in the pharmaceutical industry. In *IEEE Symposium on Swarm Intelligence*.

Murase, A., H. Roberts, and A. Converse (1970). Optimal thermal design of an autothermal ammonia synthesis reactor. *Industrial & Engineering Chemistry Process Design and Development 9*(4), 503–513.

Nakrani, S. and C. Tovey (2004). On honey bees and dynamic server allocation in internet hosting centers. *Adaptive Behavior 12*(3-4), 223.

Nestor, M., O. Oscar, and S. Ivan (2002). Natural gas network optimization and sensibility analysis. In *SPE International Petroleum Conference and Exhibition in Mexico*.

Obayashi, S., K. Deb, C. Poloni, and M. Tadahiko (1999). *Evolutionary multi-criterion optimization*. Springer.

Odom, F. and F. Langenbacher (1990). Tutorial on Modeling Gas Turbine Driven Centrifugal Compressors. In *22nd Annual Meeting Pipeline Simulation Interest Group (PSIG)*, pp. 18–19.

Opricovic, S. and G. Tzeng (2004). Compromise solution by MCDM methods: A comparative analysis of VIKOR and TOPSIS. *European Journal of Operational Research 156*(2), 445–455.

Osiadacz, A. (1987). *Simulation and analysis of gas networks*. Gulf Publishing Company, Houston, TX.

Oski, J. (1988). *Multicriteria truss optimization*. Springer.

Ouyang, L. and K. Aziz (1996). Steady-state gas flow in pipes. *Journal of Petroleum Science and Engineering 14*(3-4), 137–158.

Papalexandri, K. and T. Dimkou (1998). A parametric mixed-integer optimization algorithm for multiobjective engineering problems involving discrete decisions. *Industrial & engineering chemistry research 37*(5), 1866–1882.

Parker, N. (2004). Using natural gas transmission pipeline costs to estimate hydrogen pipeline costs. *Institute of Transportation Studies 1*, 1–86.

Patankar, S. (1980). *Numerical heat transfer and fluid flow*. Hemisphere Pub.

Pérez Escobedo, J. L. (2010). *Multiobjective optimization of New Product Development in the pharmaceutical industry*. Ph. D. thesis, Institut National Polytechnique de Toulouse.

Pettersson, F., A. Biswas, P. Sen, H. Saxen, and N. Chakraborti (2009). Analyzing Leaching Data for Low-Grade Manganese Ore Using Neural Nets and Multiobjective Genetic Algorithms. *Materials and Manufacturing Processes 24*(3), 320–330.

Pettersson, F., N. Chakraborti, and H. Saxén (2007). A genetic algorithms based multi-objective neural net applied to noisy blast furnace data. *Applied Soft Computing 7*(1), 387–397.

Ponsich, A. (2005). *Stratégies d'optimisation mixte en Génie des Procédés– Application à la conception d'ateliers discontinus*. Ph. D. thesis, Institut National Polytechnique de Toulouse.

Pugnet, J. (1999). Pompage des compresseurs. *Techniques de l'ingénieur. Génie mécanique BL2*(BM4182), BM4182.1–BM4182.18.

Ramteke, M. and S. Gupta (2009). Biomimetic Adaptations of GA and SA for the Robust MO Optimization of an Industrial Nylon-6 Reactor. *Materials and Manufacturing Processes 24*(1), 38–46.

Rangaiah, G. (2009). *Multi-Objective Optimization: Techniques and Applications in Chemical Engineering*. World Scientific Publishing Company.

Rangaiah, P. (1985). Studies in constrained optimization of chemical process problems. *Computers & Chemical Engineering 9*(4), 395–404.

Ray, W. and J. Szekely (1973). *Process optimization, with applications in metallurgy and chemical engineering*. John Wiley & Sons.

Reeves, G. and R. Reid (1988). Minimum values over the efficient set in multiple objective decision making. *European journal of operational research 36*(3), 334–338.

Ren, L., Y. Zhang, Y. Wang, and Z. Sun (2007). Comparative analysis of a novel m-topsis method and topsis. *Applied Mathematics Research eXpress 1*, 2–15.

Rhoads, G. (1983). Which flow equation-does it matter? In *PSIG Annual Meeting*.

Ríos-Mercado, R., S. Wu, L. Scott, and E. Boyd (2002). A reduction technique for natural gas transmission network optimization problems. *Annals of Operations Research 117*(1), 217–234.

Rodriguez, G., L. Pibouleau, C. Pantel, and S. Domenech (2010). Optimization of Gas Transmission Networks under Energetic and Environmental Considerations. *International Journal of Chemical Reactor Engineering 8*(Article A136), 1–31.

Romeo, E., C. Royo, and A. Monzon (2002). Improved explicit equations for estimation of the friction factor in rough and smooth pipes. *Chemical engineering journal 86*(3), 369–374.

Sauer, R. N., A. R. Colville, Jr., and C. W. Burwick (1964). *Computer Points the Way to More Profits*, Volume 49. Hydrocarbon Processing & Refiner.

Schouten, J., J. Michels, and R. Janssen-van Rosmalen (2004). Effect of hydrogen-injection on the thermodynamic and transportation properties of natural gas. *International journal of hydrogen energy 29*(11), 1173–1180.

Schroeder, D. (2001). A tutorial on pipe flow equations. In *33rd Annual Meeting Pipeline Simulation Interest Group (PSIG)*, pp. 17–19.

Service, T. C. (2010). A no free lunch theorem for multi-objective optimization. *Information Processing Letters 110*(21), 917 – 923.

Shashi Menon, E. (2005). *Gas Pipeline Hydraulics*. CRC Press.

Sherif, S., F. Barbir, and T. Veziroglu (2005). Towards a hydrogen economy. *The electricity journal 18*(6), 62–76.

Shu, L., S. Ho, S. Ho, J. Chen, and M. Hung (2004). A Novel Multi-objective Orthogonal Simulated Annealing Algorithm for Solving Multi-objective Optimization Problems with a Large Number of Parameters. In *Genetic and Evolutionary Computation–GECCO 2004*, pp. 737–747. Springer.

Sletfjerding, E. and J. Gudmundsson (2003). Friction factor directly from roughness measurements. *Journal of Energy Resources Technology 125*, 126–130.

Smith, J. and H. Van Ness (1998). *Introduction to Chemical Engineering Thermodynamics*. McGraw-Hill Book Company Book Company.

Smith, K., R. Everson, and J. Fieldsend (2004). Dominance measures for multi-objective simulated annealing. In *Evolutionary Computation, 2004. CEC2004.*, Volume 1, pp. 23–30. IEEE.

Srinivas, N. and K. Deb (1994). Muiltiobjective optimization using nondominated sorting in genetic algorithms. *Evolutionary computation 2*(3), 221–248.

Stoner, M. (1969). Steady-state analysis of gas production, transmission and distribution systems. In *Fall Meeting of the Society of Petroleum Engineers of AIME*.

Stoner, M. (1972). Sensitivity analysis applied to a steady-state model of natural gas transportation systems. *Old SPE Journal 12*(2), 115–125.

Suming, W., R. Rios-Mercado, E. Boyd, and L. Scott (2000). Model relaxations for the fuel cost minimization of steady-state gas pipeline networks. *Mathematical and Computer Modelling 31*(2-3), 197–220.

Sun, C., V. Uraikul, C. Chan, and P. Tontiwachwuthikul (2000). An integrated expert system/operations research approach for the optimization of natural gas pipeline operations. *Engineering Applications of Artificial Intelligence 13*(4), 465–475.

Sung, W., D. Huh, J. Lee, and O. Kwon (1998). Optimization of Pipeline Networks With a Hybrid MCST-CD Networking Model. In *SPE Production & Facilities*, Volume 13, pp. 213–219. Society of Petroleum Engineers.

Surry, P. and N. Radcliffe (1997). The COMOGA method: constrained optimisation by multi-objective genetic algorithms. *Control and Cybernetics 26*, 391–412.

Surry, P., N. Radcliffe, and I. Boyd (1995). A Multi-Objective Approach to Constrained Optimization of Gas Supply Networks: The COMOGA Method, A Evolutionary Computing. In *AISB Workshop*, pp. 166–180.

Tabkhi, F. (2007). *Optimisation de Réseaux de Transport de Gaz*. Ph. D. thesis, Institut National Polytechnique de Toulouse.

Tabkhi, F., L. Pibouleau, G. Hernandez-Rodriguez, C. Azzaro-Pantel, and S. Domenech (2009). Improving the performance of natural gas pipeline networks fuel consumption minimization problems. *AIChE Journal 56*(4), 946–964.

Taboada, H. and D. Coit (2006). Data mining techniques to facilitate the analysis of the Pareto-optimal set for multiple objective problems. In *Proceedings of the Industrial Engineering Research Conference*.

Tanaka, M., H. Watanabe, Y. Furukawa, and T. Tanino (1995). GA-based decision support system for multicriteria optimization. *Systems, Man and Cybernetics, 1995. Intelligent Systems for the 21st Century., IEEE International Conference 2*, 1556–1561.

Teixeiro de Almeida, A., C. De Miranda, and A. Cabral Seixas Costa (2004). Multicriteria model for prioritization of research and development projects. In *Journal of the Academy of Business and Economics*.

Tian, S. and M. Adewumi (1994). Development of analytical design equation for gas pipelines. *Old Production & Facilities 9*(2), 100–106.

Turinsky, P., P. Keller, and H. Abdel-Khalik (2005). Evolution of nuclear fuel management and reactor operational aid tools. *Nuclear Engineering and Technology 37*(1), 79–90.

Turner, W. and M. Simonson (1984). A compressor station model for transient gas pipeline simulation. In *PSIG Annual Meeting*.

Turner, W. and M. Simonson (1985). Compressor station transient flow modeled. *Oil & Gas Journal Technology 1*, 79–83.

Upreti, S. and K. Deb (1996). Optimal design of an ammonia synthesis reactor using genetic algorithms. *Computers & Chemical Engineering 21*(1), 87–92.

Valero, A., M. Lozano, L. Serra, G. Tsatsaronis, J. Pisa, C. Frangopoulos, and M. Spakovsky (1994). CGAM problem: definition and conventional solution. *Energy-The International Journal 19*(3), 279–286.

Veziroglu, T. and F. Barbir (1998). Hydrogen energy technologies. *Emergyng Technologies Series 1*, 1–20.

Whaley, T. and G. Long (2001). Pipelines. *Wiley Online Library 1*, 1–18.

Williams, T. and R. Otto (1960). A generalized chemical processing model for the investigation of computer control. *AIEE Trans 79*, 458–468.

Wolpert, D. and W. Macready (1997). No free lunch theorems for optimization. *IEEE transactions on evolutionary computation 1*(1), 67–82.

Zadeh, L. (1963). Optimality and non-scalar-valued performance criteria. *Automatic Control, IEEE Transactions 8*(1), 59–60.

Zhaoxu, S. and H. Min (2010). Multi-criteria decision making based on promethee method. In *Computing, Control and Industrial Engineering (CCIE), 2010 International Conference on*, Volume 1, pp. 416–418. IEEE.

List of Figures

List of Tables